Effects of Organic Matter on Shrinkage and Water Retention Behaviour of Organic Dredged Sediment

S.A. Chin A Moei

Faculty of Civil Engineering & Geosciences, Geo-Engineering

TU Delft Delft University of Technology

Challenge the future

Effects of Organic Matter on Shrinkage and Water Retention Behaviour of Organic Dredged Sediment

by

S.A. Chin A Moei

in partial fulfillment of the requirements for the degree of

Master of Science
in Civil Engineering

at the Delft University of Technology,
to be defended publicly on Wednesday December 14, 2016

Supervisor:	Dr. ir. L.A. van Paassen	TU Delft
Thesis committee:	Prof. Dr. C. Jommi	TU Delft
	Dr. C. Chassagne	TU Delft
	MSc. N.H.M. Zain	TU Delft

An electronic version of this thesis is available at http://repository.tudelft.nl/.

TU Delft Delft University of Technology

ABSTRACT

Peatlands in the Netherlands suffer from continued surface subsidence and accumulation of suspended sediments which leads to poor water quality. Excess suspended sediments are currently being deposited in depots on peatlands as a sustainable method for reusing sediment and to compensate for surface subsidence. The general consensus of researchers is to credit the majority of surface subsidence of peatlands to oxidation of organic matter. To assess this, the effect of organic matter and initial water content on the shrinkage and water retention behaviour was studied. Additionally, the effect of organic matter on gas formation was researched, along with the main mechanism for such an occurrence. From the peatland Wormer & Jisperveld, dredged sediments were collected from a depot and core samples were also taken over the course of three years. Soil characterisation tests were carried out and a novel approach of combining the extended evaporation method with computed tomography was used. Experiments were varied by differing the organic and initial water contents, through chemical removal (H_2O_2) of organic matter and fan drying, respectively. Results show that decreasing the organic content reduced liquid limit of the sediment. The effect of organic matter on the shrinkage characteristics is not significant for the range of water contents relevant during the desiccation process observed in the field. Only normal shrinkage was observed at near saturated conditions, where the loss of water volume is equal to the loss of bulk soil volume. Additionally, the effect of organic matter on the water retention characteristic greatly reduces the water content at a given suction level. Varying the initial water content changes the onset of the water retention characteristic, while the curve's shape was barely influenced. Slight variation of retention behaviour likely due to natural oxidation of organic matter. For the shrinkage characteristic only the onset was influenced. Computed tomography illustrated that the effect of organic matter stimulates gas formation within the sediment. Gradual movement of the gas, aggregation, bubble growth and ebullition events were also observed. The main mechanism of gas formation could not be determined with the applied test methods. However, it is considered to have been caused by either exsolution of dissolved methane, oxidation of organic matter or a combination of both. Further research would be needed for verification.

ACKNOWLEDGEMENTS

First and foremost, I would like to thank my thesis supervisor Dr.ir Leon van Paassen for his guidance throughout the final phase of my education. His knowledge and passion for his work is an immense inspiration to me and undoubtedly for his former students of TU Delft and for the many more to come at Arizona State University. I wish you best of luck as you begin a new chapter in your life in Arizona.
I would further like to thank the rest of my committee members, Prof Dr. Cristina Jommi, Dr. Claire Chassagne and Msc. Nor Zain for their patience and constructive feedback. A special mention to Dr. ir. Dominique Ngan-Tillard for her assistance with Avizo and logistic forms.
Secondly, I would like to express my gratitude to the lab technicians, Arno Mulder, Ellen Meijvogel, Joost van Meel, Guus Lohlefink, Han de Visser and Wim Verwaal. I would have been completely lost without their help and guidance in the laboratory.
Lastly, I would like to thank my friends and family, you mean the world to me. I know I am far from an ideal student and a hopeless case at times, so I am very grateful to my family for their love and continued support. My friends, thank you all for the moral support during the difficult moments and for the unforgettable good times.

Stephen Chin A Moei
Delft, December 2016

CONTENTS

NOMENCLATURE

ρ_s	Particle density
ρ_w	Water density
θ	Volumetric water content ($\frac{V_w}{V_s}$)
M_s	Mass of solids
M_w	Mass of water
CH_4	Methane
CO_2	Carbon dioxide
CT	Computed Tomography
e	Void ratio ($\frac{V_v}{V_s}$)
EEM	Extended Evaporation Method
G_s	Specific gravity
GHG	Greenhouse Gases
H_2O_2	Hydrogen peroxide
n	Porosity ($\frac{V_v}{V_t}$)
NaOH	Sodium hydroxide
NO_2	Nitrous oxide
S	Degree of saturation ($\frac{V_w}{V_v}$)
SCC	Soil shrinkage characteristic
SWRC	Soil water retention curve
V_a	Volume air
V_g	Volume of gas
V_s	Volume solids
V_v	Volume voids
V_w	Volume water
VGC	Volumetric gas content ($\frac{V_g}{V_s}$)
w	Gravimetric water content ($\frac{M_w}{M_s}$)

List of Figures

List of Tables

1

INTRODUCTION

The master thesis represents the final work for a Master of Science degree of the Delft University of Technology. A specific topic was researched for a 9 month period, which will be awarded 40 ECTS (European Credit Transfer and Accumulation System) for good result.

This master thesis was carried out under the supervision of the academic faculty of Delft University of Technology. The supervising body formed a committee with their role of overseeing, guiding and grading the student during their graduate time. This document represents the final product of the master thesis.

In this thesis, the influence of organic matter on the shrinkage behaviour of dredged sediment was studied. This chapter discusses the motivation and objectives for this research, together with general information of the field. Subsequent chapters include the theoretical background related to the subject, methodology involved for the study, processing procedure of the data, results acquired after processing, analysis and evaluation of the results and finally recommendations for further research.

1.1. PROLOGUE AND PROBLEM DEFINITION

During the Holocene period peat formation took place in the Netherlands above the Pleistocene layers. These peatlands were reclaimed from the 12th century for agricultural purposes. Ever since the reclamation of these lands the peat meadows has been subsiding. Where peatlands were on average between one to three meters above sea level, peatlands have now subsided to one to two meters below average sea level [1].
Surface subsidence of peat is triggered by drainage of the land and consists primarily of three processes: consolidation due to loss of buoyant force, shrinkage due to drying and oxidation of organic matter[2].

Where many different type of research have been carried out in the course of the years on the topic of peat subsidence, the general belief is that the long term subsidence is mainly attributed to oxidation of organic material. Researchers such as van den Akker[3], were able to correlate surface subsidence with the corresponding CO2 emissions but accounted the long term subsidence only due to oxidation. Another well-known paper is from Schothorst et al 1977 [4], assumed that higher content of mineral elements in the top layers is due only to oxidation, making it possible to estimate that oxidation by comparing the bulk density of mineral elements in the layers above and below groundwater level. Schothorst concluded that approximately 15% of the total subsidence could be attributed to shrinkage of the upper layer, which subsequently leaves 85% to be ascribed to oxidation of organic matter.

Whereas, Pons and Zonneveld [5] stated that half of the total moisture loss and consequently half of the settling, was caused by oxidation of most of the organic matter. Zonneveld's statement appears to be a more accurate assessment of the peat subsidence situation in the Dutch polders, but was misinterpreted for quite some time.
This is supported by soil classification of peat wetlands in Oostknollendam. Peat samples were taken over the course of three years. When examining the volume balances of the samples, it appears that 90 to 95% of the total volume consists of water. Such simple volume balance calculations indicates that it is impossible to

attribute the majority of peat subsidence due to oxidation of organic material.

1.2. PROJECT CONTEXT

1.2.1. WORMER & JISPERVELD

Wormer & Jisperveld is a peat wetland and nature reserve of about 2400 ha. It lies in the Dutch province Noord-Holland between Wormer, de Rijp, Purmerend and Wormerveer. The area consists of a network of ditches and 3 shallow lakes, namely: De Poel, Het Zwet and De Marken. Of the total area, 240 ha is constructed on, 500 ha is water and 1660 ha are peatlands. The area is independently preserved and maintained by the organizations Natuurmonumenten and Natura 2000, with Natura 2000 maintaining the majority of the region. Main function of the land is agriculture (dairy farming), serving secondly as a nature reserve for preserving its unique wildlife and for recreational activities. The project area is shown in Figure 1.1

Around 1000AD peatlands were reclaimed mainly for agriculture. Under the influence of drainage and agriculture, the peat began to subside ever since. Around the 12th century, the surface subsided till the sea level. Low lying embankments were needed to protect the area and surrounding villages from flooding. In the beginning of the 17th century the landscape changed once again due to drainage of Beemster in 1612 and the Wijdewormer in 1626, which significantly increased the water management issues. As a result, it was decided in 1630 to construct embankments around the entire Wormer and Jisperveld. During this time, many other low lying polders in the area were enclosed with embankments. With the embankments in place, this prevented the entry of brackish water supplied from the Zaan river. However, flooding still occured every so often, resupplying the area with brackish water. In 1932, the Afsluitdijk was constructed, which significantly reduced the influence of brackish water. The salinity of the water reduced from 6 gram chloride per liter in 1930, to 0.5 gram per liter at present day.

Currently, the peat's thickness is estimated to be 2m, where the original thickness is estimated to be 5m around 1000BC. The continued subsidence due to maintaining the lowered groundwater table, brings up the question of how to reverse this phenomenon and to eventually restore the residing peat. Additionally, large amounts of supended sediments are being produced yearly in the peat wetlands, which causes a number of hazards for the area. For this reason along with continued surface subsidence has led to the creation of the ongoing pilot project "Liftup of Lowlands" since March 2013.

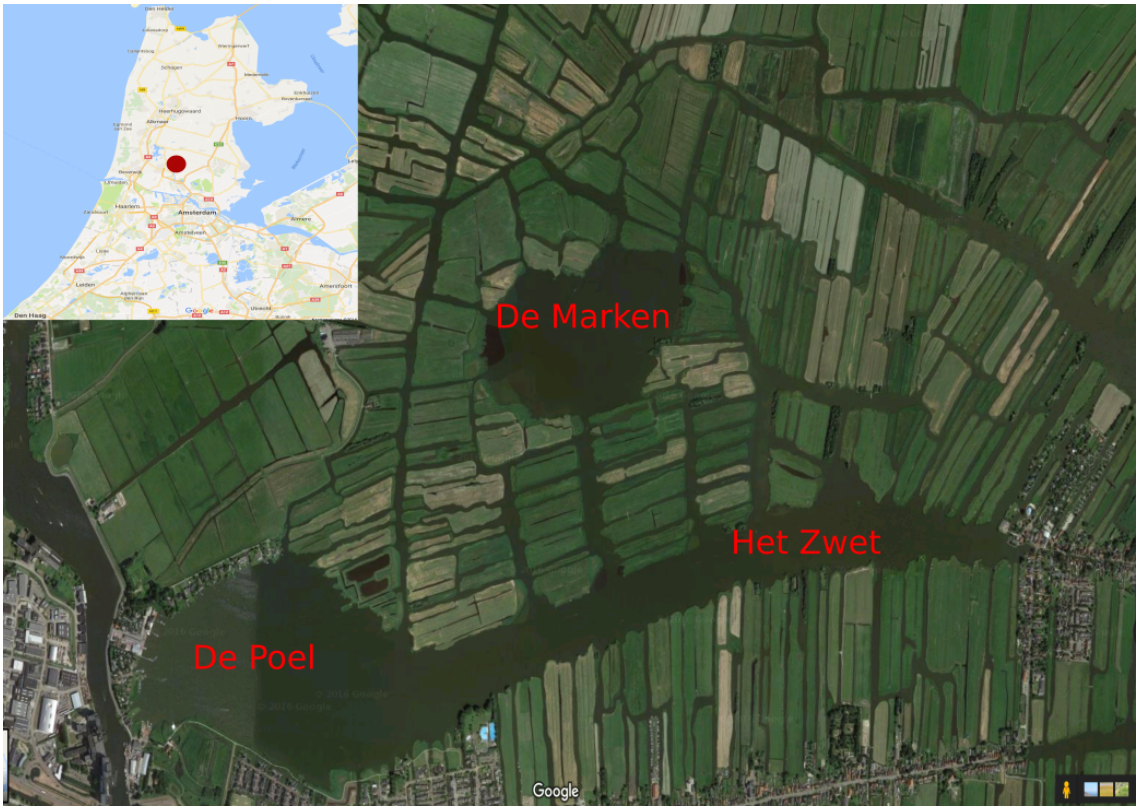

Figure 1.1: Project location - Wormer & Jisperveld

1.2.2. LIFTUP OF LOWLANDS

In peat wetlands such as Wormer & Jisperveld, large amounts of suspended sediments are generated due to the wetland's unstable conditions. Shore erosion and sediment transport throughout the waterways causes significant hindrance for the environment and the community directly involved with the area. Models have estimated a total amount of 1 million m^3 of mobile suspended sediments flowing throughout the area. Current environmental issues concerning mobile suspended sediments are eutrophication of the water and spreading of mercury pollution present in the sediments. Obstruction of waterways due to sediment accumulation is a less severe secondary problem, which is treated regularly by dredging. Continued subsidence is another major issue with peat wetlands, although less related to suspended sediments. "Liftup of Lowlands" is a pilot project which aims to upgrade and reuse suspended sediments as a resource which can contribute to a more global sustainability. Various parties are involved in the "Liftup of Lowlands" pilot project. The Hoogheemraadschap Hollands Noorderkwartier is the regional water authority in charge of the area. Companies such as Witteveen+Bos, Tauw and Arcadis are directly involved in the project and researchers from the Delft University of Technology and Wageningen University are also assigned to the pilot project.

Mercury pollution was caused due to a paint manufacturer, De Uil, in the late 19th century. De Uil used to lie to the south-east of the Poel, where sulfuric acid and mercury were used to produce a crimson coloured paint. This caused region to be polluted with mercury. Presently, a few areas in De Poel exceed intervention levels of 10 mg/kg mercury. Overall, the average mercury concentrations are between 1.20 - 5.50 mg/kg. These levels exceeds the biotanorm of 1.2 mg/kg mercury for eels, but are still below the norm for fish consumption. Research of the area has shown that the risks of the current mercury pollution is low as there is little to no mobilisation of dissolved mercury when subjected to suspension and aerobic conditions. The largest risk to mercury exposure appears to be in the top layer, 0-20 cm, of the sediment. Removal of this top layer is a good short term solution, but in the long term the removed sediment will eventually be replaced by formation of new sediment. A likely effective mitigation method would be to create an underwater sediment depot, a so called Sediment Storer. This would isolate and cover the mercury rich top layer.

Eutrophication is the depletion of oxygen in water due to an excess of nutrients, mainly phosphates. The excess nutrients causes an explosive growth of plants and algae, which consumes the oxygen in the water, resulting in the death of aquatic animals. Muddy water is distinguished by high concentrations of phosphates, little amount of aquatic plants and a large amount of algae and biomass. Where the current situation in Wormer and Jisperveld is described as eutrophic, with muddy water and eroding lakesides. Although the phosphates supplied by the waterways is not particularly high, it is the phosphate rich sediment that is transported throughout the Wormer and Jisperveld that causes disturbances with sunlight penetration and physical and chemical disturbances of the sediment. Ways to mitigate sediment transport, are isolation of certain key parts of the water system (Sediment Storer), screens to capture mobile sediment (Sediment Settler) and shore protection to prevent erosion.

The Sediment Storer mentioned previously is a novel method designed by Tauw. It involves the use of Geotubes and a synthetic woven cloth. The Geotube is filled with sand, and submerged to the bottom of the water. The synthetic cloth is then strung from the Geotube to a waterbuoy on the surface of the water. The Sediment Storer is meant to retain the dredged sediment in the buffer, acting as an underwater depot and are placed along the shore. A schematic view of the Sediment Storer is illustrated in Figure 1.2. The same technique is used for shore protection in combination with breakwater structures made out of wooden piles placed in a row. A Sediment Settler has a similar design, but are placed perpendicular where sediment flow is dominant. The Sediment Settlers allow the flow of water through holes at the top of the screen, but captures sediments from below. Schematic view of the Sediment Settler can be seen in Figure 1.3. The Sediment Storers that are currently located in De Marken are illustrated in Figure 1.4

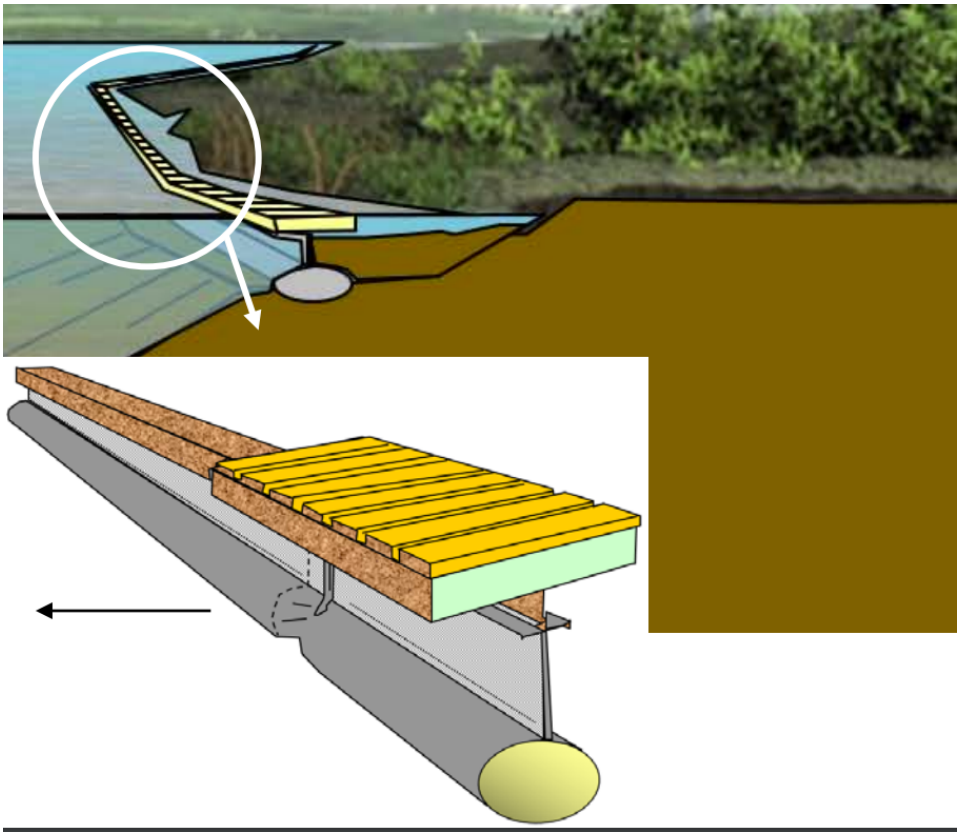

Figure 1.2: Schematic view of a Sediment Storer [6]

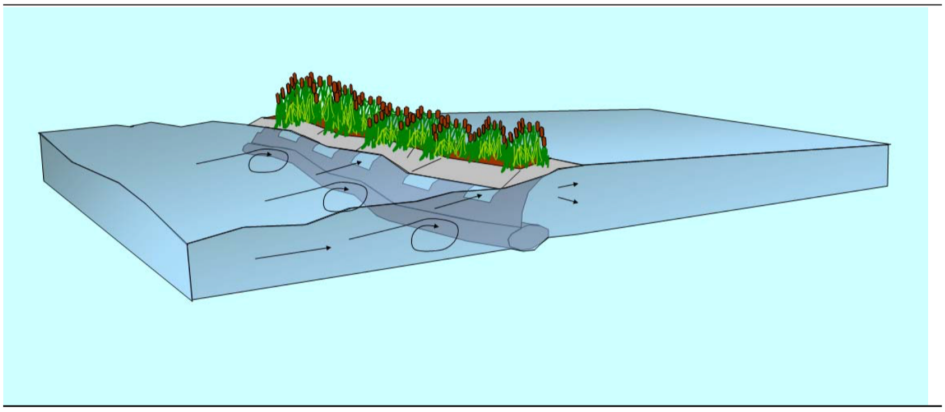

Figure 1.3: Schematic view of a Sediment Settler [7]

Figure 1.4: Sediment Storers located in de Marker

The usual method for disposing excess suspended sediment is at sea or at upland disposal facilities. The "Liftup of Lowlands" project attempts to reuse the suspended sediments by means of physical ripening on depots and to compensate for subsidence. Depots are created by excavating 30cm of the top layer of the soil to create an enclosed embankment. Excess suspended sediments are then dredged in the depots where physical ripening can take place. This process is illustrated in Figure 1.5. Advantages of using depots is the storage of excess dredged sediments and possible improvement of soil quality when the dredged material is dewatered/ripened. Land is usually reclaimed after a set period of time, usually three years. Disadvantages are finding suitable areas for the depots and an increase of settlement rate of the original peat layer. From an economical standpoint, farmers would rather not relinquish their property for such an extended period of time. Concerning settlement rate, an increased settling rate is possible due to the additional sediment weight placed on the soil.

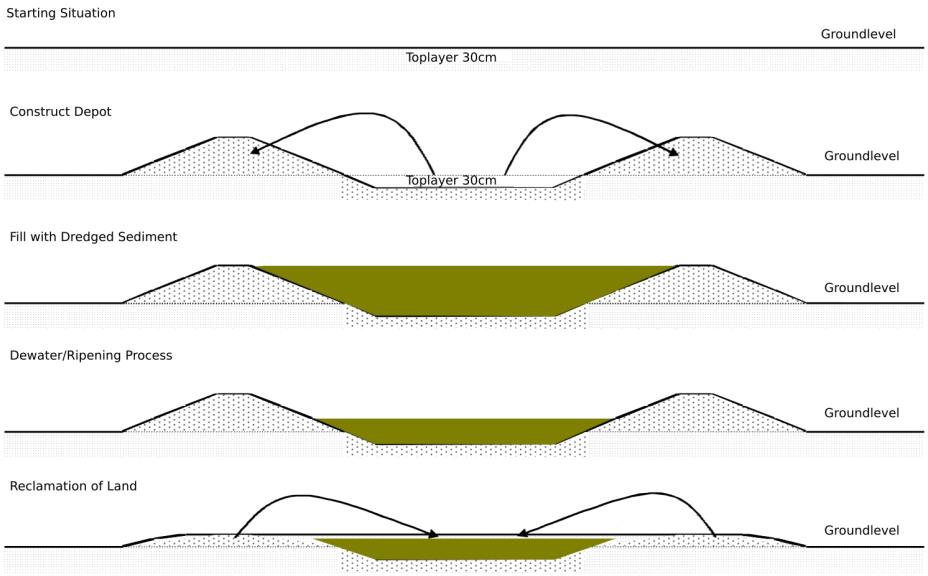

Figure 1.5: Schematic view of construction and reclamation of depot - Edited from Hoogheemraadschap Hollands Noorderkwartier [8]

All the aforementioned mitigation techniques are currently being implemented in Wormer & Jisperveld as part of "Liftup of Lowlands". The pilot project has been ongoing since March 2013. Research being carried out by Delft University of Technology and Wagingen University focuses on the dredged sediment placed for ripening on the depots.

The current research being done by Delft University of Technology and Wagingen University are focused on the dredging depots, in particularly Depot X, illustrated in Figure 1.6. Depot X was constructed in 2013 and will be dismantled at the end of 2016. The ripened dredged sediment will then be cultivated for agriculture. Research topics being carried out by the universities include ripening of dredged sediments and its functional requirements for reuse, dewatering of dredged sediment and formation of dessication cracks and coupling decomposition of organic soils to volume changes. The Settlement Storers, Sediment Settlers and shore protection were carried out by companies such as Tauw and Witteveen+Bos. Results of these techniques are still to be processed and analysed by these companies.

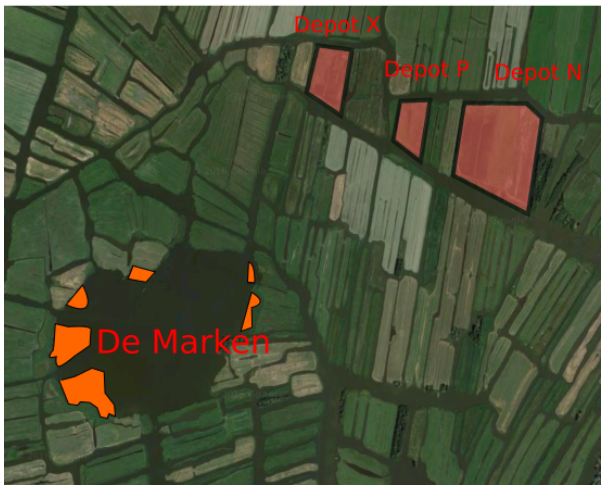

Figure 1.6: Dredging Depot X, P and N

1.2.3. GREENHOUSE GASES IN PEAT WETLANDS

Although not a topic being researched for the “Liftup of Lowlands” project, emission of greenhouse gases (GHG) from wetlands are directly related to drainage of peat soils. Peat wetlands are considered to be large carbon sinks, able to store and release carbon and nitrogen gases. Due to their large carbon reservoirs, these areas are of great climatic interest. The main GHG released by these wetlands are carbon dioxide (CO_2) , methane CH_4 and nitrous oxide (NO_2), where CO_2 and CH_4 are seen as most influential to GHG emissions.

Peat degradation is considered as one of the main mechanisms to GHG emissions. Peat degradation is a consequence of continued drainage. The lowered water table depth causes aeration of the soil. Aeration of the soil results in the oxidation of its organic components, which subsequently releases CO_2 and contributes to surface subsidence.

CH_4 is also produced by methanogenic bacteria that are most commonly found in waterlogged anoxic soils, which may become supersaturated in peat pore water, providing the potential for a gas phase to develop as bubbles. CH_4 can be emitted to the atmosphere via three pathways: diffusion through the pore water, ebullition (gas bubble release) and plant mediated transport. Studies of GHG emissions are based mainly on diffusive CH_4 emissions, but have largely ignored the presence of entrapped gas in peat, which may cause miscalculations in their GHG prediction models. Other effects entrapped gas can have on peatlands are peat buoyancy, pore water gradients, and nutrient and contaminant transport. In the field at Wormer & Jisperveld, peat buoyancy is an occurrence observed numerous times, causing waterways to be blocked and crashing of boats. Peat mats as large as 30x30m were reported. Figure 1.7 illustrates one of numerous floating mats seen in Wormer & Jisperveld. Besides floating peat mats, a great amount of gas bubbles were visible at the surface water when the site was visited on 25 August 2016.

Figure 1.7: Floating peat mat in Wormer & Jisperveld - Captured on 25 August 2016

1.3. RESEARCH QUESTIONS

The MSc thesis is closely related to one of the the previously stated research topics of "Liftup of Lowlands" project, namely coupling decomposition of organic soils to volume changes, which is currently being carried out by a PhD student from TU Delft. The goal for this study is to understand the effect of organic matter on the shrinkage and water retention behaviour of the dredged sediment under natural drying conditions. Additionally, since shrinkage behaviour is being researched during natural drying, air entry into the soil and possible biogenic gas formation will be studied as well. The main research question is:

- How does organic matter influence water retention and shrinkage behaviour of dredged sediments from peat meadow areas under natural drying conditions?

With the following sub-questions:

- How does the initial water content influence the water retention and shrinkage behaviour?
- What is the effect of organic matter on gas formation?
- What is the main mechanism for gas formation in organic dredged sediments?

1.4. RESEARCH PROGRAM

To answer these questions, the research program devised consisted of a series of evaporation tests, chemical oxidation of highly organic dredged material and are supported by a series of CT-scans (Computed Tomography) . Natural drying of the dredged sediment is simulated by the commercial Hyprop device. The Hyprop is a cylindrical column where soil is placed in and utilises the Extended Evaporation Method (EEM) to measure the water tension and soil weight as the sample naturally dries. A series of Hyprop campaigns were carried out with the dredged sediment with varying organic and water content. The water content was adjusted by naturally drying the sediment in the open air before being utilised in the Hyprop. Organic content was reduced by chemically oxidizing the dredged sediment with hydrogen peroxide (H_2O_2). To study the volume changes, CT-scans were made during the drying process of the Hyprop. With the help of 3D analysis software, Avizo 9.0, the soil and gas volume can be accurately calculated. The test procedures are described more in depth in chapter "Materials & Methodology". Overall, the Hyprop experiments carried out are:

1. **Non-oxidised** (initial organic content) - **Undried** (initial water content)
2. **Non-oxidised** (initial organic content) - **Partially Air dried** (lowered initial water content)
3. **Oxidised** (lowered organic content) - **Undried** (initial water content after oxidation)
4. **Oxidised** (lowered organic content) - **Partially Air dried** (lowered initial water content after oxidation)

1.5. CONTENT OF THE REPORT

Thus far, the context of the thesis and the research questions have been discussed. The second chapter, "Literature Review", reviews the theoretical background related to the subject. Afterwards, the third chapter "Material & Methods" defines the dredged sediment and the methods used for the investigation. This includes a description of the material, the testing devices and the testing procedures. The "Data Processing" in the fourth chapter describes how the results are processed and the corrections utilised. Subsequently, the processed data is then displayed and critically analysed in the fifth chapter,"Results & Analysis". The next to last chapter, "Discussion", reviews the thesis. Emphasis is put on evaluating the applied methodology and data processing. The results will also be discussed in depth and a critical assessment will be done. The final chapter, "Conclusions & Recommendations", concludes the results of the thesis, value of the research is discussed and recommendations are given related to the methodology, data processing, results for future research.

2

Literature Review

2.1. Peat

2.1.1. Morphology

Peat is an accumulation of organic matter or partially decayed vegetation that takes thousands of years to develop. Conditions for peat to develop are determined by climate and topography. An excess of water throughout the year is needed, the landscape must be such that a sufficient amount of this water is retained to support growth of vegetation and is a permanent reservoir is required to preserve the remains, which ultimately becomes the peat. Lakes and basins are ideal habitats for the forming of peat. River banks are also suitable but requires that the water flow is not too powerful. The final component is the geology, which influences the chemistry and concentration of nutrients in the water entering the mires in the basins and valleys.

Three morphological stages can be identified during the development of peatlands, namely: (1) the rheotropic stage, (2) the transitional stage and (3) the ombrotrophic stage. (1) Rheotrophic stage is the stage where mires develop in mobile water in lakes, basins and valleys. In this stage nutrients are being brought in by stream flow, runoff and percolating groundwater. Supplied nutrients are rich, in calcareous regions and is further enriched by sediment that is washed in. This type of peat is referred to as fen peat, is in most cases alkaline and are generally underlain by very soft organic muds.
(2) Transitional stage is when the mire changes from rheotrophic to ombrotrophic growth due to upward growth. The mire becomes increasingly dependent on precipitation, while still receiving nutrients, although to a lesser extent.
(3) The final stage, the ombrotrophic stage, is the phase where the mire has grown beyond the maximum physical limits of the groundwater. It solely relies on the precipitation for its water supply. The peatland starts to function as a reservoir, holding water above the level of the groundwater. Nutrient conditions here are insufficient due to the small amounts of salts that is taken up as sea spray in rough weather. This type of peat is named bog peat, and is acidic.

2.1.2. Water in Peat

Peat has a unique characteristic in its ability to hold water. For the Wormer and Jisperveld approximately 90% of the total volume consists of water. Three states of retention can be recognized in peat soils according to Hayward and Clymo (1982), namely: (1) intracellular water held within the internal cells under a suction of less than 10kPa, (2) interparticle water held by capillary forces under a suction exceeding 10kPa and (3) adsorbed water retained under a suction not exceeding 20MPa [9]. Whereas, the majority of the water is held as intracellular and interparticle water. The proportions and total quantity of each is dependent upon the struture, morphology and degree of humification of the various plants present. Where humification is defined as the degree of decomposition. Drainage and the type of plants in the peat also influences the proportions and quantity. Where ombotrophic plants tend to have higher intracellular water contents than minetrophic plants and bog peats have higher interparticle and total water contents than fen peats. Water in state (1) is more likely to flow during drainage, water in states (1) and (2) can be expelled by consolidation and all water can be removed by oven drying at 105 °C.

It is a common occurence that fibrous peats, with low humification, have higher total water contents than peats with high humification. This is explained by the destruction of the cellular structure as the organic material decomposes, which causes a decrease in intracellular water. Where generally the proportion of intracellular water is higher than interparticle water in fibrous peats. This cellular structure is remarkable as it must have microscopically thin walls, which must possess a significant shear strength to be able to ensure structural integrity in an essentially liquid mass. A powerful agency must be present to give the peat its strength and stability. Hypothesized, is that this powerful agency must be attributed the adsorbed water adhering to the surface of the cell tissue. The adsorbed water zone is controlled by the cation exchange ability (CEA) of the cell tissue and the chemistry of water containing the nutrient supply. The higher the cation exchange ability, the stronger the degree of adsorption and the greater the interparticle adherence.

Various peat forming plants has shown that the water retention is inversely related to the concentration of minerals in the water supply. Floristic change gradually occurs as the nutrient supply declines, which is then accompanied by an increase in cation exchange ability. This ultimately results in strengthening of the adsorption complex and an increase in the water content. This explains the larger water contents of bog peats, the high cation exchange abilities of bog plants enables them to extract very small amounts of nutrients in rain, giving up hydrogen ions in exchange. The exchange of hydrogen ions results in acidifying the water and peat. Figure 2.1 illustrates the relationship of the pH and exchangeable cations versus the organic content.

Thus, if low humification causes higher total water contents, i.e. high liquid limits, then the opposite is also true. Liquid limit declines with increasing humification presumably due to the destruction of cell tissue which results in the weakening of the adsorption complex. Therefore, in peat, the fibrous state would be expected to have a higher liquid limit than amorphous state.

Furthermore, water contents over peat can vary over a wide range from a few hundred per cent of dry weight to greater than 2000% in a span of a small distance. This is due to plants of different character live in communities and the non uniform decomposition of throughout the mass of soil [10].

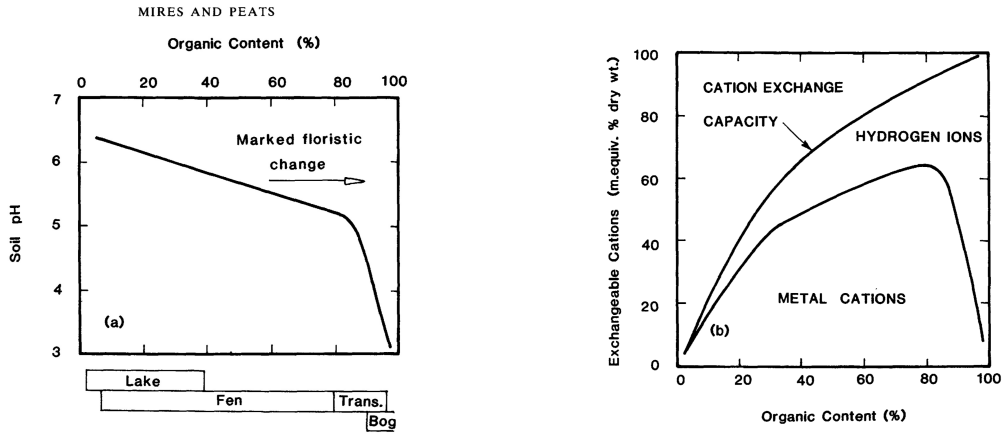

(a) Soil pH vs organic content

(b) Exchangeable cations vs organic content

Figure 2.1: Gorham's pH and cation exchange ability in relation to the organic content of lake, fen and bog [11]

2.1.3. GAS FORMATION IN PEAT

Two main mechanisms can be distinguished in the formation of gas in peat. The first is decay of organic matter which releases carbon dioxide (CO_2) into the atmosphere, and the second is exsolution of methane (CH_4) which is supersaturated in the pore water. Drainage of peatlands results in a lowered water table depth. Consequently, aerobic conditions prevail in the top layer of the soil, which enables CO_2 to be produced via bacterial and fungal decomposition of plant litter and soil organic matter. Methane is almost exclusively produced by the strictly anaerobic methanogenic bacteria that are most commonly found in waterlogged anoxic soils, such as natural wetlands[12]. Much current peatland studies are concerned with the source and release of atmospheric methane (CH_4) and their effect on the environment. Methane is lost to the atmosphere from peatlands via three mechanisms: (1) diffusion through pore water to the water table and thus through the zone above the water table to the peatland surface, (2) diffusion or active transport through vascular plants and (3) via ebullition, where bubbles move to the peatland surface. Schematic view of the three pathways of methane emission and CO_2 release are illustrated in Figure 2.2. Until recently, the general consensus was that the first two mechanisms were the most influential pathways for CH_4 losses to the atmosphere. However, Recent work has suggested that a significant portion (>40%) of methane lost from peatlands does so as bubbles (ebullition) [13]. The presence of these bubbles has important biogeochemical effects, including the development of localized methane diffusion gradients, alteration of local flow paths affecting substrate delivery, peat buoyancy, and the potential episodic release of CH_4 via ebullition events[14].

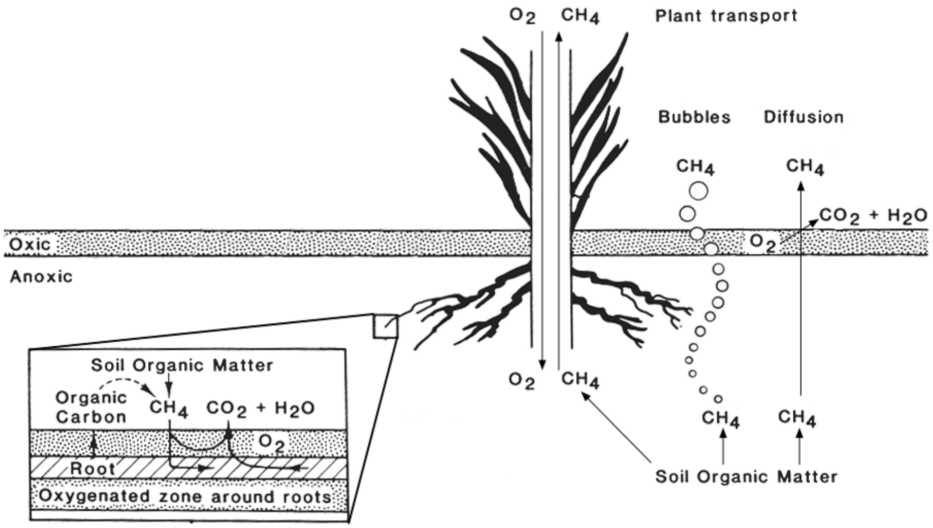

Figure 2.2: Schematic process of CH_4 and CO_2 emissions from peat soils [15]

Bubbles may be attached to peat fibres, they may occur within the cellular structure of peat fibres, or they may be found freely within the voids of pores between fibres. Buoyant forces of bubbles attached or within the peat fibres must overcome the surface tension of the gas-water interface for the bubbles to move. Bubbles in pores are able to move freely until they encounter some restrictions to that movement, such as pores with a smaller diameter than the bubbles. Bubbles are also able to increase in size through aggregation and production. As bubbles become stuck in pores, they have the potential to reduce greatly the water and solute transfer from surrounding areas. [16]

Ignoring the process of ebullition and production of gas due to decay, entrapped gas volume is influenced by a change in either atmospheric pressure or temperature. Consequences are the expansion or contraction of the gas according to the ideal gas law and the movement of gas between the gaseous and dissolved state according to Henry's law. The ideal gas law is the equation state of a hypothetical ideal gas and Henry's law describes that the amount of dissolved gas is proportional to its partial pressure in the gas phase. The ideal gas law is often written as:

$$PV = nRT \tag{2.1}$$

where,

- P is the pressure of the gas,
- V is the volume of the gas,
- n is the amount of gas in moles,
- R is the ideal gas constant,
- T is the absolute temperature of the gas.

And Henry's solubility law defined via concentration is:

$$H^{cp} = c_a / p \tag{2.2}$$

where,

- H^{cp} is Henry's solubility constant,
- c_a is the molar concentration of a species in aqueous phase,
- p is the partial pressure of that species in the gas phase

Temperature increase causes dissolved gas to come out of solution, leading to an increase of volume gas content and also causing existing bubbles to expand. Temperature also positively influences the production of CH_4. However, currently it is not clear the how much of the increase in gas bubbles is due to CH_4 production, thermal expansion or gas coming out of solution[17].

2.2. SOIL PHASE RELATIONSHIPS

For a civil engineer, soil is understood to be the weathered material in the upper layers of the earth's crust. Non-weathered material in this crust is denoted as rock. Natural weather process of rock degenerates into stones under long-term influence of sun, rain and wind. Course stones that are created in mountainous areas are transported downstream by gravity, often together with water in rivers. Internal friction gradually reduces the size of the stones becoming gravel, sand and eventually silt. Generally in the Netherlands, the soil consists of weather material, mainly sand and clay. The material has been deposited in earlier times in the delta formed by rivers. Other fine material has also been deposited by flooding of the land by the sea and the rivers.

Soils are commonly described as phases, namely: the solid phase consisting of minerals and organic matter, the gas phase and the water phase. These components (particles, water and air) of the three phases are used to describe a soil. Various parameters are used to define the distribution of these three components, and their relative contribution to the volume of a soil.

Soils can be either of two-phase or three-phase composition. In a completely dry soil the two phases are the solid soil particles and the pore air. A fully saturated soil also consist of two phases, the solid soil particles and the pore water. Only when a soil is partially saturated does it consist of three phases, the solid soil particles, pore water and pore air. The components of a soil is represented by a phase diagram in Figure 2.3. The distribution of these three components and their relative contribution to the volume of soil can be defined in various parameters and will be discussed in the following sections.

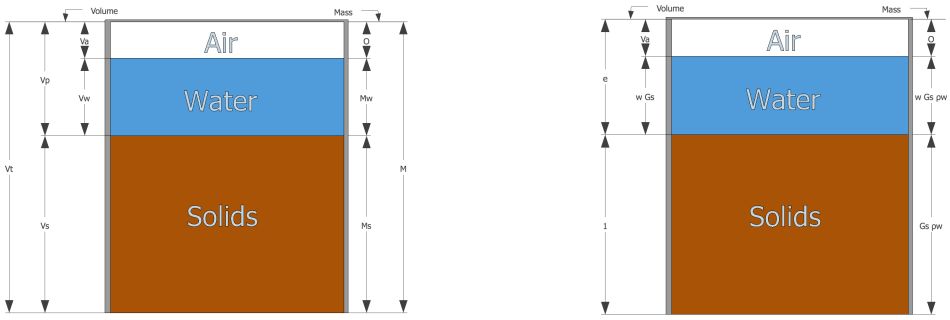

(a) (b)

Figure 2.3: Phase diagrams

2.2.1. POROSITY

The porosity, n is an important basic parameter which defines the ratio of volume of pore space and the total volume of soil,

$$n = \frac{V_v}{V_t} \tag{2.3}$$

The total volume is expressed as the sum of pore volume and the volume of the solids , $V_t = V_p + V_s$. The pore space of soil contains the water and air phase of the soil, therefore expressed as: $V_V = V_w + V_a$. When the porosity is small the soil is called densely packed and when the porosity is large it is loosely packed. Another method of expressing the amount of pores is the void ratio, e ,

$$e = \frac{V_v}{V_s} \tag{2.4}$$

This quantity is generally the preferred method, because it expresses the pore volume with respect to the fixed volume of solids. Porosity can not be smaller than 0 and can not be greater than 1. Whereas, the void ratio can be greater than 1. Both void ratio and porosity can be expressed interchangeably as:

$$e = \frac{n}{(1-n)} \qquad n = \frac{e}{(1+e)} \tag{2.5}$$

Since this thesis deals with highly shrinkable soils, a clear distinction must be made with what is considered air/gas when cracks appear in the soil. Air/gas-filled pores is defined as three cases in this thesis: (1) the gas is completely entrapped by the encompassing soil, (2) air/gas-filled pores open to the atmosphere by a narrow passage on the surface or (3) air-filled pores open to the atmosphere by large distinct passages. This is conceptually illustrated in Figure 2.4. In Figure 2.4 a schematic shrinking procedure of the dredged sediment can be seen. Highlighted in blue are entrapped gas bubbles formed during the drying process, and in red gas/air open to the atmosphere by air passages. The initial state signifies the start of the drying procedure, with little to no air/gas visible. Once evaporation starts, only vertical shrinkage and gas accumulation is observed in stage 1. Stage 2 signifies increased vertical shrinkage with lateral shrinkage as well. Gas accumulation continues, accompanied with bubble growth. In stage 3 vertical and lateral shrinkage continues with air/gas-filled pores connected to the atmosphere by narrow passages. In the end, we see in stage 4 the soil being detached from the side boundaries, large bubbles are formed and air/gas-filled pores are open to the atmosphere.

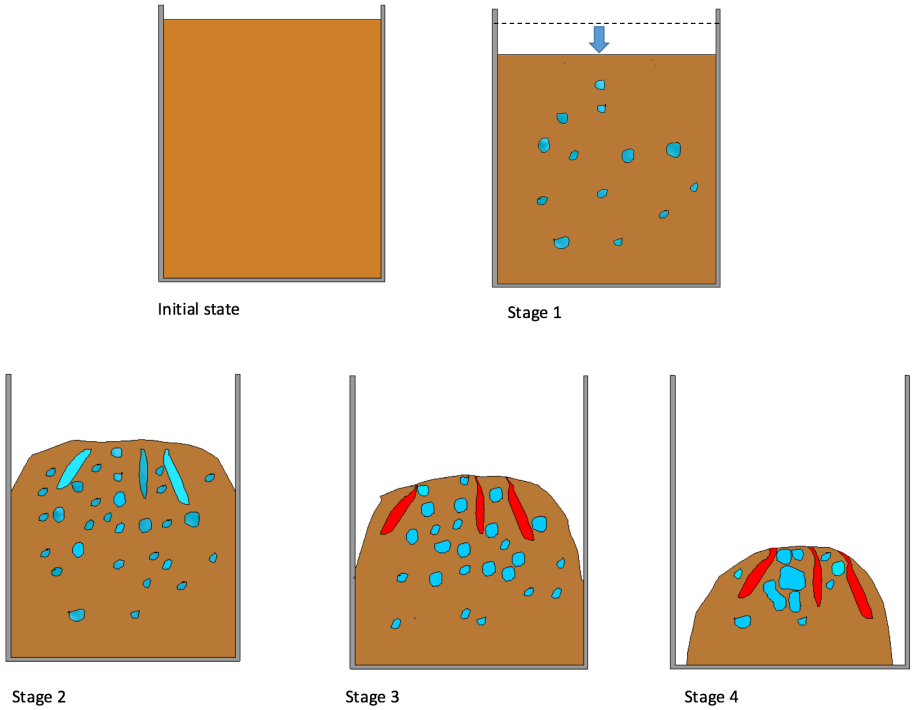

Figure 2.4: Schematic illustration of shrinkage procedure. Highlighted in blue represents entrapped gas bubbles. Highlighted in red represents air/gas-filled pores open to the atmosphere.

The distinction between entrapped gas bubbles and open air/gas-filled pores must be made as gas volume can differ greatly if for example narrow air passages open to the atmosphere are connected to large air/gas-filled pores.

2.2.2. DEGREE OF SATURATION

The degree of saturation, S , describes the amount of water present in the pores, as pores can contain water and air. Degree of saturation is expressed as

$$S = \frac{V_w}{V_v} \tag{2.6}$$

If $S = 1$ the soil is completely saturated and conversely if $S = 0$ the soil is completely dry.

2.2.3. WATER & GAS CONTENT

The water content, or moisture content, describes the quantity of water contained in a material. It is defined as dimensionless ratio based either on mass (gravimetric) or volume (volumetric). In geotechnical engineering the water content is determined by weighing a sample of the soil and then drying the sample in an oven at a temperature of 105-110 °C and reweighing. The gravimetric water content is described as the mass of water over the mass of the dry solids:

$$w = \frac{M_w}{M_s} \tag{2.7}$$

In engineering applications, volumetric water content can be described as the volume of water over the total volume or the volume of solids. Total volume is used in aggregate soils where the total volume does not vary as much. For this case, the soil being studied is highly organic and shrinkable, thus water volume will be expressed over a fixed volume of solids. Assuming no loss of organic material. Usually, the gravimetric water content is determined first and then converted to volumetric water content based on the water (ρ_w) and soil particle density (ρ_s) or the specific gravity ($G_s = \frac{\rho_s}{\rho_w}$). This is done because mass relations are usually more easily available.[18]

$$\theta = \frac{V_w}{V_s} = \frac{M_w}{M_s} \cdot \frac{\rho_s}{\rho_w} = w \cdot G_s \tag{2.8}$$

Similarly, the volumetric gas content (VGC) can be described as the volume of gas over the volume of solids.

$$VGC = \frac{V_g}{V_s} \tag{2.9}$$

2.3. SOIL SUBSIDENCE

In wetlands, two types of subsidence occurs once the area is drained, namely: primary and secondary subsidence. When drained, primary subsidence occurs when the soil sinks under its own weight due to a loss of buoyant force. Secondary subsidence is caused by several processes, such as oxidation of organic material due to microbial decomposition, shrinkage on drying and loss of material by fire [19]. Burning and microbial decomposition are both forms of oxidation, where burning can cause large changes in elevation quickly.

In the period between the 9th and 14th century low polders were reclaimed under the influence of drainage and agriculture [4] .In order to maintain suitable conditions for agriculture drainage is used to keep surface water levels in the polders low, and thus also the groundwater tables [20]. The drained area causes primary subsidence. In time, this cycle repeats itself, surface water levels must be lowered again to once again maintain agriculture conditions, which ultimately leads to more subsidence of the peat wetlands.

2.3.1. SOIL SHRINKAGE

Soil shrinkage is the loss of moisture in soil, as a result soil decreases its height by subsidence. During soil evaporation, shrinkage can be divided into various phases. The first phase, structural shrinkage, is when the loss of water due to draining of the macropores is larger than the volume changes, so that the soil structure behaves stable. Followed by normal shrinkage, also known as proportional shrinkage, where the volume change caused by shrinkage is proportional to the water loss. The third phase, residual shrinkage, is when the loss of water volume is greater than the total decrease in sample's volume. In the final phase, zero shrinkage, the sample's volume does not decrease any further and a small amount of water evaporates [21]. An example of a typical shrinkage characteristic curve (SCC) with its distinct phases is illustrated in Figure 2.5.

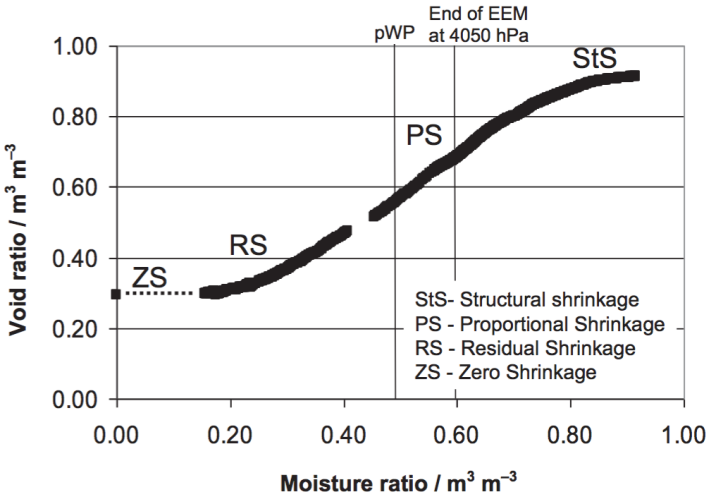

Figure 2.5: Shrinkage Curve Example - Schindler 2015 [21]

2.3.2. ORGANIC OXIDATION PROCESS

Organic oxidation is defined as the loss of organic matter in either gas or in solution and the disappearance of physical structure and change in chemical state. The high organic contents present in peat decomposes if the rate of decay is greater than the rate of addition. Inversely, peat accumulates if the rate of decay is slower than the rate of addition. Oxidation of organic matter is attributed to soil microflora, bacteria and fungi, which are responsible for aerobic decay. The end product results in carbon dioxide and water, which is essentially a biochemical oxidation. Oxidation can be reduced when peat is immersed in water, reducing the supply of oxygen. The reduction of oxygen reduces aerobic microbial activity and encourage anaerobic decay, which is much less rapid. If the conditions are suitable, such as excess of rainfall and the ground is fully drained, then peat is able to accumulate [22].

Besides the oxygen supply needed for oxidation, metabolic activity is greatly influenced by temperature, acidity and the availability of nitrogen. The optimum temperature and acidity for decomposition of organic matter lies in the range of 35-40 °C and pH 7 to 7.5 respectively. Decomposers tend to be most active in neutral to weakly alkaline conditions, thus higher acidity of peat results in greater resistance to decomposition. Nitrogen supply increases the activity of decomposers, i.e. when making garden compost, decomposition is accelerated when nitrogen is added [10].

2.4. ORGANIC MATTER REMOVAL BY CHEMICAL REAGENTS

Removal of organic matter by chemical reagents is a common pretreatment method for analysis of the mineral phase of soils, such as particle-size distribution. The most commonly accepted reagents for organic removal are hydrogen peroxide (H_2O_2), sodium hypochlorite (NaOCl) and disodium peroxodisulfate ($Na_2S_2O_8$). The use of hydrogen peroxide was proposed by G.W. Robinson in 1922 and has become the most widely used chemical reagent for organic matter removal. The remaining two chemical reagents has only been recently applied to soils in an attempt to improve the efficiency of organic carbon removal and to reduce the effects of hydrogen peroxide on minerals. Although, till this day, there is very little consensus regarding the correct protocol for organic removal as well as much uncertainty regarding the effects of oxidative reagents on the soil.

The removal of organic matter is controlled by the reaction conditions (pH, temperature, contact time, chemical additives) and soil properties (minerology, organic matter content and quality). The use of chemical reagents will always be incomplete and the extent of oxidation varies from one soil to another. Factors responsible for the incomplete removal of carbon are the presence of carbonates, the soil reaction, chemically resistant organic compounds and protection of organic matter by mineral surfaces [23].

2.5. CAPILLARITY IN SOIL

Water flows from regions with higher potential to regions with lower potential. The total potential energy of soil water is the sum of three forces: gravity (gravitational potential), the attraction between dissolved ions and water (osmotic potential), and the attraction between the soil particles and the water (matric potential). Where osmotic potential is the least relevant.

Water that drains freely from the soil under the influence of gravity occurs when the cohesive forces between the water molecules exceed the matric forces. As the water drains out of the soil, the matric potential and the total water potential decrease and become negative. The matric forces now exceed the force of the gravity, and in turn the water is held in the soil. The opposite is also possible, where the water rises and is being held above the saturated zone, this is called capillary water. This water is retained in small pores by a negative total potential due to negative matric forces.

This capillarity can be explained by the water-air interaction in soils. The affinity of one fluid for a solid surface in the presence of a second or third fluid or gas refers to wettability. A measure of wettability is the contact angle resting on a solid surface in the presence of another fluid or gas. The interface between the fluid and gas meets the solid surface at a contact angle θ. It is a property related to interactions of solids and a fluid with another fluid or gas, defined as:

$$cos(\theta) = \frac{\sigma_{as} - \sigma_{ws}}{\sigma_{aw}} \tag{2.10}$$

where σ_{as} is the interfacial tension between air and solid, σ_{ws} is the interfacial tension between water and solid, and σ_{aw} is the interfacial tension between air and water. If the angle is less than 90°, the reference fluid, in this case the water, is referred to as the wetting fluid for a given solid surface. If the angle is greater than 90°, then the reference liquid is referred to as the nonwetting phase. Water can either be a wetting or nonwetting fluid depending on the soil minerology. The contact angle for a reference fluid on a solid surface is shown in Figure 2.6.

(a) Contact angle less than 90°

(b) Contact angle greater than 90°

Figure 2.6: Wettability of water and air on a solid surface

Matric suction or capillary pressure refers to the pressure discontinuity across a curved interface separating two fluids, or a fluid and gas in this case. This pressure difference exists because of the interfacial tension present in the fluid-gas interface. The matric suction causes porous media to draw in the wetting fluid and repel the nonwetting fluid and is defined as the difference between the pressure of the nonwetting and wetting fluid. For a two-phase system of water and air, the matric suction ψ is

$$\psi = u_n - u_w \tag{2.11}$$

where u_n and u_w are the nonwetting (air) and wetting fluid (water) pressure respectively. Assuming soil pores have cylindrical shapes, the interface between the two liquids in each tube form a subsection of a sphere. Capillary pressure is then related to the pore radius, contact angle and the interfacial tension between the two liquids. Figure 2.7 models a soil pore as a capillary tube. Capillary stresses can be estimated with the following equation:

$$\hat{P}_c = \rho g d_c = \frac{2\sigma_{aw} cos(\theta)}{r_p} \tag{2.12}$$

where $\hat{P}_c$ is the capillary pressure at air entry, σ_{aw} is the air-entry interfacial tension, θ is the contact angle defined previously and r_p is the tube radius. If capillary pressure, P_c (defined as ψ in Equation 2.11) is larger than $\hat{P}_c$ the air invades the pores. As the soil continues to dry, the water phase becomes disconnected and remains in the form of menisci or liquid bridges at the interparticle contacts. The curved water-air interface produces a pore water tension, which generates interparticle compressive forces.

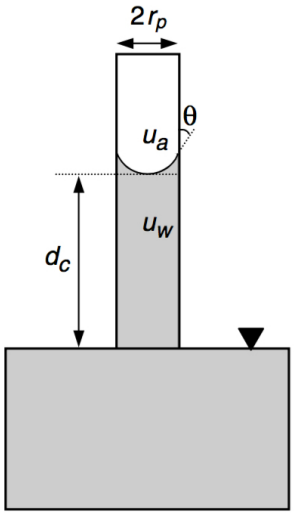

Figure 2.7: Soil pore modelled as a capillary tube [24]

Thus, because water is attracted to soil particles and because water can develop surface tension, suction develops inside the pore fluid when a saturated soil begins to dry. This suction acts like a vacuum and directly contributes to the effective stress.[24]

2.5.1. SOIL WATER RETENTION CURVE

Soils contains a range of different pore sizes, which drains at different capillary pressures as higher air pressure is required for air to enter water-saturated fine-grained soil than course-grained material. This leads to a soil water retention curve (SWRC) which characterises the relationship in which the matric suction is plotted against the volumetric water content. It is a common relationship used in various hydrological and plant-physiological studies to define the unsaturated behaviour of soils.

The curves are determined during air invasion of a water saturated soil sample. As the water content decreases due to evaporation or drainage, the matric suction increases. When water infiltrates into the soil the reverse occurs where the water content increases and the matric suction decreases. However, when rewetting and drying cycles take place, different wetting and drying paths may be distinguished, this is known as hysteresis. This can be caused by the inability of water to escape through smaller openings for larger water-filled pores, the entrapment of air during rewetting of soil or due to irreversible change in soil fabric and shrinkage during drying. Figure 2.8 is given of a soil water retention curve with the aforementioned hysteresis phenomenon.

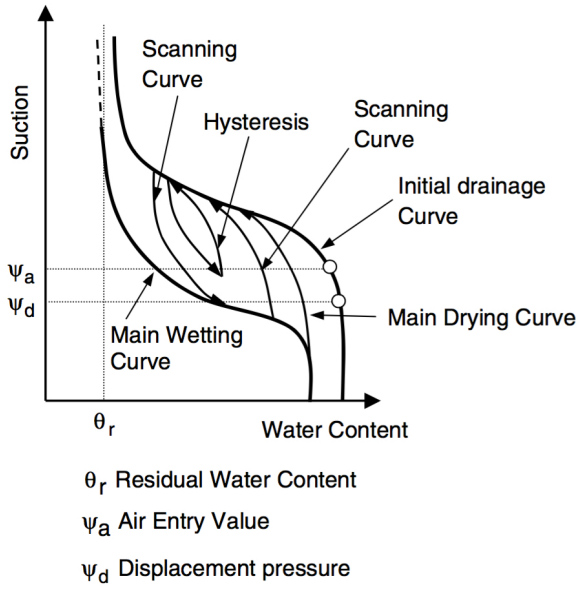

Figure 2.8: An example of a soil water retention curve with hysteresis effect [24]

2.6. RESEARCH CONSIDERATIONS

This literature review gave insight on crucial key theory needed for this master thesis. Although plenty of research have been done of water retention characteristics on a variety of soils, a limited amount of research has been done on studying the water retention and shrinkage behaviour of highly organic dredged sediment. Thus, this thesis will attempt to study these characteristics of highly organic dredged material utilizing the Hyprop and medical CT-scanner, a combination that has not been seen before in past literature. Utilizing the Hyprop on highly shrinkable soils has only recently been carried out by U. Schindler in 2015 [21]. Schindler's method involves using a rubber membrane to support the soil and measures the sample perimeter at a select few locations. Because we are dealing with a dredged sediment, the rubber membrane would not be able to support this soil and the limited amount of spatial measurements would not be sufficient to study shrinkage behaviour. Therefore, it was suggested to use a macro CT-scanner where volume measurements of the soil, air and gas can be accurately measured.

The application of X-ray computed tomography for studying peat has become more frequent in recent years due to its ability to non-destructively visualize a material in high resolution and in 3D. Additionally, the cost of CT-scanners has reduced substantially in recent years making them available to scientists. Hence, lately CT imaging has been used to evaluate three dimensional pore geometry and hydraulic properties in peat. Peatland studies associated with CT imaging are for example visual analysis of entire peat cores for measuring gas content and peat structure (Kettridge [25]) or CT analysis of sub-sample cores maintained at constant hydraulic head by means of twin pressure plates (Rezanezhad [26], [27]) to study the influence of pore size on unsaturated hydraulic conductivity. However, thus far no studies have been carried out involving CT imaging to measure gas bubbles during the dessication process of peat cores. Therefore, CT imaging of organic dredged sediment will be researched to study the effect of gas bubbles on the shrinkage behaviour during dessication.

3

MATERIALS & METHODS

3.1. WORMER DREDGED SEDIMENT

Dredged sediment samples from Wormer & Jisperveld - Depot X was retrieved in 2013, a month after the construction of the depot. The samples were stored in large air tight containers and placed in a 10 °C climate room. The dredged sediment is a thick brown slurry, illustrated in Figure 3.1. Before usage the slurry must be mixed well, to acquire representative samples as the majority of the sediment settled to the bottom. Upon mixing and when air dried a strong odour is released from the dredged sediment. In addition to the dredged sediment, core samples were also taken during a three year period.

A number of classification tests were performed on the material by previous researchers, such as: particle size distribution, hydrometer tests, X-ray defraction (XRD) and X-ray fluorescence (XRF) for the minerology and chemical composition, environmental scanning electron microscope (ESEM) for microscopic imaging of the material, Rock-eval for measuring the amount of carbon, Atterberg limits, water content, fibre content and Loss on Ignition (LoI) for the organic content. Particle size distribution by means of wet sieving and hydrometer tests were particularly difficult to carry out as the majority of the sludge consists of water with little dry solid material. Furthermore, hydrometer tests are usually carried out on samples with little to no organic matter. The large amounts of organic matter in the dredged sediment made hydrometer test very problematic to perform. The accuracy of these two test would mostly likely yield varying results when retested. For this reason it was not repeated. XRD, XRF and ESEM tests also were not repeated, as it is outside the scope of this project. Atterberg limits, water content and organic content tests were performed once again on the original dredged sediment and Hyprop experiments. The ASTM and RAW standards were followed when performing these tests. Atterberg limits of the oxidised material were not performed on as there was limited oxidised material to test on.

The original and retested classification results of the original non-oxidised and oxidised dredged material is listed below in Table 3.1

Properties	Unit	Non-Oxidised	Oxidised
Water Content[1]	%	1296	282
Organic Content	%	51.44	28.10
Mineral Content	%	48.56	71.90
pH	-	7-7.5	2-2.5
Fibre Content	%	15*	7*
Specific Gravity	-	1.8.-1.82*	1.86 - 2.03*
Liquid Limit	%	546	171[2] (270*)
Plastic Limit	%	205 (228*)	127*
Plasticity Index	%	341	143*

Table 3.1: Selected classification properties
[1] = Gravimetric water content
[2] = Estimated - single point measurement
* = Results from N.H.M. Zain [28]

Figure 3.1: Dredged sediment from storage container

3.1.1. OXIDATION PROCEDURE

Oxidised Wormer dredged material was obtained by pretreating the sample with hydrogen peroxide (H_2O_2). Hydrogen peroxide is thermodynamically unstable and decomposes into oxygen and water when added to the dredged material.

$$H_2O_2 \rightarrow \frac{1}{2}O_2 + H_2O \tag{3.1}$$

The surplus of oxygen created by the hydrogen peroxide then reacts with the organic material, or organic carbon(C), which causes rapid oxidation of the organic material.

$$CH_2O + O2 \rightarrow CO_2 + H_2O \tag{3.2}$$

The pretreatment was carried out based on the British Standard 1377-2:1990 [29]. Figure 3.2 illustrates the general procedure for oxidising the dredged sediment.

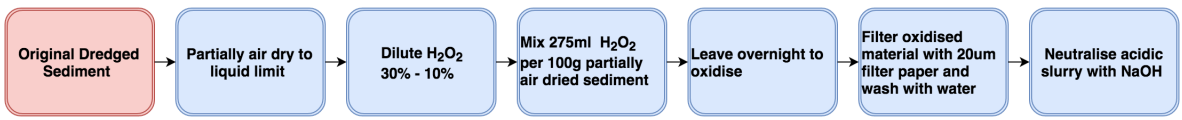

Figure 3.2: Flowchart oxidation procedure

Wormer slurry was temporarily air dried to around the liquid limit (546%), hydrogen peroxide was then slowly added to the slurry while being mixed gently with a glass rod. The amount of hydrogen peroxided needed was calculated based on the total organic carbon (TOC) content per 100g of wet soil. A conversion factor of 1.724 from Schumacher [30] has been used to convert organic matter to organic carbon. There are no universal conversion factors, where conversion factors range from 1.724 to as high as 2.5. The conservative lower boundary conversion factor was taken to ensure that an adequate amount of H_2O_2 was supplied to the slurry. According to Equation 3.2 one electron acceptor O_2 is needed to oxidise the same amount of organic carbon. Thus, if the amount of moles organic carbon is present in 100g of temporarily air dried soil, then the amount of oxygen needed is also known. Equation 3.1 then indicates that twice the amount of moles hydrogen peroxide is needed to supply the electron acceptor. With the amount of moles hydrogen peroxide known, the amount of hydrogen peroxided needed for 100g of slurry is 275ml of a 10% H_2O_2 solution. The calculation method can be seen in Appendix A. Most protocols for sample preparation propose the use of 30% H_2O_2 solutions. Other protocols have suggested 10 and 50% (wt/wt) H_2O_2. McLean [31] has shown that doubling the H_2O_2 concentration from 6 to 12% resulted in little increase in C removal from soils. This suggests that the concentration is not decisive for carbon removal efficiency [23]. Thus, a 10% solution was deemed suitable for the oxidation of the organic carbon. The organic dredged sediment was spread on a tray and was left to air dry temporarily at room temperature of 20-25°C. A fan was used to accelerate the drying process. The desired water content was around the liquid limit of approximately 550%, this was periodically checked with the cone penetrometer test. Batches of 100, 200 and 300g partially dried slurry were oxidated in beakers of 1, 2 and 3L respectively. This is done to ensure that the same process of oxidation was applied consistently. The amount of hydrogen peroxide was scaled according to the weight of the batch of partially dried slurry, 275ml H_2O_2 10% (wt/wt) per 100gr partially dried soil. Immediate frothing occurred when hydrogen peroxide was added. Occasional stirring was done to subdue the excessive frothing. The sample was covered with a watch-glass or a petri dish and left to stand overnight. The lack of visible frothing and bleached soil colour indicated a complete reaction, but frothing may have continued due to the decomposition of excess H_2O_2 at mineral surfaces[23]. Oxidised samples in 2 and 3L beakers can be seen in Figure 3.3

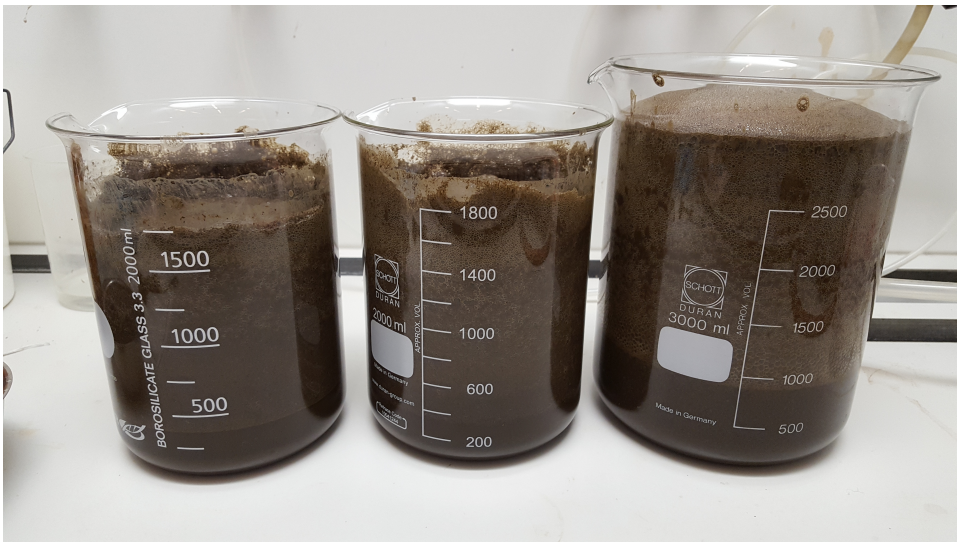

Figure 3.3: Oxidised samples in 2 and 3L beakers

The next day, once the frothing ceased, the oxidised slurry was filtered with the help of a vacuum pump, 20μm filter paper and washed with demineralised water. The pH of the filtered oxidised slurry was then checked with a Consort pH meter. Levels of pH ranged from 2 - 2.5 after oxidation, which is considered to be highly acidic and unsafe to work with. The acidic slurry was neutralised with sodium hydroxide (NaOH 2M) . Small amounts of NaOH 2M of around 1ml was added to the oxidised material and mixed thoroughly. After mixing the pH was rechecked with the Consort pH meter and the process was repeated until the mixture reached safe levels of pH 5.5 - 7. This arduous titration procedure was repeated for the initial few batches to understand its neutralisation behaviour, displayed in Appendix B. The exact amount of NaOH needed for each batch varied slightly, as it was dependent on the amount of oxidised dredged sediment and the initial pH value. However, the amount of NaOH needed was roughly estimated based on previous attempts. Once the pH was neutralised, the oxidised slurry was then ready to be processed for Hyprop experiments and Loss on Ignition (LoI) tests. Preferably, acquiring the Atterberg limits after oxidation was desired, but this was not possible due to the limited amount of oxidised material.

Figure 3.4: Filter attached to vacuum pump

3.2. HYPROP

The Hyprop is a device used to determine the water retention characteristics and unsaturated hydraulic conductivity. The method the Hyprop uses is the extended evaporation method (EEM) developed by U. Schindler in 1980 [32]. The EEM is widely used due to its simplicity, easy computation and small data demand. The pressure head is measured in two depths with miniature tensiometers and the total weights are continuously recorded as the sample desaturates. Water retention curves can then be derived by correlating the soil water tension with the water content and unsaturated hydraulic conductivity is calculated according to Darcy Buckingham's law [33].

The Hyprop consists of the main body, a sampling ring and two tensiometers. The main body, or sensor unit, measures and records the soil water tension and the temperature. All electrical components and pressure transducers are located in the main body. The original Hyprop consists of two metal fastening clips to secure the sampling ring to the main body. The sampling ring is needed to hold the soil in place. The original sampling ring has an inner diameter of 8 cm and a cylinder height of 6 cm. The original Hyprop configuration can be seen in Figure 3.5a.

Two tensiometers are fixed into the main body where the pressure transducers are located. The long and short tensiometers have a length of 50 and 25mm, which protrude into the soil 37.5 and 12.5mm respectively. The tensiometers consist of a porous ceramic tip which allows water to move freely in or out of the tube. As the soil dries out, water inside of the tensiometer's shaft is sucked out through the ceramic tip, creating a vacuum inside of the tensiometer which is read by the pressure transducer in the main body. If the soil is wetted, water will then flow back into the tensiometer and consequently the vacuum decreases and the tension reading is lowered. Measuring limits of the tensiometers are approximately +100 kPa to -85 kPa. Tensiometers can achieve higher tension measurements than their design limit of -85 kPa if boiling retardation occurs in the water of the tensiometers. If boiling retardation does not occur, then air enters the ceramic cups and the tension will drop.

Because the CT-scanner was used on the whole Hyprop device, the majority of the metal components had to be removed from the Hyprop to minimize the amount of artefacts in the CT-images. Thus, the metal fastening clips and metal sampling ring were replaced with a new PVC system. The PVC fastening system consists of a PVC base, two plastic screw threads through the base and a PVC top beam to fasten the Hyprop to the base with 2 plastic screws. The height of the new PVC sampling ring has been extended to 12 cm to prevent punching of the top tensiometer through the soil surface as it shrinks. The new sampling rings are slightly thicker than the original, which results in a slight decrease of the inner diameter, approximately 7.5 cm. The sampling ring is filled with soil up to a column height of approximately 10 cm to prevent spillingn of soil when making CT-scans. Figure 3.5b shows a schematic view of the new modified Hyprop components. In Figure 3.6 illustrates the actual modified Hyprop.

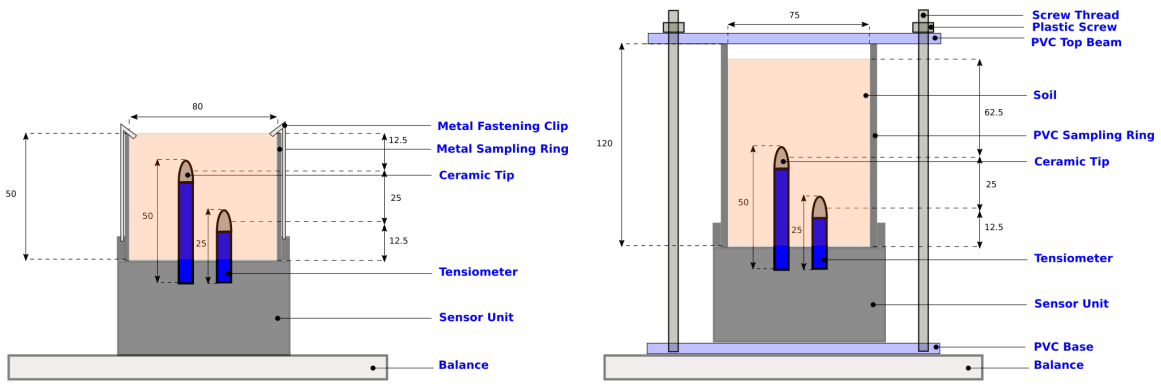

(a) Original Hyprop

(b) Modified Hyprop

Figure 3.5: Schematic view of the original and modified Hyprop

Figure 3.6: PVC Hyprop components

3.2.1. HYPROP PREPARATION

Before carrying out a Hyprop experiment the tensiometers and the sensor unit in the Hyprop's body needs to be filled with demineralised and degassed water. The degassing of the tensiometer and sensor unit was initially done manually with syringes, but later a vacuum pump from the Hyprop's manufacturer (UMS) was acquired and utilised. The tensiometers and sensor units were put under vacuum at a range of 800-1000 hPa, and was left overnight to degas. Once degassed, the tensiometers were removed from the syringes/vacuum pump and the tensiometers were screwed into the shaft of the Hyprop's sensor unit. Paying careful attention not to damage the pressure transducers by exceeding 3 bar of pressure. Additionally, special care was made not to touch the ceramic tips of the tensiometers with the fingers, as grease, sweat and soap residues influences the ceramic's performance. A silicone gasket was then placed on the bottom of the sensor unit to prevent unwanted soil particles entering the sensor unit's shaft. Once the tensiometers and the silicone gasket were assembled to the main body, the ceramic tips were then covered with a rubber cap filled with water to keep the tips moist. The extended sampling ring was then lubricated with silicone grease to prevent slurry sticking to the sides of the ring as it dried. The final step is to add the soil to the Hyprop and fasten it tightly to prevent soil loss. Depending on how liquid the slurry behaved two methods of fastening the slurry to the Hyprop was utilised. If the slurry was pourable, then the sample ring was first fastened to the main body and the slurry was poured into the the Hyprop directly. If the slurry behaved more viscous and less pliable, then the sample ring was placed on a flat tile or plastic cap and filled carefully with a spoon or spatula. The plastic cap was only used once, because it appeared to negatively influence the results. Therefore, it was later replaced with the flat tile. The sensor unit with the tensiometers attached was flipped upside down and carefully placed on the soil sample. The assembly was then placed back upright and the flat tile was slowly slid off the ring or the plastic cap was pulled off. Excess slurry was then removed from the ring untill a column height of approximately 10cm was achieved. The assembly was then fastened with the PVC fasteners, which concludes the assembly process of the Hyprop. CT scans were made after Hyprop assembly. The measuring campaign was then set to start after the initial scan. In some Hyprop campaigns, use was made of an air pump to quicken the evaporation process.

3.2.2. HYPROP TESTS

Previously mentioned in Chapter 1.4, in total four Hyprop tests were carried out to assess the research questions, namely: (1) non-oxidised and undried, (2) non-oxidised and air dried, (3) oxidised and undried and finally (4) oxidised and air dried. Table 3.2 displays the initial water content at the start of the Hyprop test, and the dry solid and organic content determined with LoI tests. For the oxidised tests an air pump (Eheim Air Pump 400) was utilised to accelerate the drying process, evaporation periods would be too long otherwise. Initial experimentation of the air pump was employed for the non-oxidised & undried campaign for a couple of days, but was later switched off. The air pump setup is illustrated in Figure 3.7 for the non-oxidised & undried campaign. Test log of the various Hyprop campaigns can be viewed in Appendix C.

Hyprop #	Initial Water Content[1] [%]	Dry Solid Content [%]	Organic Content [%]
1) Non-Oxidised & Undried	1296	7.16	51.44
2) Non-Oxidised & Air Dried	997	9.12	48.70
3) Oxidised & Undried	282	26.20	28.10
4) Oxidised & Air Dried	172	36.73	29.95

Table 3.2: Selected Hyprop campaign soil properties
[1] = Gravimetric water content

Figure 3.7: Eheim Air Pump 400 setup for the non-oxidised & undried campaign

3.3. MACRO CT-SCANNER

A macro CT-scanner (Computed tomography) uses a motorized x-ray source that rotates around a circular opening, called a gantry. During the CT-scans of the Hyprop, X-ray tubes rotates around the device, shooting beams of X-rays through the soil. The CT-scanners are equiped with special digital X-ray detectors, located directly opposite of the X-ray source. As the X-rays leave the soil, they are then picked up by the detectors and transmitted to a computer. Each time the X-ray source completes a full rotation, a 2D image slice of the soil is constructed. The thickness of a slice can be set by the CT machine and usually varies between a few millimeters. The scanning process is then repeated to produce another image slice, until the desired number of slices are collected. These image slices can be displayed individually in a 2D plane, or stacked together to generate a 3D image of the soil.

Common issues with CT-scans are undesired artefacts in the image slices. There are many different CT artefacts such as noise, ring, beam hardening, scatter, pseudoenchancement, motion, cone beam, helical, out of field artefacts and metal artefacts. In depth knowledge of all these artefacts are outside the scope of this thesis. However, discerning the major influence of artefacts in the CT-scans is of importance. In this case, metal components in the Hyprop causes significant amount of artefacts in the CT images. These metal components causes beam hardening and scatter artefacts on the CT images, discernible by dark streaks between two high attenuation objects such as metal. A high attenuation object is presented as white on an image, due to absorption of X-ray photons. Beam hardening can be explained as the loss of X-ray energy more quickly as it passes it through metal , where scatter is caused by X-ray photons to change directions and thus end up in a different detector [34]. An example of beam hardening and scatter can be seen in Figure 3.8.

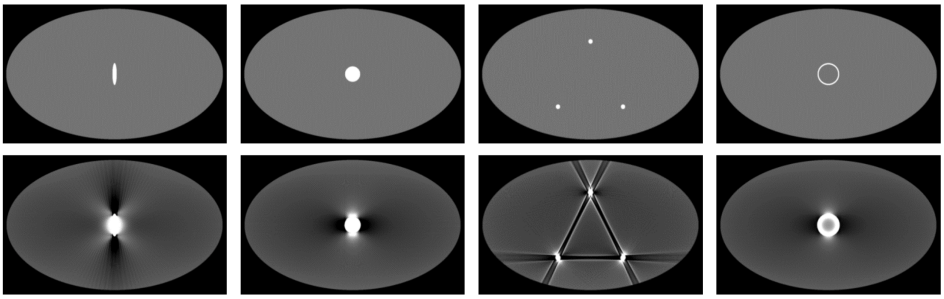

Figure 3.8: Beam and scatter effects - F.Boas [34]

For the Hyprop experiments, the CT-scanner was used once to three times a week. CT-scans were made of the Hyprop devices while their campaigns were still running. The Siemens Somatom Definition CT-Scanner was used for the experiments at the Geoscience & Engineering laboratory of TU Delft. Voxel size of the CT images were 0.4 x 0.4 x 0.6 mm with a voxel resolution of 512 x 512 x 512 in a local 3D (XYZ) coordinate system. Other scan settings were:

Beam Type	Spiral
Voltage	140 kV
Electric Current	250 mAs
Slices	0.6 mm
Pitch	0.6 mm
Rotatation Time	0.5 s/rot
Scan Time	4.44 s
Kernel	B50f
Field of View	150 mm

Table 3.3: Macro CT-Scan Settings

4

DATA PROCESSING

This chapter shall describe the methods used to process the data acquired from the Hyprop campaigns and the CT-scans. Raw data acquired from the two test methods must be processed in such a way to make the results presentable for final analysis.

4.1. HYPROP DATA

The Hyprop generates a substantial amount of data during the course of the experiment. Output data that the Hyprop registers are the time, tension measurements, gross weight and the temperature of the soil. Four Hyprop campaigns have been carried out, namely: (1) Non-Oxidised & Undried, (2) Non-Oxidised & Partially Air Dried, (3) Oxidised & Undried and (4) Oxidised & Partially Air Dried.

Data processing procedure for the Hyprop is divided into the weight measurements and tension measurements. Processing procedure for the weight and tension measurements includes determining net weight of the soil and applying correction methods for negative initial pore water tension.

4.1.1. WEIGHT MEASUREMENTS

The Hyprop is placed on a balance and the weight is constantly measured as the Wormer dredged sediment evaporates. Consequently, the weight of the Hyprop and its components must also be registered to attain the net weight of the soil. The various components of the Hyprop consist of: the body of the Hyprop without the metal fastening clips, the tensiometers, silicone ring and the soil fastening system. The soil fastening system consists of the PVC sample ring, 2 plastic screws, the PVC base, PVC top beam and 2 plastic screw threads. Weight of the components for each Hyprop experiment are listed in Table 4.1.
To obtain the net weight of the soil, the gross weight that the Hyprop measures was subtracted by their corresponding components.

Components	Unit	Hyprop 1	Hyprop 2	Hyprop 3	Hyprop 4
Body (without metal fastening clips)	[g]	328.91	328.23	328.04	329.01
Long and short tensiometers	[g]	1.89	1.58	1.58	1.58
Silicone ring	[g]	7.07	7.08	7.03	7.03
Fastening system	[g]	440.25	453.11	440.27	453.11

Table 4.1: Weight properties of Hyprop components
Hyprop 1 = Non-oxidised & undried campaign
Hyprop 2 = Non-oxidised & partially air dried campaign
Hyprop 3 = Oxidised & undried campaign
Hyprop 4 = Oxidised & partially air dried campaign

4.1.2. TENSION MEASUREMENTS

A number of measures had to be taken to process the tension measurements due to the difficult nature of the dredged sediment and the preparation method of the experiment. The first problem observed while running Hyprop campaigns are the initial negative tension measurements. Based on existing literature, very little Hyprop tests were carried out on shrinking soils and soils exceeding liquid limit. For this study, the non-oxidised slurries in the Hyprop campaigns had approximately exceeded more than twice the liquid limit. Initial tension measurements for the non-oxidised cases were generally around hydrostatic pressure based on the slurry column height in the sample ring. In Figure 4.1 an example is given of the negative initial tension encountered for the non-oxidised undried campaign. The figure shows an initial negative tension of around 10hPa, which coincides with the hydrostatic pressure of the initial slurry column height of 10cm. Negative tension is slightly greater than 10hPa due to lack of Hyprop calibration for this campaign.

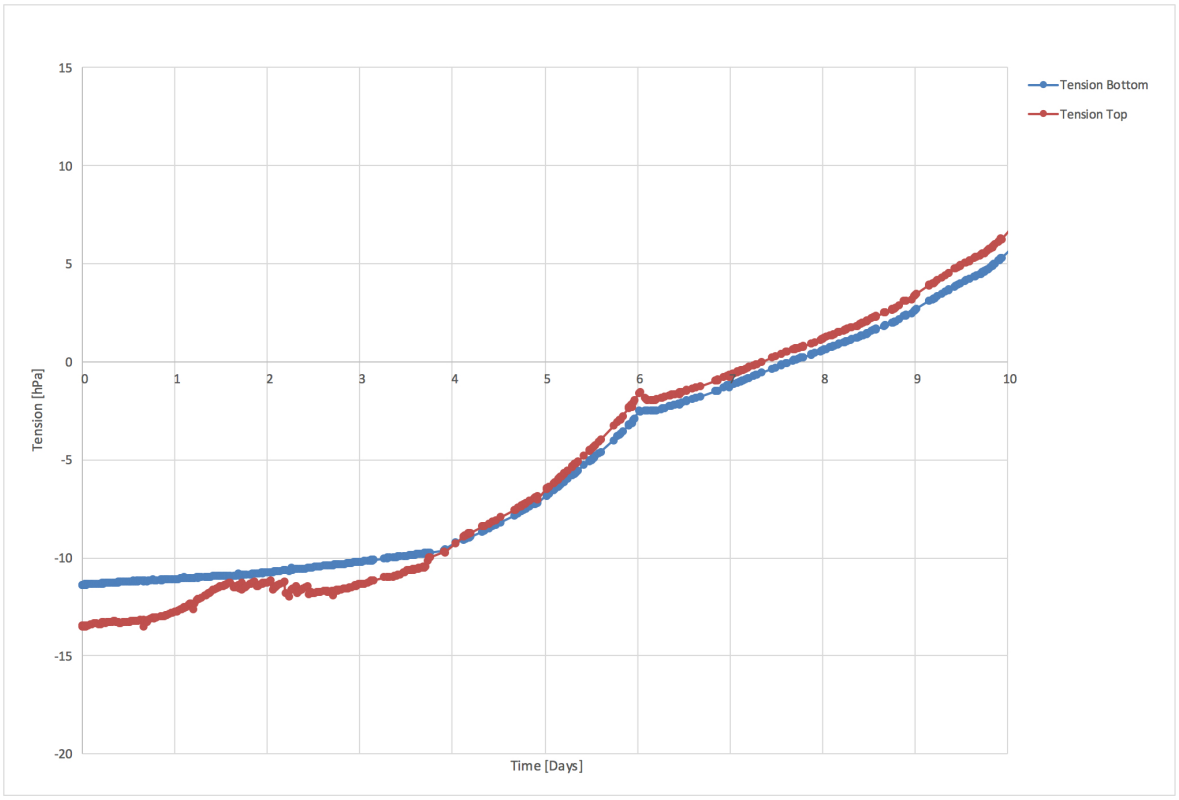

Figure 4.1: Non-oxidised undried campaign - Displaying negative initial tension

These negative tensions are unwanted primarily because it gives a false image of suction development in the early stages of the tests. According to Figure 4.1 positive tension would only have taken place after 7 days of the test. While in reality, during this period tension build up must have taken place as well. Additionally, negative tension is unwanted because it complicates further analysis of the results, where these results are ideally displayed in log scale. The negative tension was corrected by essentially "lifting up" the values according to the initial slurry column height and by associating the loss of slurry column height to positive tension. Correlating the loss of slurry column height to positive tension is done under the assumption that in the initial stage of evaporation there is only vertical shrinkage. The volumetric shrinkage is then equal to the change of height multiplied by the surface area. Therefore, the change in slurry column height results in the decrease of hydrostatic pressure or an increase of tension [35]. Figure 4.2 illustrates the result of implementing the corrections. For this case, initial values are still negative due to calibration errors of the original measurements. Slurry column height was around 10 cm, and was "lifted up" for 10 hPa. Hence, the initial values are still negative. This correction is only noticeable for the early stages of the experiment and minimally influences remainder of the measurements. The following case will show a more accurate correction where the Hyprop was calibrated beforehand.

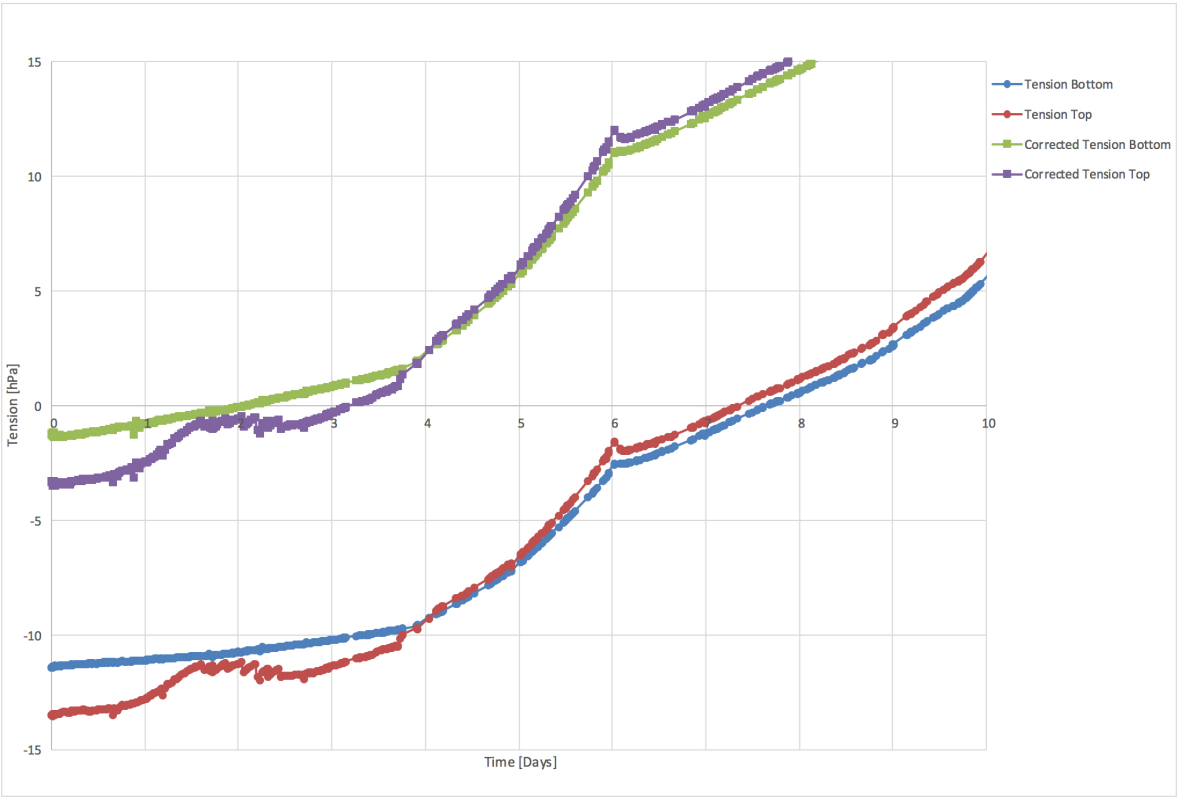

Figure 4.2: Non-oxidised undried campaign - Original vs corrected tension measurements

The second issue encountered were erratic initial tension measurements caused by the assembly method of the Hyprop. An example of this is shown in Figure 4.3. For this test calibration did occur beforehand, evident by the bottom tensiometer. This tensiometer shows negative initial tension expected from a 10 cm slurry column, i.e. 10 hPa hydrostatic pore pressure. However, the top tensiometer displays high initial tension of 30hPa. Unlike the first campaign, non-oxidised and undried, where the dredged sediment was poured into the sample ring. This method caused no disturbance during the assembly of the Hyprop. In this case, the partially dried sediment was too viscous to be poured into the sample ring. As explained in Chapter 3.2.1, assembly of the Hyprop involved placing the sample ring on a flat tile and the ring was carefully filled with slurry using a spoon and spatula. For this test, the plastic cap was used instead of the flat tile. The Hyprop's sensor unit with the tensiometers attached was then flipped upside down and carefully placed on the soil sample. The full assembly was then placed back upright and the plastic cap was subsequently pulled off. This pulling motion of the cap caused a vacuum disturbance in the soil, resulting in the positive initial tension. To prevent this disturbance for future tests, the cap was then replaced with a flat tile.

Once again the two correction methods were applied, namely: "liftup" of the measurements based on the initial slurry column height and correlating the loss of slurry column height to positive tension. The corrected measurements can be seen in Figure 4.4. Here the corrected measures removes the majority of negative tension due to pre-calibration.

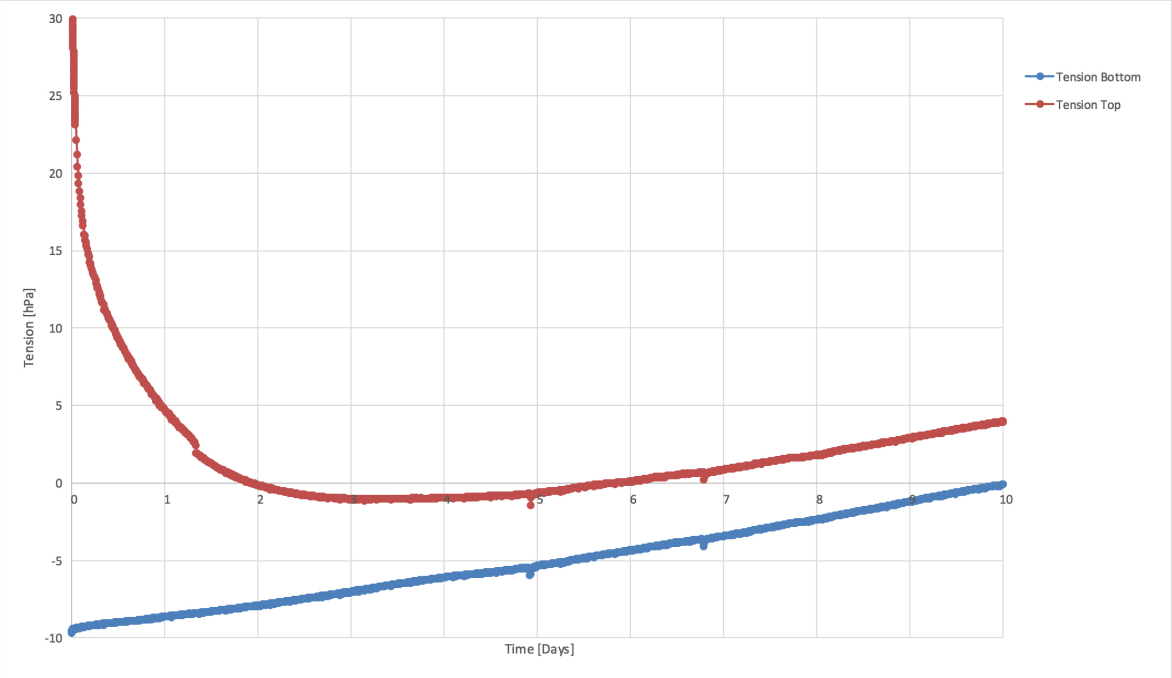

Figure 4.3: Non-oxidised partially air dried campaign - Irregular initial tension measurements

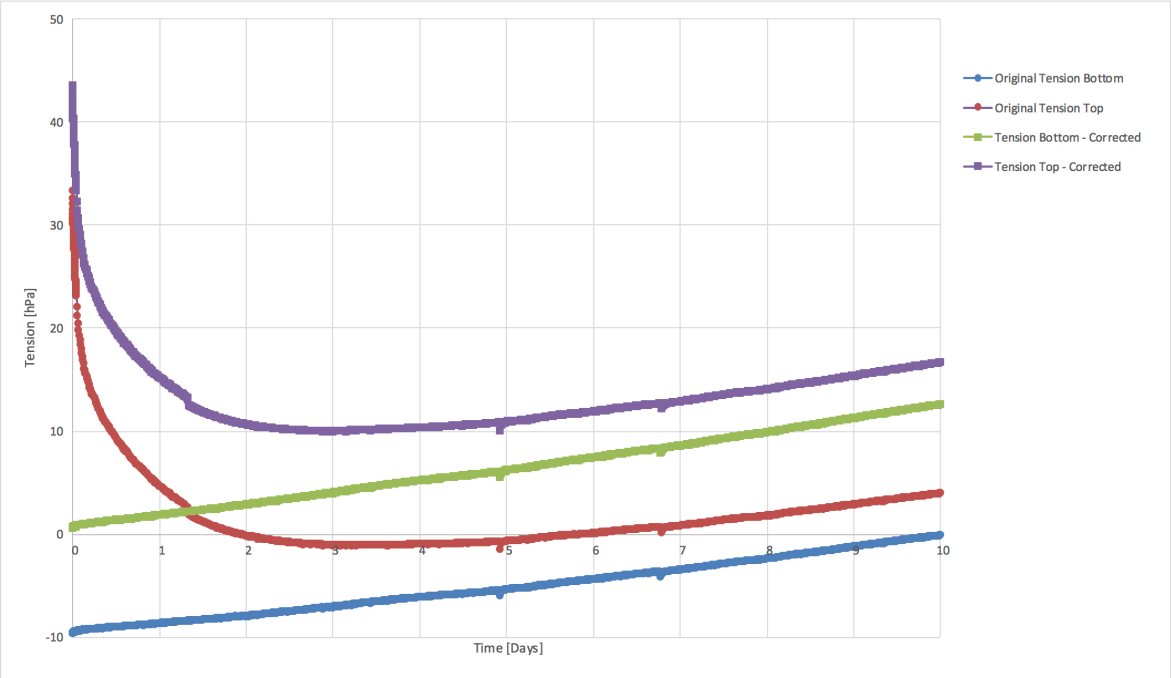

Figure 4.4: Non-oxidised partially air dried campaign - Corrected measurements by extrapolating and removing negative tension

These correction methods were consistently applied to the other tests. For the oxidised campaigns more assembly disturbances were encountered when connecting the sensor unit to the sample ring. Initial water content for the two tests were much lower, causing the dredged sediment to behave much stiffer during the penetration of the tensiometers into the soil. For non shrinking soils, the usual method is to use an auger to drill a hole for the tensiometers. But, due to the wet soil with water contents above the liquid limit the auger was not used, as the drilled hole would collapse back immediately.

Figure 4.5 shows the stiff response the bottom tensiometer experienced when penetrating the oxidised soil. A resistance of -35hPa occurred for the bottom tensiometer as it penetrated the soil, followed by a sudden vacuum surge till 10hPa shortly after. The sudden surge in tension could have been caused by the removal of the flat tile, but it does not explain why the top tensiometer did not behave the same. Possibly an adverse effect to the initial pressure (or negative tension). For the top tensiometer the initial tension was 0hPa. This slowly equalized after a day of evaporating, emphasizing the disturbance caused by the assembly procedure. The same amount of time was needed for the bottom tensiometer to equalize. Correction procedure was applied once more to remove the majority of negative tension.

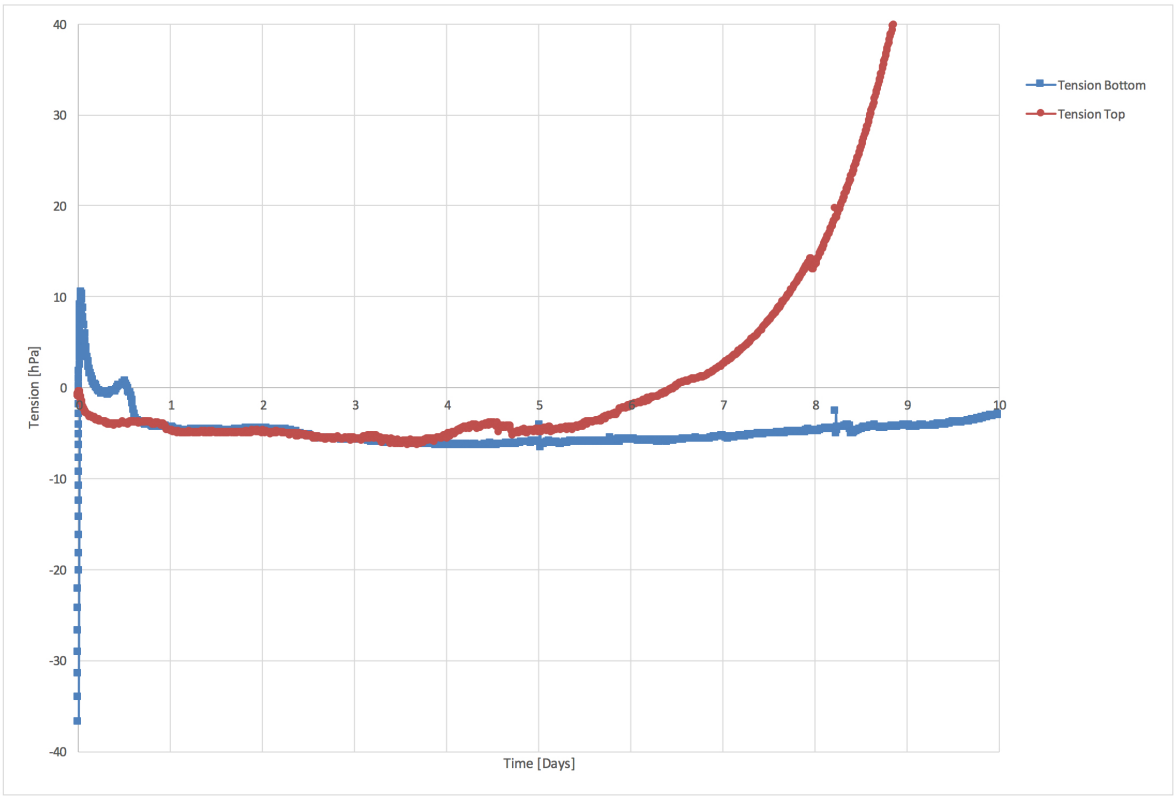

Figure 4.5: Oxidised undried campaign - Irregular tension measurements due to Hyprop assembly

4.2. HYPROP DATA TO SOIL WATER RETENTION CURVE

From the data acquired from the Hyprop, the soil water retention curve (SWRC) can be constructed using the net weight of the soil and the corrected tension measurements. The soil's water retention behaviour is described by plotting the water content over the matric suction. Explained previously in Chapter 2.2.3, water content can be expressed gravimetrically or volumetrically. Throughout this thesis, the gravimetric and volumetric water contents were used interchangeably, depending on context. Gravimetric water contents were used for initial characterisation of the soil and the volumetric water contents were used to construct graphs, such as as the SWRC and the SCC.

Net weight measurements were used to calculate the gravimetric water content ($\frac{M_w}{M_s}$). Total soil water content at the beginning of the evaporation experiment was calculated by summation of the amount of water evaporated during the Hyprop test with the residual amount of storage water derived from the water loss on oven drying (105 °C). Mass of water per time step can then be computed by subtracting the total amount of water from the evaporated weight change during the Hyprop test. Mass of solids was computed from the residual weight after oven drying and was considered to be constant during evaporation, thus assuming no loss of organic material. Gravimetric water content was then computed by dividing the mass of water corresponding to each time step by the constant mass of solids. Subsequently, the volumetric water content was determined by multiplying the gravimetric water content with the specific gravity. The volumetric water content was then plotted over the corresponding tension measurements to obtain the SWRC.

4.3. CT IMAGE PROCESSING

A CT scanner produces cross sectional images, or slices, of the object. The CT data is then processed in Avizo 9.0, a 3D image analysis software that translates the images into voxels. The CT data can then be constructed into 3D images or into individual orthogonal slices (ortho slices). Ortho slices are illustrated in grayscale, where differing densities can be distinguished. The slices can be viewed singularly in various planes (i.e. XY-, YZ- and ZX plane) or simultaneously within a single viewer. The purpose for the CT-scans are to acquire a set reconstructed images of the soil's desiccation process and to calculate the volume of the soil as it shrinks in the Hyprop.

The processes continuously applied when analysing the CT-scan data from the Hyprops were: Interactive Thresholding, Volume Edit, Separate Objects, Image Segmentation, Generate Surface and Label Analysis. The order of these processes are illustrated in a flowchart in Figure 4.6. For every Hyprop dataset the analysis is divided into portions, namely: the soil and water portion of the analysis and the gas portion. Evident in the flowchart is that the two portions have a varying analysis procedure.

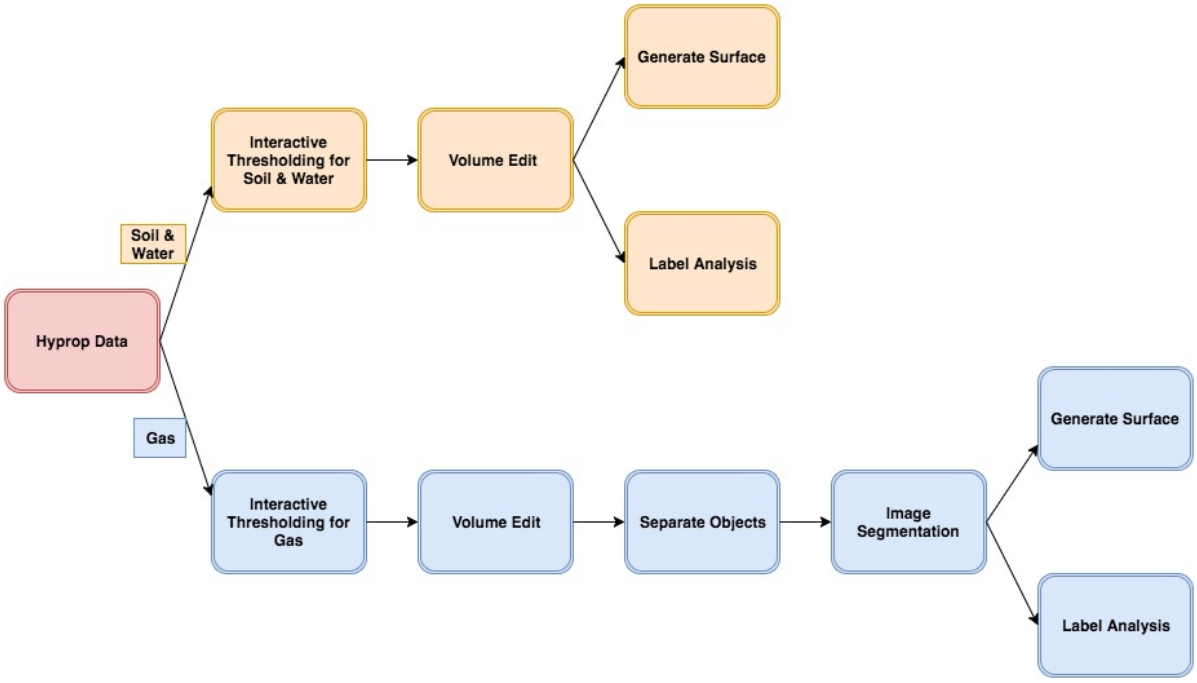

Figure 4.6: CT-Images processing steps in Avizo

Interactive Thresholding module is a binary level of analysis and is the first step of the data processing procedure. The interactive thresholding module transforms a gray level image into a binary image by means of detection, where the pixels of a specific gray level interval are isolated and stored separately. This is called binary, because the threshold criterion determines if a pixel is of binary value 1 or 0. Subsequently, the newly formed image consist solely of pixels having a value 1 or 0. To process the CT-data, the interactive threshold is set to two criterias. The first is to only isolate the soil and water, displayed in Figure 4.7a and 4.8a. Figure 4.7a displays CT-imagery histogram of the non-oxidised & air dried Hyprop campaign, with the voxel distribution on the vertical axis and the voxel intensity on the horizontal axis. The highlighted area indicates the chosen threshold values. Figure 4.8a displays the thresholded area in an image slice, highlighted in blue. The second criteria is to threshold solely the gas, indicated in Figure 4.7b and 4.8b.

The separation of materials is based on density dependent attenuation of X-rays, where CT imagery visualizes greater density as lighter gray scale colours and lesser density as darker gray scale colours. Attenuation is defined as the reduction in intensity of X-ray beams as it traverses matter either by absorption or deflection. Solid and liquid fractions of the histograms were not separated, as there is currently no effective way to segment out the soil from the surrounding water. Mineral solids and organic compounds are also not discernable from each other. The selected threshold area is determined visually with Avizo. Because separation of the soil is based on density, the threshold criteria differs as desiccation of the soil takes place. Bulk density increases as soil

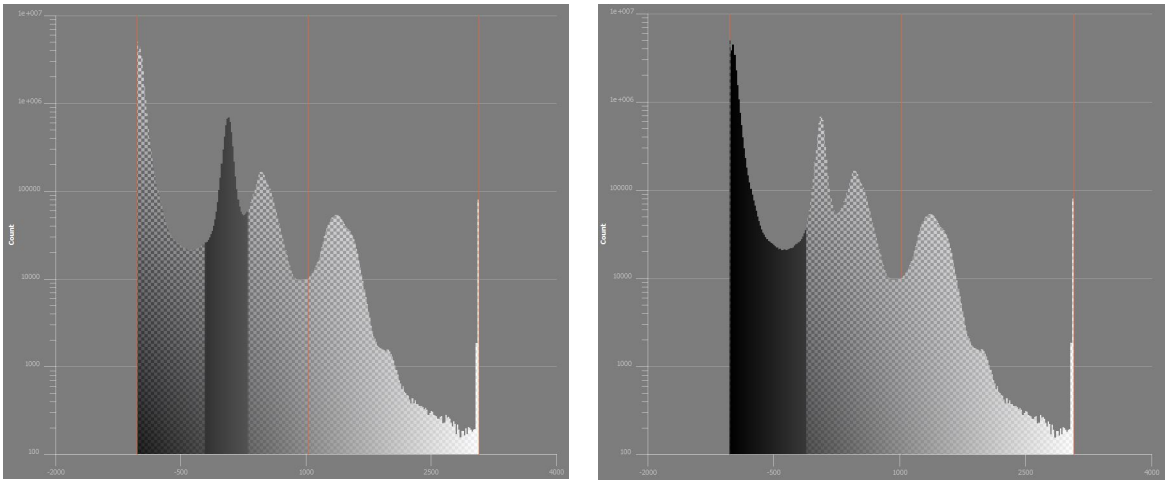

(a) Thresholded area for soil and water

(b) Thresholded area for gas

Figure 4.7: Histogram with their selected threshold area for the non-oxidised & air dried Hyprop campaign

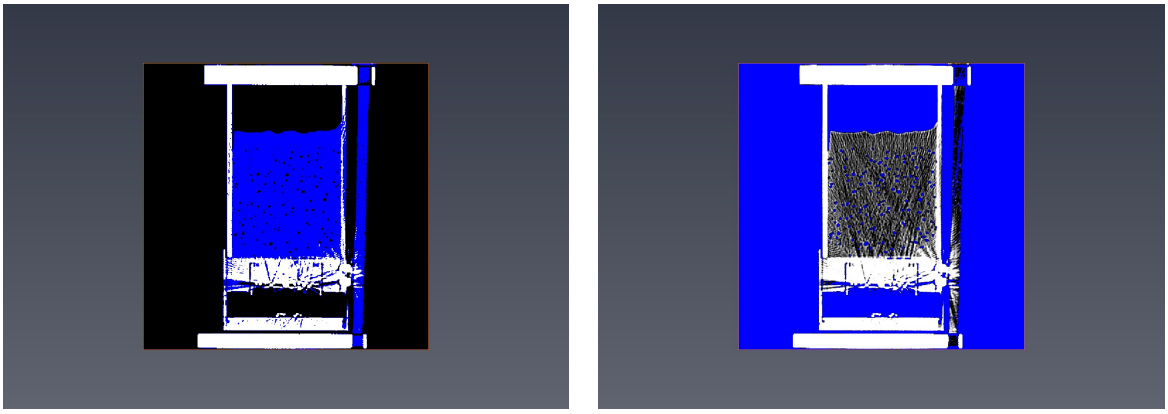

(a) Selecting the soil and water

(b) Selecting the gas

Figure 4.8: Isolating the gas from the soil and water with interactive thresholding for the non-oxidised & air dried Hyprop campaign

Once the binary image is obtained, then undesired objects such as the Hyprop device or surrounding air are removed with the Volume Edit module. This module provides tools, e.g. the draw tool, for interactive modification of 3D image volumes. The draw tool was used to encircle a specific region, followed by removing the not encircled (exterior) region, indicated in Figure 4.9 for both processing phases.

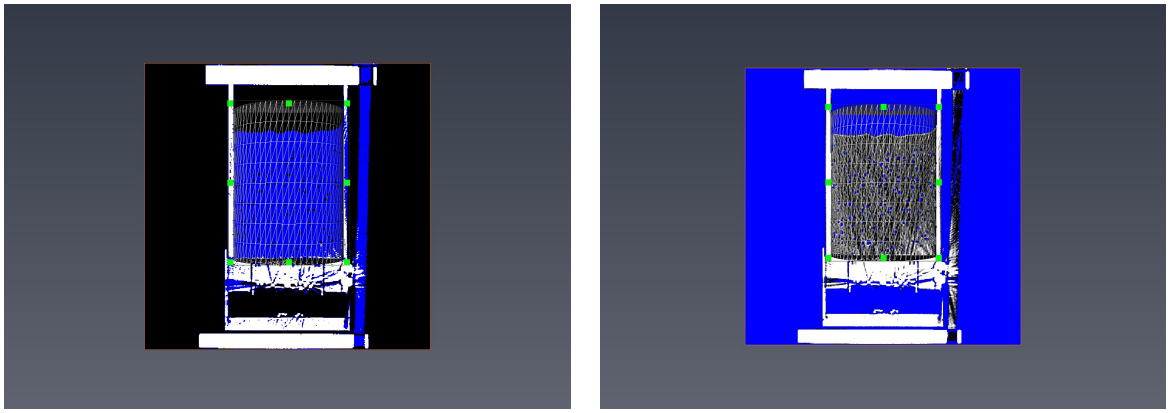

(a) Separating undesired objects from the soil and water (b) Separating undesired objects from the gas

Figure 4.9: Volume edit for both phases

From this point onward, the analysis procedure differs. The soil and gas phase is basically over, all that has to be done from this point onward is to create a 3D image with Generate Surface module and to calculate the volume of the soil and water with the Label Analysis module. Generate Surface is used because smoothing of the 3D image is possible with this module. The Label Analysis module computes a group of measures on each cell or connected component of the input image, and generates a spreadsheet with the result values. For our case, the Label Analysis is programmed for calculating the bulk volume of the selected criteria based of Interactive Thresholding. The generated surface of the soil and water phase is seen in Figure 4.10. These last two steps ends the data processing for the soil and water phase.

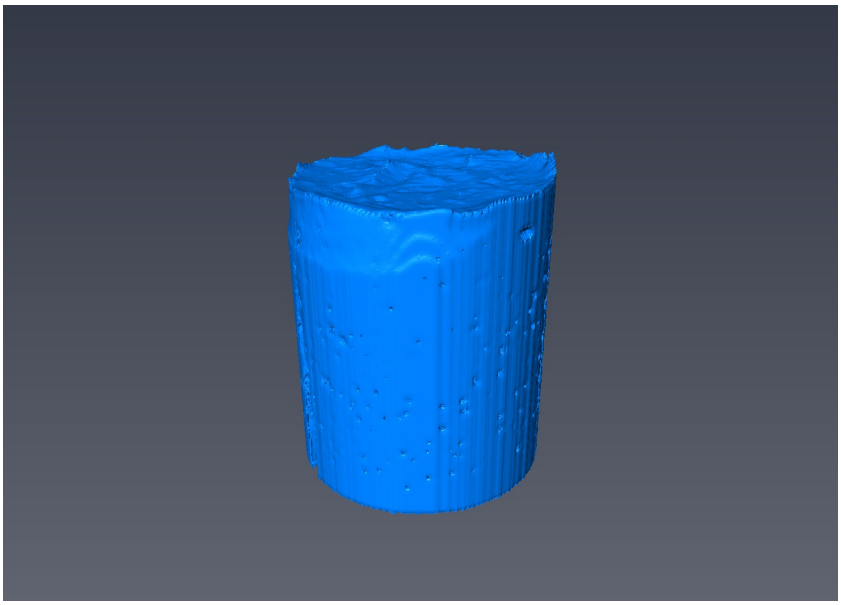

Figure 4.10: Generated surface of soil and water

Back to the gas phase, the subsequent module applied after Volume Edit is the Separate Objects module. This module is needed because some gas bubbles appear to be touching, but ideally should be separated for proper analysis. The connecting particles are due to the resolution being too low to distinguish the objects' boundaries. Interactive Thresholding cannot avoid this type of output when the CT-data is too coarse or noisy, thus Separate Objects module is used to separate connected particles. Once the Separate Objects module is applied then manual image segmentation was carried out. This involved manually removing as much artefact

errors caused by the metal disturbance of the Hyprop device. Secondly, manual image segmentation was needed to remove any unwanted objects (such as surrounding air) that the Volume Edit failed te remove. Finally, image segmentation was also used to differentiate between gas completely enclosed by the dredged sediment and cavities exposed to the atmosphere. The segmentation of artefacts from the gas can be seen in Figure 4.11, indicated with the salmon colour.

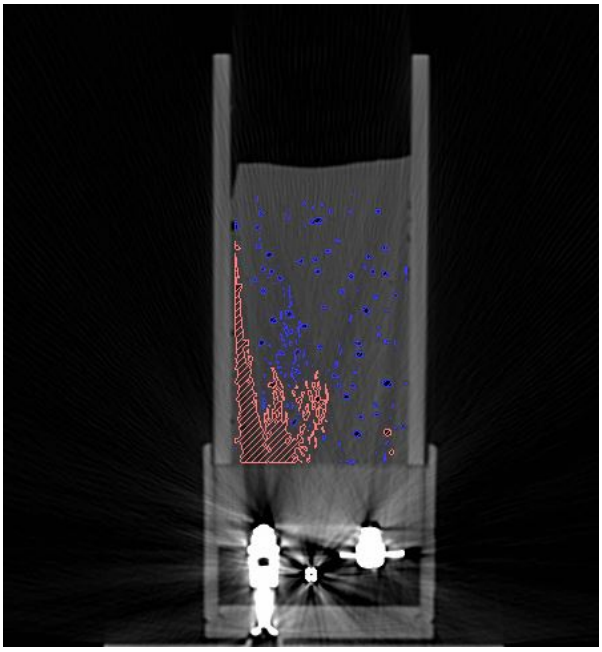

Figure 4.11: Manual removal of artefacts

Once the artefacts and exposed caveties separated then two previous steps are once again applied: Generate Surface and Label Analysis. The Generate Surface result of the gas is shown in Figure 4.12, with the blue and the salmon colour indicating the entrapped gas and artefacts respectively.

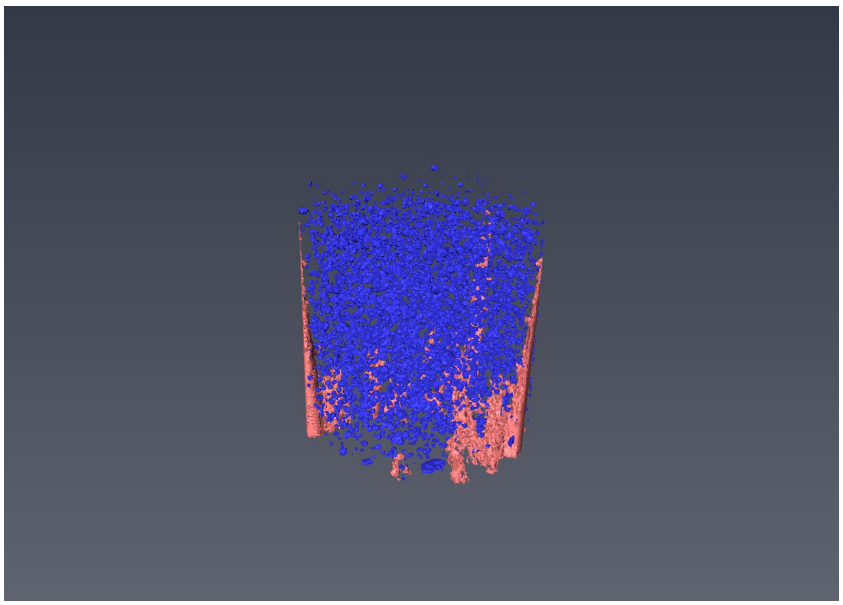

Figure 4.12: Generated surface of the entrapped gas and artefacts

The final steps are to overlap the two generated surfaces over each other. The colour of the generated surface is first changed to a transparent shade, illustrated in Figure 4.13. Now the two surfaces can be overlain, resulting in the final 3D image. This is demonstrated in Figure 4.14. The overall process is repeated for all Hyprop CT-scans.

(a) Original generated surface of soil and water

(b) Transparent generated surface of soil and water

Figure 4.13: Altering the shading of the generated surface

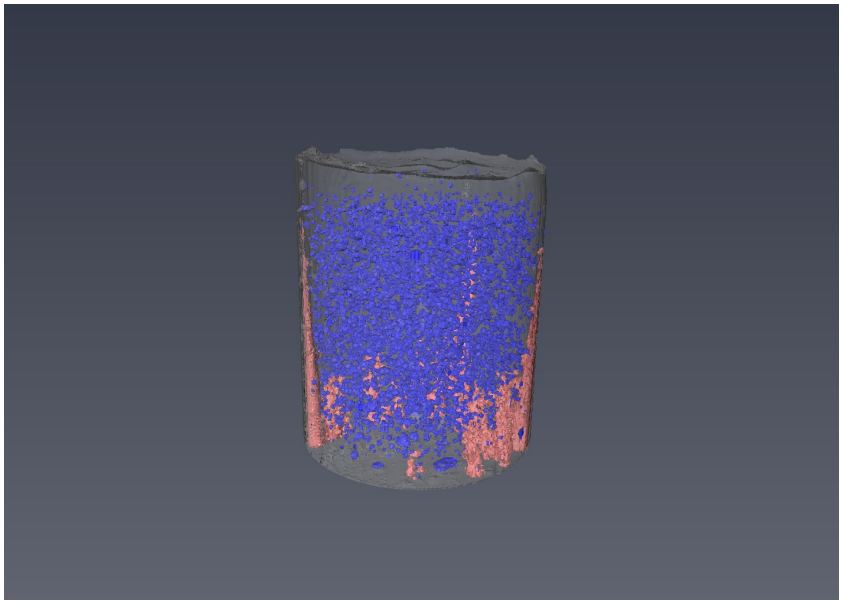

Figure 4.14: Final image of combining Figure 4.12 and Figure 4.13b

4.4. HYPROP AND CT DATA TO SOIL SHRINKAGE CURVE

The combined data from the Hyprop and the CT-scans resulted in the soil shrinkage curve (SCC). The SCC was constructed by plotting the void ratio over the volumetric water content. Volumetric water contents were computed as previously described in Chapter 4.2. The void space is defined as the water and air phase of the soil. Water volume was derived from the water mass of the soil during evaporation and the gas volume was computed from the CT-scans. For the SCC the total amount of gas and air is considered, since air entry points are key characteristics for shrinkage curves. The SCC is dependent on the gas volume measurements, as such data points were limited to the number of CT-scans. As a direct result, the SCC was not as continuous as the SWRC. Calculation sheet concerning the SCC is illustrated in Appendix D. Here the various volume measurements are displayed, which are needed to calculated various ratio values for the SCC.

5

RESULTS & ANALYSIS

5.1. INTRODUCTION

The previous chapter presented how the data acquired from the Hyprop and CT-scans were processed. The Hyprop data involved applying correction methods to irregular initial tension measurements caused by the modified Hyprop assembly procedure and the unique characteristics of the dredged sediment. Processing the CT-scan data with Avizo composed of isolating the gas fraction from the soil and water fraction, removing any unwanted objects (Hyprop device, surrounding air and artefacts), creating a complete 3D image and finally carrying out a volume analysis of the gas phase and the soil and liquid phase. The results of the Hyprop and the volume measurements from the CT-scans will be combined to produce various graphs, such as the shrinkage and water retention characteristics. The results of these curves and the 3D images generated with Avizo will be analysed in depth in this chapter. Additionally, the results from the core samples are discussed as well.

5.2. CORE SAMPLE ANALYSIS

Core samples were taken from the depot and were measured for their gravimetric water and organic content. Results are displayed in Appendix E. From the results we see that a substantial amount of water was lost over the years. Gravimetric water content averaged over the core sample's depth from March 2014 was approximately 1730%, and the latest measurement from August 2016 indicated a gravimetric water content of roughly 550%. While there was steady loss of water from the depot, the organic content appeared to have increased marginally from 53% to 57% averaged over the core sample's depth. Visually, immense amount of plant growth was noticeable, which will contribute to increased soil strength.

5.3. HYPROP

The Hyprop registers the soil tension, gross weight and the corresponding time in short intervals. These values of the various campaigns can be presented together in graphs. Soil properties of the Hyprop campaigns are represented in Table 3.2. In absolute terms the mass balance composition of the slurry for the various tests are presented in Table 5.1. Images of the dredged sediment after the Hyprop experiment are illustrated in Appendix F. This section shall interpret the results of the direct output of the Hyprop experiments.

Hyprop #	Total Water [g]	Water Evaporated [g]	Solids [g]	Organic [g]
1) Non-Oxidised & Undried	445.33	429.07	34.37	17.68
2) Non-Oxidised & Partially Air Dried	436.48	411.29	43.79	21.33
3) Oxidised & Undried	375.77	339.07	133.41	37.49
4) Oxidised & Partially Air Dried	337	280.16	195.60	58.88

Table 5.1: Mass composition of dredged sediment during tests

Figure 5.1 illustrates the weight change of the soil column due to evaporation over time. More or less linear evaporation rates are prevalent for all instances. The non-oxidised undried campaign shows a sudden

increase in evaporation rate from 9.1g/day to 43.9g/day. This was caused by utilizing an air pump (Eheim Air Pump 400) for approximately two days. Later it was decided to turn the pump off and let evaporation occur naturally. If the fan was not used for two days, then evaporation was expected to last around 45 days. The non-oxidised & partially air dried sample ran for almost 50 days without the use of a fan. This campaign would have been only slightly longer than the undried sample if the fan was not used. Longer duration of the test is caused by the lower evaporation rate of the partially dried soil. The only varying parameters between the two tests is the amount of moisture in the soil and the amount of solids. Assuming that the rate of evaporation was not influenced by the lowered water content, because both samples were still over-saturated with approximately twice the liquid limit. Which implies that the additional amount of dry solids reduces the evaporation rate. The oxidised samples also shows similar result, where the partially air dried variant has a lower evaporation rate compared to the undried sample. For the oxidised tests, the fan was used for the whole duration of the experiment. Unfortunately the oxidised and non-oxidised tests cannot be compared as their test conditions were not equal.

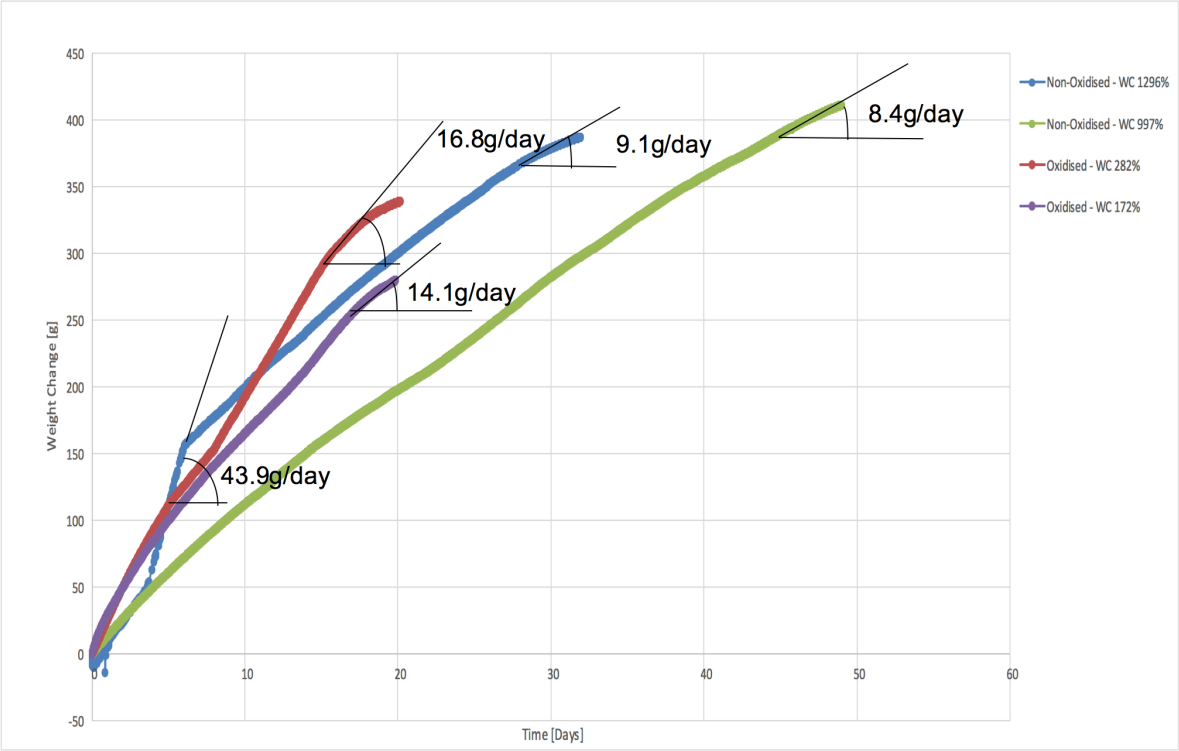

Figure 5.1: Weight change vs time for all Hyprop campaigns

Figure 5.2 displays tension measurements over time of all the Hyprop tests carried out. More or less the same tension shapes are seen in the figure, with a few exceptions for the oxidised samples. The bottom measurements for the oxidised undried variant appears to immediately drop to 0 hPa when air entry takes place. Where usually, air entry occurs followed shortly after by the bubble point which subsequently leads to a complete loss of tension. Other common traits are the long initial periods of little to no tension development. This period varies between 8 to 20 days and is influenced by the initial water content and amount of fines in the soil.
Top measurements experience tension development sooner due to the drying front starting from the surface. Finally, maximum tension peaks decrease with greater initial water contents. The partially air dried samples developed higher tension peaks due to the increasing amount of fine grained solids in absolute sense.

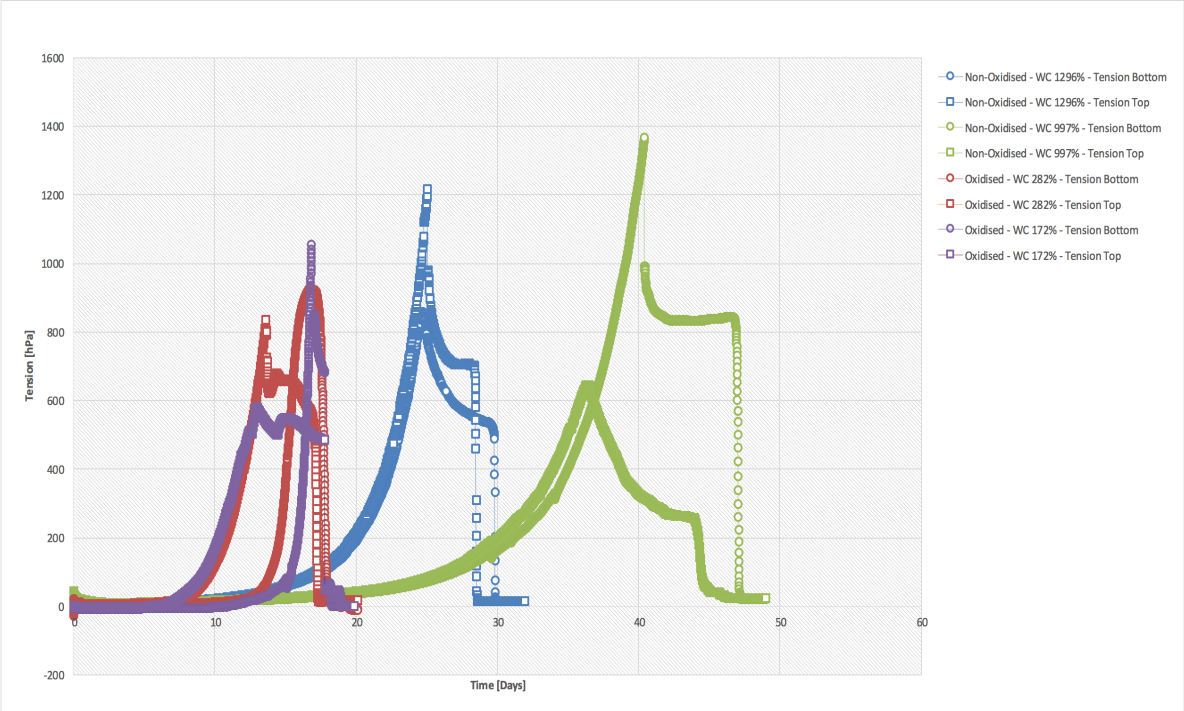

Figure 5.2: Tension vs time for all Hyprop campaigns

The tension vs weight change diagram is illustrated in Figure 5.3. The general shape of the graphs are the same due to the linear evaporation rate. Bottom tensions are generated later in the graphs due to the drying front advancing from the surface downward. The peculiar sudden bubble point of the oxidised undried bottom tensiometer without initial air entry is more visible in this graph. Notable is the large amount of weight loss with minimal suction development. The majority of water evaporated during this period corresponds to the same moderate slopes in Figure 5.2, where 8-20 days little to no tension developed. This indicates a large portion of vertical shrinkage with very little horizontal shrinkage, which is also apparent in the corresponding CT-scans.

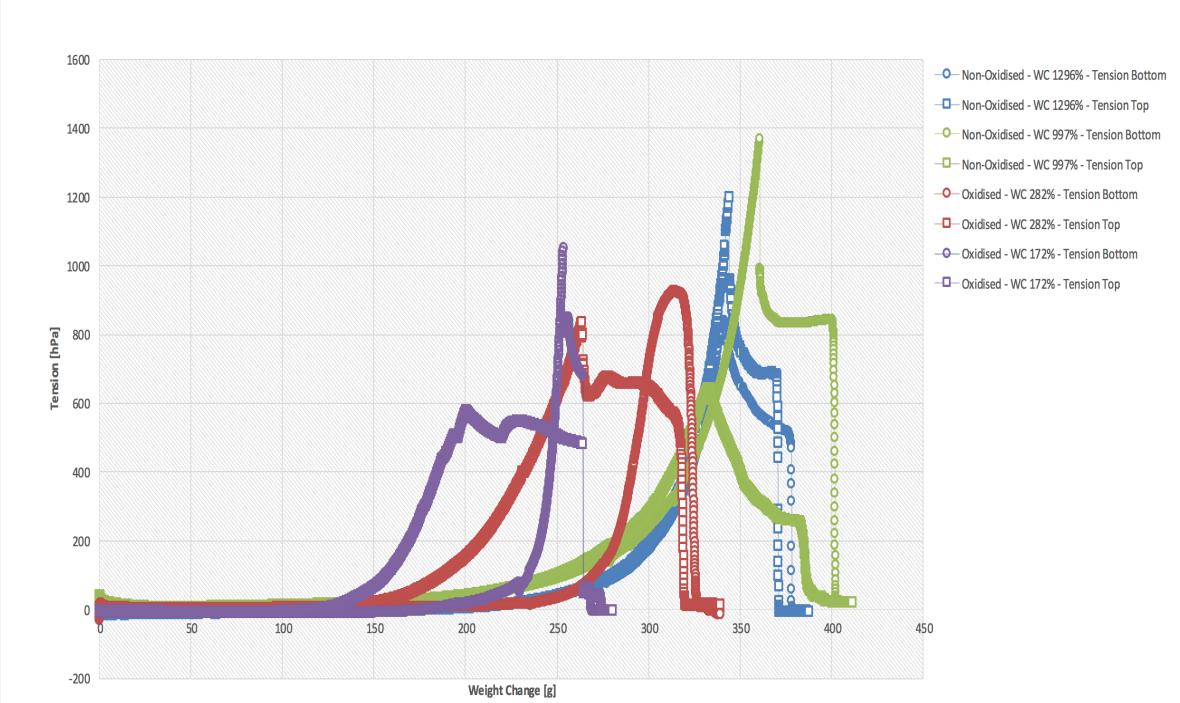

Figure 5.3: Tension vs weight change for all Hyprop campaigns

Figure 5.4 illustrates the soil water retention curve. The water retention curve is plotted volumetrically by converting the mass based water content with the help of the specific gravity G_s. Here can be seen that varying the initial water content for the non oxidised and oxidised samples more or less retains its basic shape for their respective subdivision. Regarding the non-oxidised campaigns, lowering its initial water content appears to slightly change the shape of the function when compared to its undried form. Expected was that the lowered water content would continue along the path of the undried sample, which is apparently not the case. Possible explanation for this is due to the loss of organic matter, approximately 3%, when the sample was partially air dried prior to testing. Hypothesised, is that the partially air dried sample had less organic matter for water to bond on, thus changing its water retention behaviour.
Regarding the oxidised campaigns, the start displays irregular initial values due to the assembly procedure of the Hyprop. Connecting the sensor unit with the tensiometers to the soil caused excessive initial tension to build up, which would dissipate after a couple of days and then follow its regular path. Illustrated with the dashed lines, the liquid limit of the oxidised campaigns decreased significantly, caused by the loss of organic material and the broken down structure of the oxidised soil. Hence, the soil's ability to retain water is greatly reduced when oxidised. Furthermore, removal of organic matter appears to significantly change the path of the water retention function. However, when lowering the initial water content the curve then follows the same path of its oxidised counterpart.
Thus, the soil water retention curve illustrates that varying its initial water content barely influences the shape of the function. The samples within their respective subdivision, with a lower initial water content wants to follow the path of its undried counterpart, with slight variations due to loss of organic material due to natural drying. Significant removal of organic matter through chemical oxidation greatly reduces the soil's ability to retain water and changes its water retention behaviour when compared to the non-oxidise samples.

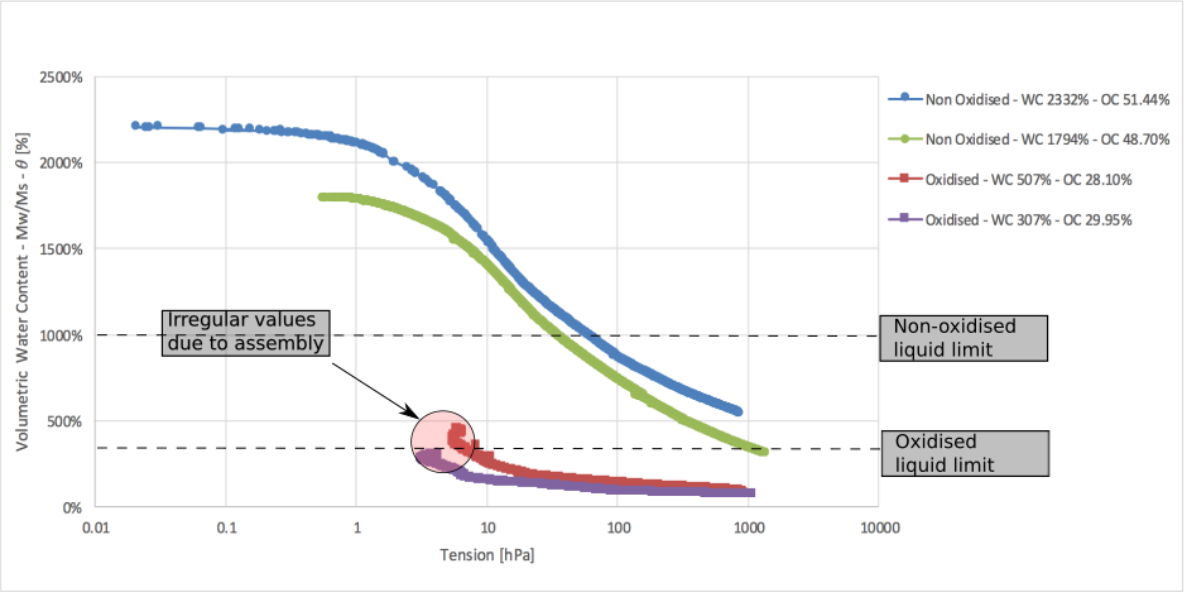

Figure 5.4: Volumetric soil water retention curves for all Hyprop tests during entire measuring campaign

5.4. CT IMAGES

In Chapter 4.3 the procedure of processing the CT-image data is described. This procedure has been repeated for the CT-scans made from the four Hyprop campaigns. The 3D reconstruction of the desiccation process of the various Hyprop campaigns are illustrated in Figures 5.6, 5.7, 5.8 and 5.9. In the following sections, the CT images of the various campaigns will be assessed separately.

NON-OXIDISED & UNDRIED

The non-oxidised undried campaign was the first Hyprop test carried out. Figure 5.6 represents the reconstructed dessication process during the Hyprop campaign. The blue in the figures represent entrapped gas, the salmon colour are artefacts created by metal disturbance of the Hyprop and the red indicates air cavities exposed to the atmosphere. This campaign had a water content of 1296%, dry solid content of 7.16% and an organic content of 51.44%. With such a high water content, the dredged sediment in its original form was essentially a liquid with very little solids. Half of the solids did consist of organic material. Due to the liquid nature of the sample, the material was easily poured into the Hyprop. The test ran for approximately 35 days, but due to issues with the Hyprop's software, tension measurements started 3 days after the start of the experiment. From day 4 to 6 the use of a air pump to accelerate the desiccation process was experimented with, but was later decided not to be used. Furthermore, the second ct-scan occurred quite some time after the initial scan, namely 15 days. In hindsight, more frequent amounts of scans should have taken place between these 15 days on account of a substantial amount of shrinkage and gas volume increase that took place by the time the second scan was made.

Noticeable from the second scan in Figure 5.6b and onwards is the way the soil shrinks isotropically, more or less retaining its shape. The increase of gas volume stops at this point, but most likely occurred much earlier. The volume of gas gradually decreases as desiccation continues. As the bulk volume of solids and liquid decrease, the bulk density increases. Aggregation of gas bubbles takes place, forming larger individual gas bubbles. Indicating the migration of gas in the sample. An additional distinction is made between gas that is entrapped by the dredged sediment and air cavities that are connected to the atmosphere. This is evident in the last scan, Figure 5.6i, depicted in red. The entrapped air at the top of the soil column came in contact with the atmosphere, thus releasing the entrapped gas to the atmosphere. Evident in the considerable drop in gas volume between Figures 5.6h and 5.6i.

Since the gas produced during the first and second scan, 25 April - 10 May, is entrapped by the dredged sediment it is hypothesised that the gas buildup is caused by exsolution of dissolved gas in the water. Where

according to Henry's Law the solubility of a gas is directly proportional to the partial pressure of the gas above the liquid. Thus, it is believed that the increased soil tension (20-30 hPa) during desiccation decreases the solubility of the gas in the water, resulting in gas formation. Oxidation of organic matter could also contribute to gas buildup.

Also notable is the decreasing degree of beam hardening and scatter effects caused by the underlying metal parts of the Hyprop device. Naturally, the area where beam hardening occurs completely disappears if the same area of soil ceases to exist due to shrinkage. Furthermore, when the bottom of the soil column is released from the Hyprop, i.e. the soil suspended in the air and supported by the tensiometers, then further dampening of artefacts occurs. Elevation of the soil first occurs on the 17th of May, more visible when viewing an orthoslice, such as Figure 5.5. Afterwards, as soil continues to elevate from the Hyprop, a continued decrease of artefacts is visible in the 3D reconstruction.

Figure 5.5: First instance of soil elevation - 17 May 2016

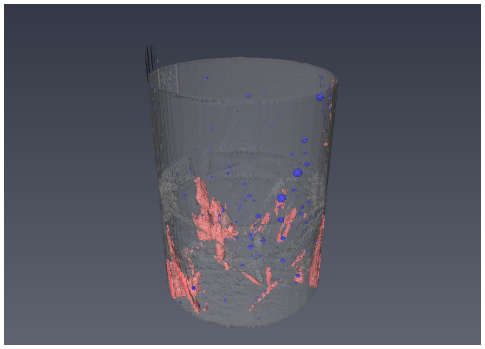

(a) 25 April 2016 - Gas: 0.7 cm^3 - Water Content: 1296%

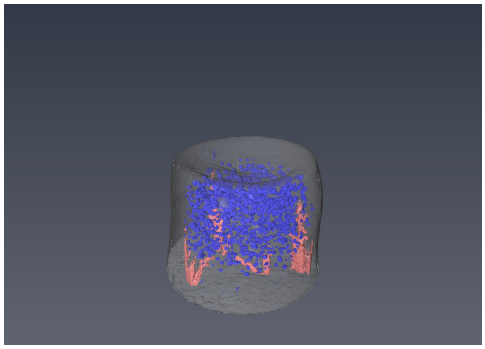

(b) 10 May 2016 - Gas: 6.0 cm^3 - Water Content: 536%

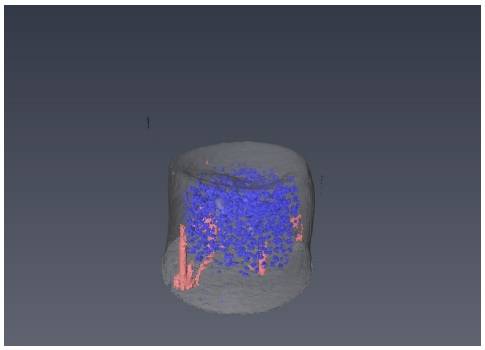

(c) 12 May 2016 - Gas: 5.9 cm^3 - Water Content: 477%

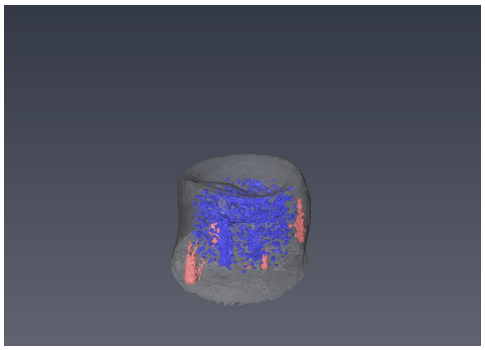

(d) 17 May 2016 - Gas: 5.1 cm^3 - Water Content: 329%

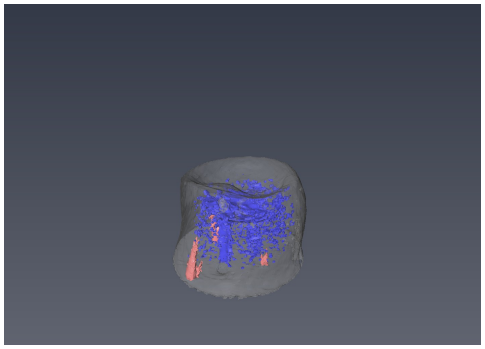

(e) 19 May 2016 - Gas: 4.7 cm^3 - Water Content: 280%

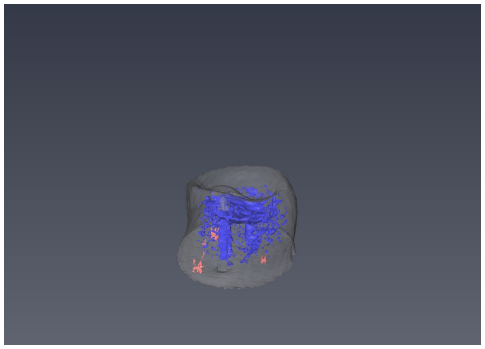

(f) 23 May 2016 - Gas: 4.1 cm^3 - Water Content: 181%

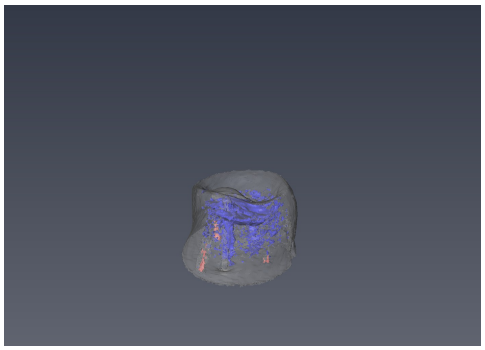

(g) 24 May 2016 - Gas: 3.8 cm^3 - Water Content: 155%

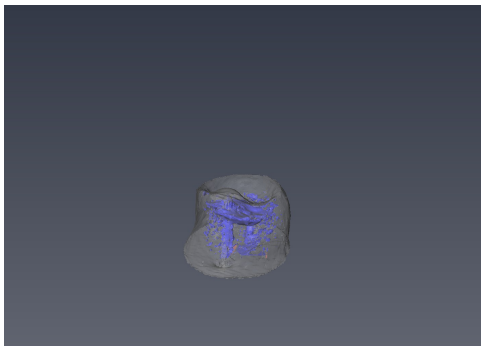

(h) 26 May 2016 - Gas: 3.3 cm^3 - Water Content: 108%

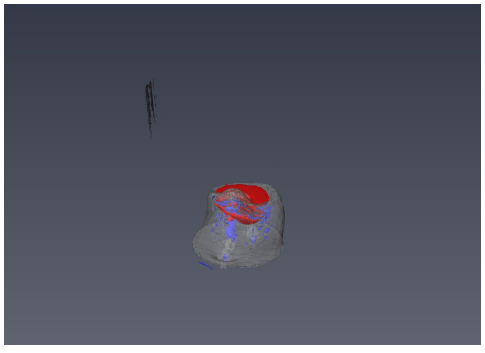

(i) 30 May 2016 - Gas: 0.74 cm^3 - Water Content: 47% -

Figure 5.6: Hyprop Campaign Non Oxidised & Undried - WC 1296% - 3D Images of Drying

NON-OXIDISED & PARTIALLY AIR DRIED

The desiccation process of the second experiment, non-oxidised and partially air dried, is illustrated in Figure 5.7. The second sample has a water content of 997%, a dry solid content of 9.12% and an organic content of 48.70%. The experiment ran for 49 days, without the use of an air pump to accelerate the desiccation process. The consistency of the partially dried sediment was of a thick slurry and definitely not pourable into the Hyprop. The sample ring was filled carefully with a spoon and spatula to avoid entrapping air in the sample. However, when viewing the 3D reconstruction in Figure 5.7a, air was nevertheless entrapped in the soil. For the second experiment, to study the accumulation of gas bubbles, more frequent scans were made in the early phase of the campaign. Gas volume quickly increased and reached its peak on 19 May, Figure 5.7c, 5 days into the experiment. Once again, a similar process occurred as the first Hyprop campaign. The gas volume slowly decreases as the bulk volume decreases. The soil slowly detaches from the sample ring and eventually detaches from the bottom of the Hyprop on 17 June. The entrapped gas was able to move gradually and formed larger gas bubbles as the total amount of gas slowly decreases. Except in this case, no air cavities were exposed to the atmosphere.

A noteworthy point during the desiccation process is the sudden surge of gas volume between the 9th and 17th of June, Figures 5.7j and Figure 5.7k respectively. Gas volume surged from 4.3 cm^3 to 5.2 cm^3. No extreme suction values were recorded during this period and the temperature barely fluctuated. Measurements errors with Avizo could be the cause for the irregularity.

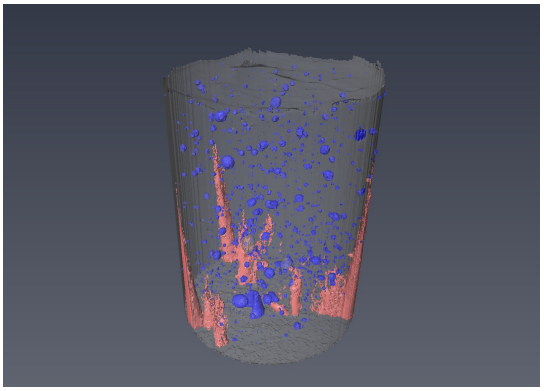

(a) 12 May 2016 - Gas: 3.7 cm^3 - Water Content: 997%

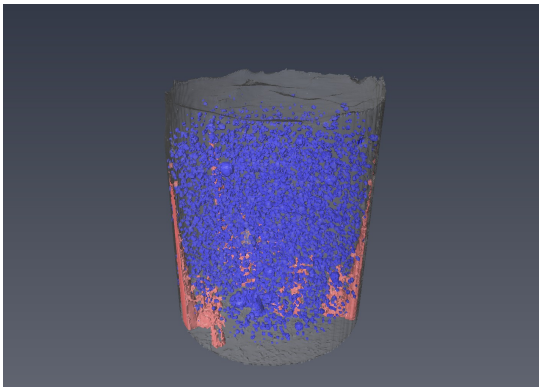

(b) 17 May 2016 - Gas: 16.8 cm^3 - Water Content: 859%

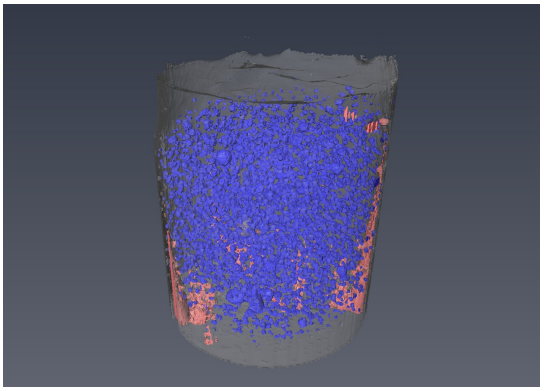

(c) 19 May 2016 - Gas: 17.1 cm^3 - Water Content: 814%

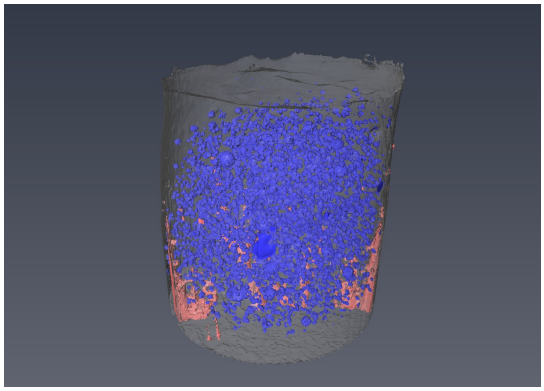

(d) 23 May 2016 - Gas: 14.5 cm^3 - Water Content: 724%

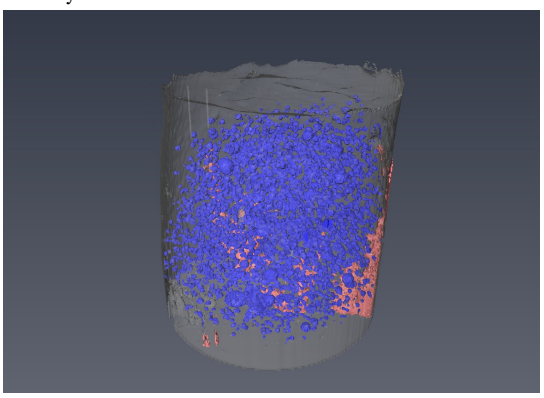

(e) 24 May 2016 - Gas: 13.8 cm^3 - Water Content: 701%

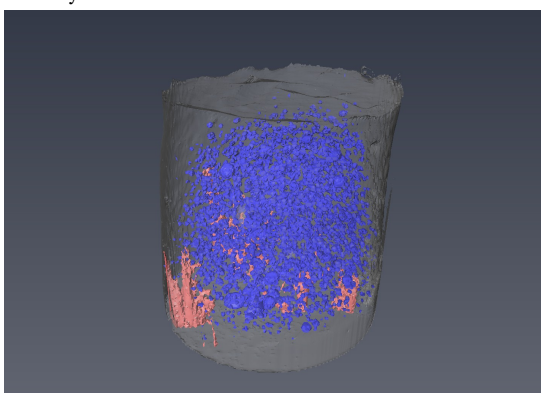

(f) 26 May 2016 - Gas: 12.4 cm^3 - Water Content: 655%

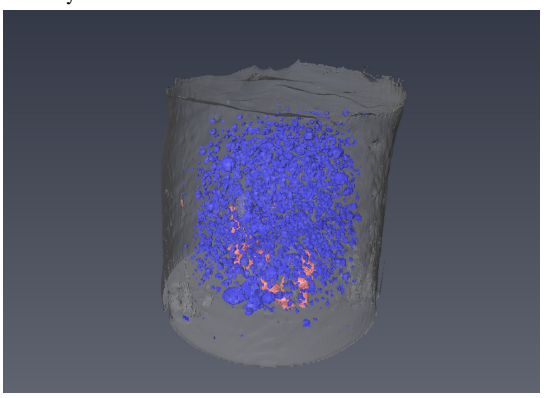

(g) 30 May 2016 - Gas: 8.6 cm^3 - Water Content: 580%

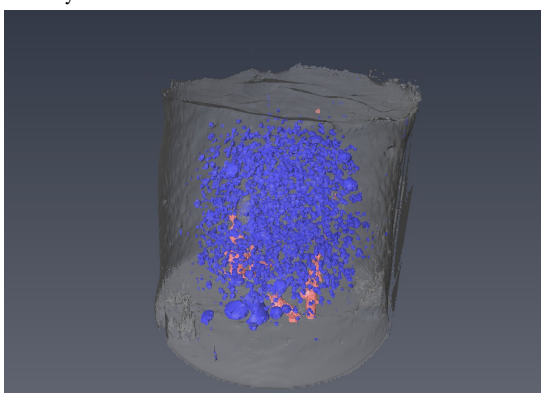

(h) 2 June 2016 - Gas: 6.8 cm^3 - Water Content: 529%

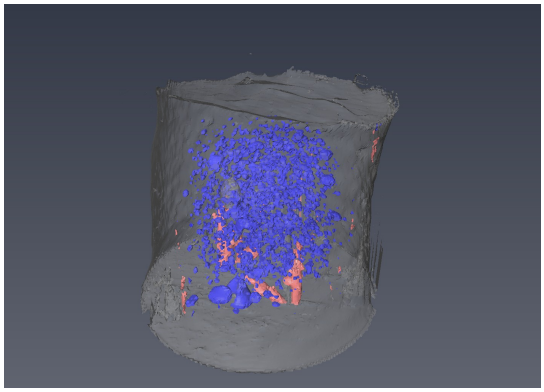

(i) 7 June 2016 - Gas: 4.9 cm^3 - Water Content: 441%

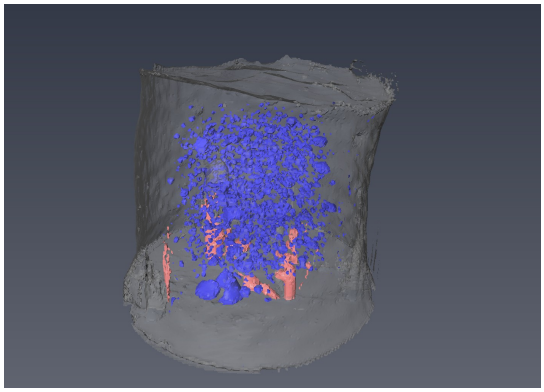

(j) 9 June 2016 - Gas: 4.3 cm^3 - Water Content: 395%

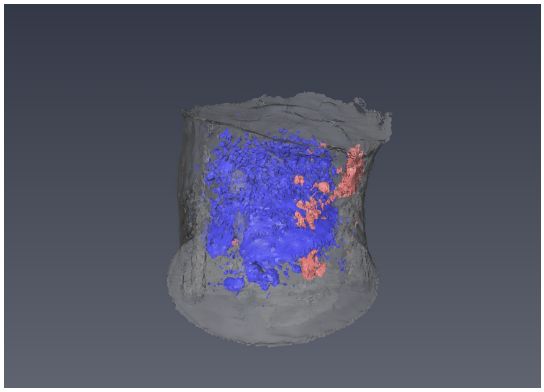

(k) 17 June 2016 - Gas: 5.2 cm^3 - Water Content: 247%

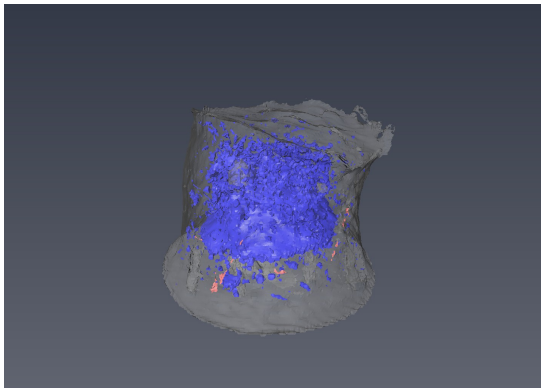

(l) 23 June 2016 - Gas: 4.1 cm^3 - Water Content: 151%

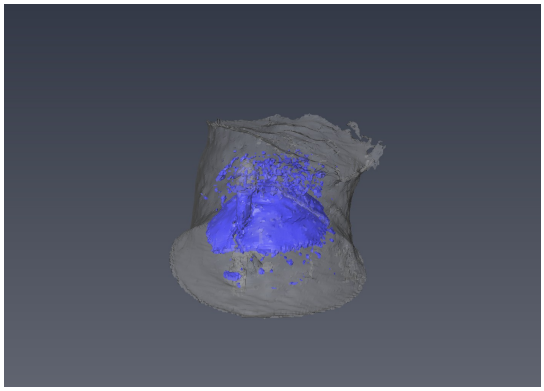

(m) 27 June 2016 - Gas: 3.3 cm^3 - Water Content: 98%

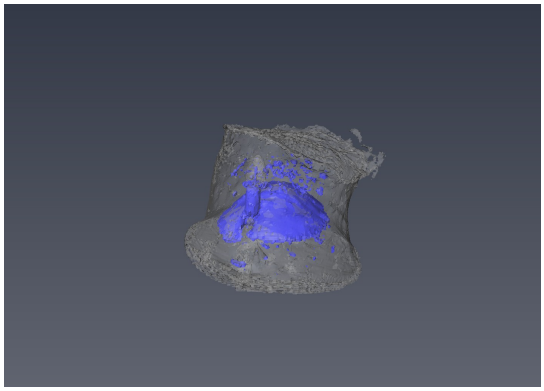

(n) 30 June 2016 - Gas: 2.9 cm^3 - Water Content: 58%

Figure 5.7: Hyprop Campaign Non Oxidised & Partially Air Dried - WC 997% - 3D Images of Drying

OXIDISED & UNDRIED

For the third Hyprop experiment, the dredged sediment was pre-treated with hydrogen peroxide (H_2O_2) to remove organic matter. After the oxidation process the Hyprop was prepared by placing the oxidised sample in the sample ring using a spoon, the same method used for the non-oxidised & air dried campaign. Water content after the oxidation procedure was 282 %. Dry solid content of the campaign was 26.20% with an organic content of 28.10%. Thus, roughly 20% of organic matter was oxidised due to the pre-treatment of hydrogen peroxide. For the oxidised set, it was decided to use an air pump (Eheim Air Pump 400) to quicken the drying process, because running another Hyprop campaign for 50 days would not be a viable option. Utilizing the fan, the duration of the experiment was 20 days. During the final phase of the experiment, large air cavities exposed to the atmosphere formed at the bottom of the soil column. A larger bulk volume of soil and water remains after the campaign has ended, which is expected due to the high dry solid content. Gas accumulation appears to not take place in this oxidised sample. Possible explanation for the lack of gas volume increase is due to the absence of dissolved gas in the water caused by the oxidation procedure. The oxidation process required vacuum filtering of the oxidised material to remove the acidic liquid. Additionally, during the filtering process the oxidised material was also washed with demineralised water. Thus, the majority of the original water present in the slurry, which contained the dissolved gases, was removed by the filtration process and partly diluted with demineralised water. The initial entrapped air is attributed to the preparation method of the Hyprop. As shrinkage takes place, the gas volume decreases and the remaining gas does not merge to form larger gas bubbles, which was previously observed in the earlier experiments.

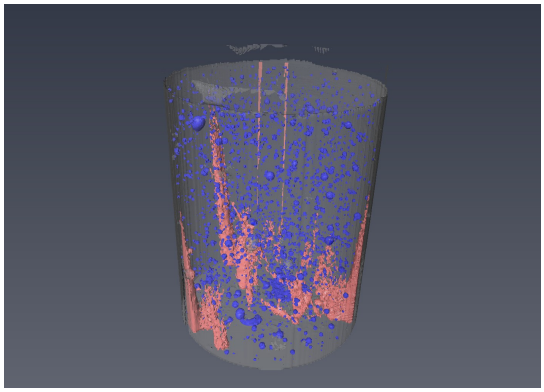

(a) 3 August 2016 - Gas: 4.4 cm^3 - Water Content: 282%

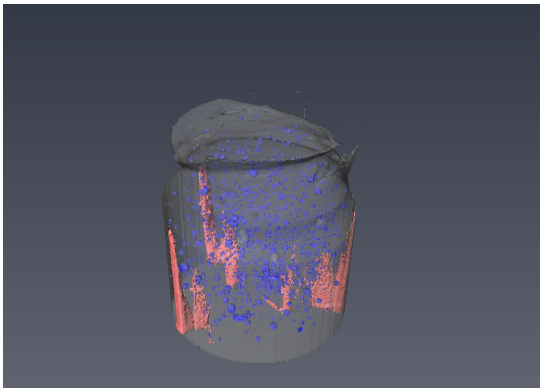

(b) 8 August 2016 - Gas: 3.4 cm^3 - Water Content: 198%

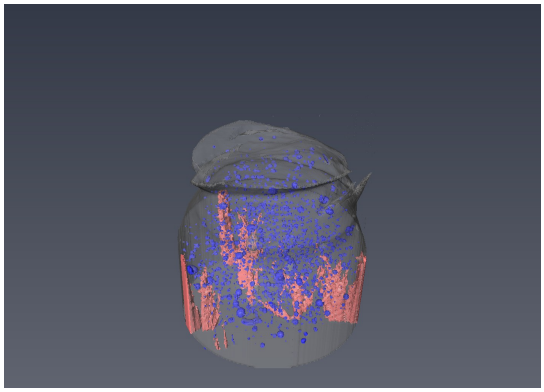

(c) 11 August 2016 - Gas: 3.1 cm^3 - Water Content: 163%

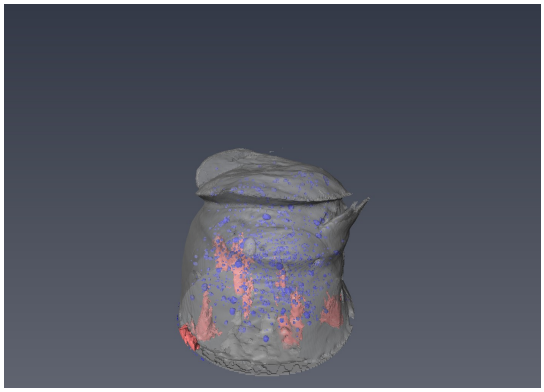

(d) 15 August 2016 - Gas: 1.8 cm^3 - Water Content: 109%

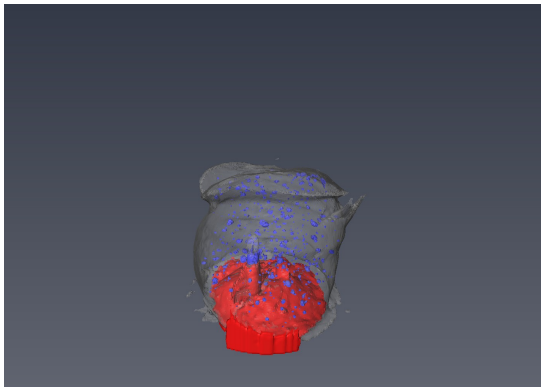

(e) 18 August 2016 - Gas: 0.91 cm^3 - Water Content: 63%

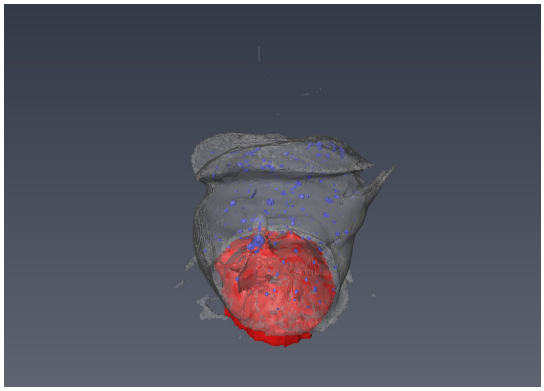

(f) 22 August 2016 - Gas: 0.55 cm^3 - Water Content: 31%

Figure 5.8: Hyprop Campaign Oxidised & Undried - WC 282% - 3D Images of Drying

OXIDISED & PARTIALLY AIR DRIED

In the final experiment, the dredged sediment was once again oxidised with hydrogen peroxide and partially dried afterwards. The oxidised sample was partially air dried until approximately the water content of the liquid limit. The falling cone was used regularly during the tray drying process until a penetration of about 20mm was achieved. Water content at around liquid limit was 172%. The dry solid content during the test was 36.73% with an organic content of 29.95%. The result of air drying prior to the Hyprop campaign was a very thick viscous slurry, which made it difficult to work with during the Hyprop preparations. The sample ring was once again prepared with a spoon and spatula, while carefully trying not to incorporate air into the soil column. However, the initial scan indicated that 12 cm^3 of air was entrapped during the Hyprop preparations. Like the previous oxidised Hyprop campaign, no accumulation of gas occured during the desiccation process, most likely due to the oxidation procedure. The gas does however converge forming larger gas bubbles, unlike the oxidised & undried campaign. As larger gas bubbles are being formed, the total volume of gas decreases as the shrinking process takes place. During desiccation cracks begin to appear on the surface and on the bottom of the soil. As a result, a portion of entrapped gas becomes exposed to the open air, and the entrapped gas is released into the atmosphere.

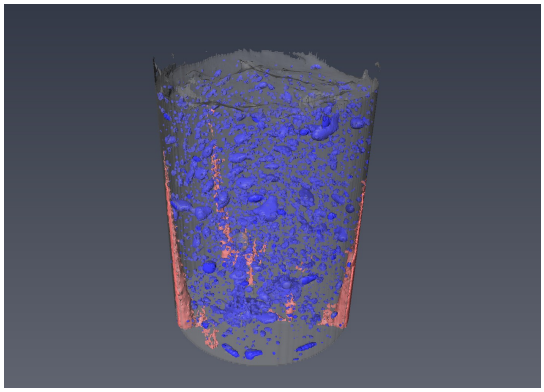

(a) 18 August 2016 - Gas: 12.1 cm^3 - Water Content: 172 %

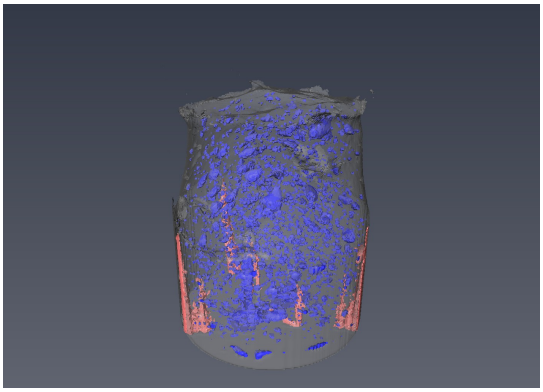

(b) 22 August 2016 - Gas: 10.2 cm^3 - Water Content: 129 %

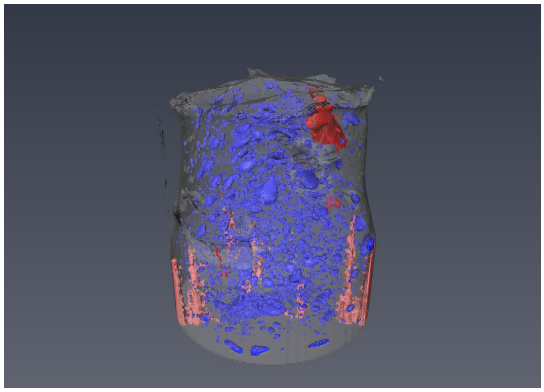

(c) 25 August 2016 - Gas: 9.6 cm^3 - Water Content: 106 %

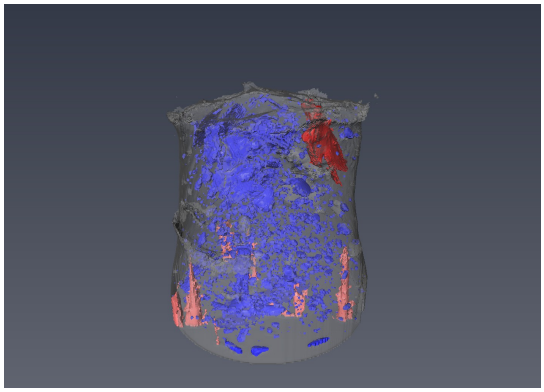

(d) 29 August 2016 - Gas: 9.5 cm^3 - Water Content: 83 %

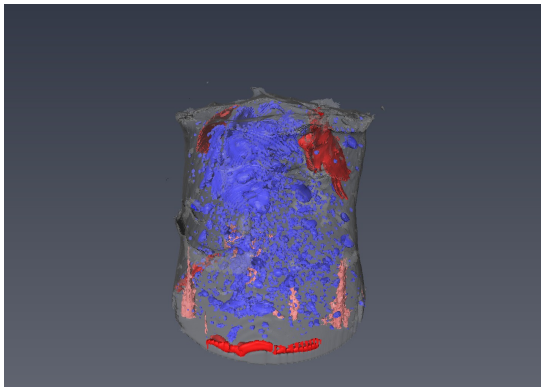

(e) 30 August 2016 - Gas: 8.3 cm^3 - Water Content: 76 %

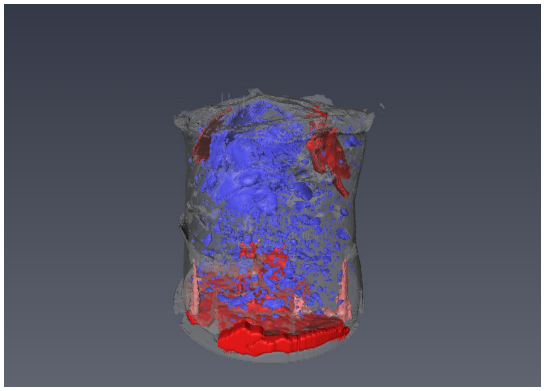

(f) 1 September 2016 - Gas: 7.5 cm^3 - Water Content: 65 %

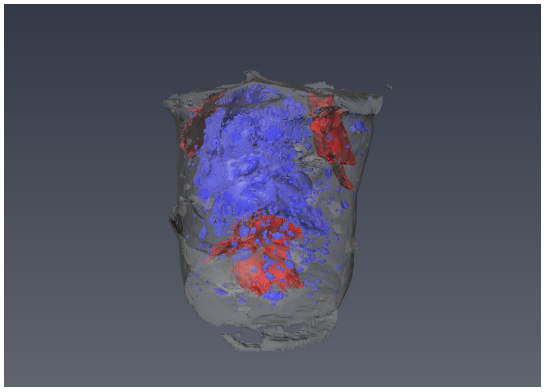

(g) 5 September 2016 - Gas: 7.1 cm^3 - Water Content: 37 %

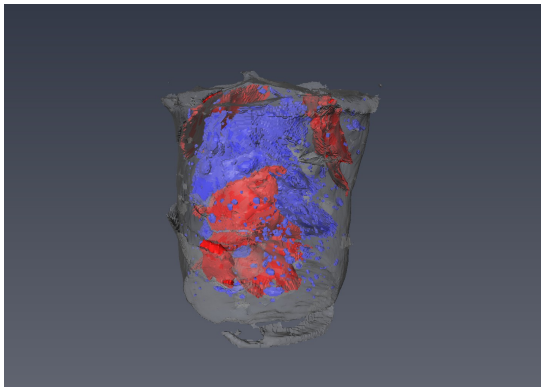

(h) 6 September 2016 - Gas: 6.9 cm^3 - Water Content: 32 %

Figure 5.9: Hyprop Campaign Oxidised & Partially Air Dried - WC 172 % - 3D Images of Drying

5.5. HYPROP AND CT-DATA COMBINED

The previous two sections described the data output for the Hyprop and CT-scans individually. When combining both data outputs various relationships can be studied, such as the soil shrinkage curves. For the upcoming graphs only the bottom tensions were applied, as their measurements were more complete in relation to the volume measurements derived from the CT-scans.

The shrinkage curve is presented in Figure 5.10, where the void ratio e ($\frac{V_{voids}}{V_{solids}}$) is plotted over the volumetric water content θ ($\frac{V_{water}}{V_{solids}}$). The basic shape of the shrinkage curves for the various Hyprop tests are straight linear lines with a gradient of approximately 1, lying essentially on the saturation line. From the four shrinkage processes described in chapter 2.3.1 (structural, normal, residual and zero shrinkage), only proportional shrinkage is evident. Experiments were stopped when zero tension was observed, before residual shrinkage could take place. If desiccation was allowed to continue, it is expected that eventually inflection points would appear, marking the point of air entry. The proportional shrinkage experienced, means that the decrease in water volume of slurry is equal to the reduction of soil's bulk volume. Seeing that the majority of the points lie essentially on the saturation line implies that the portion of air or gas is minute compared to the amount of water.

The only clear inflection point recognizable in Figure 5.10 is for the non-oxidised & partially air dried test. Ordinarily, inflection points indicates air entry of the pores, but in this situation the inflection point signifies either the exsolution of gas, thermal expansion of the gas present or gas production due to organic oxidation. Gas volume increase quickly subsides and subsequently recovers its original path. An additional inflection point is expected for non-oxidised undried campaign, but was not observed due to lack of CT-scans made during the initial stage of the test. No inflection points are observed for the oxidised tests, which indicates the lack of gas volume increase for these campaigns.

Thus, it can be concluded that the organic matter and initial water content only influences the onset of shrinkage. During the desiccation process, only normal shrinkage is observed at near saturated conditions, where the loss of water volume is equal to the loss of bulk volume.

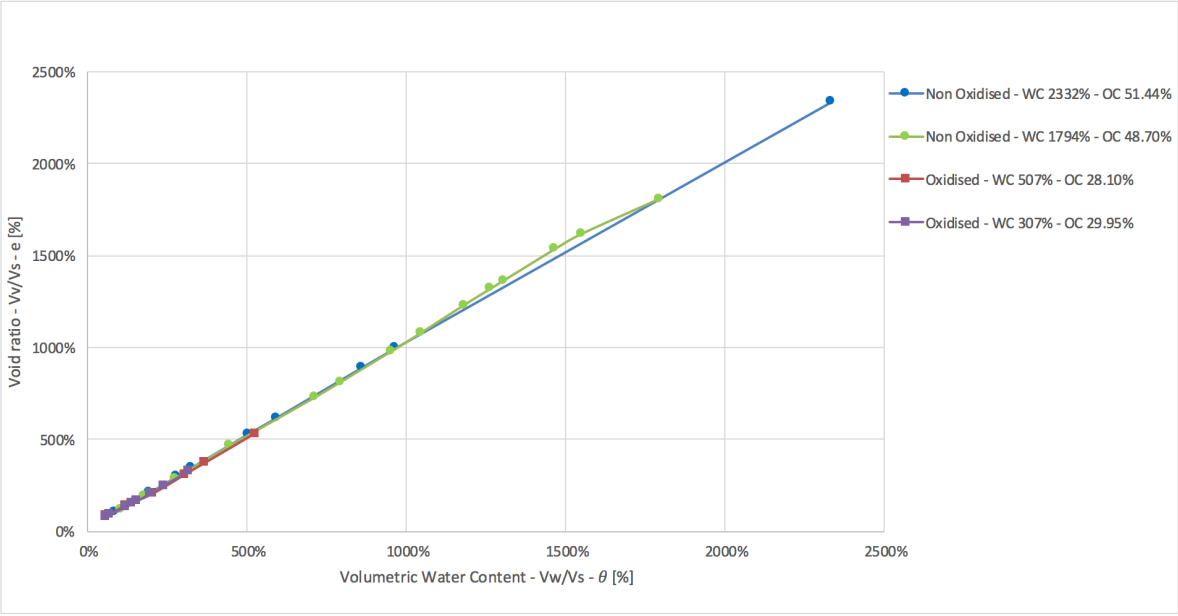

Figure 5.10: Shrinkage curves for all Hyprop tests

The scale of the shrinkage curve graph is not suitable to study the gas volume behaviour, due to the small amount of gas compared to its water volume. Thus, in Figure 5.11 the gas volume content is plotted over the volumetric water content. Where gas volume content is defined as the volume of gas over the volume of solids ($\frac{V_g}{V_s}$). Presenting the gas volume in this manner gives a more clear indication of the gas behaviour. Initial gas volume increase for the non-oxidised are clearly visible in this graph and it also clearly shows the continuous decrease of gas volume for the oxidised tests. The continuous decrease of gas volume for the oxidised tests could be explained by the lack of dissolved gases in the water due to the oxidation procedure. This supports the theory that the gas volume increase witnessed by the non-oxidised tests are at least partly due to exsolution of dissolved gases in the water. Another possible contribution to the increase gas volume is the production of gas due to oxidation of organic matter. Gradual decrease of gas volume over time is believed to be caused by diffusion of gas through the pore-water, as the gas bubbles are entrapped by soil and pore water. In the final stages of a number of Hyprop experiments, sudden gas volume decrease is attributed to forming of cracks that are open to the atmosphere, causing episodic release of gas bubbles, ebullition.

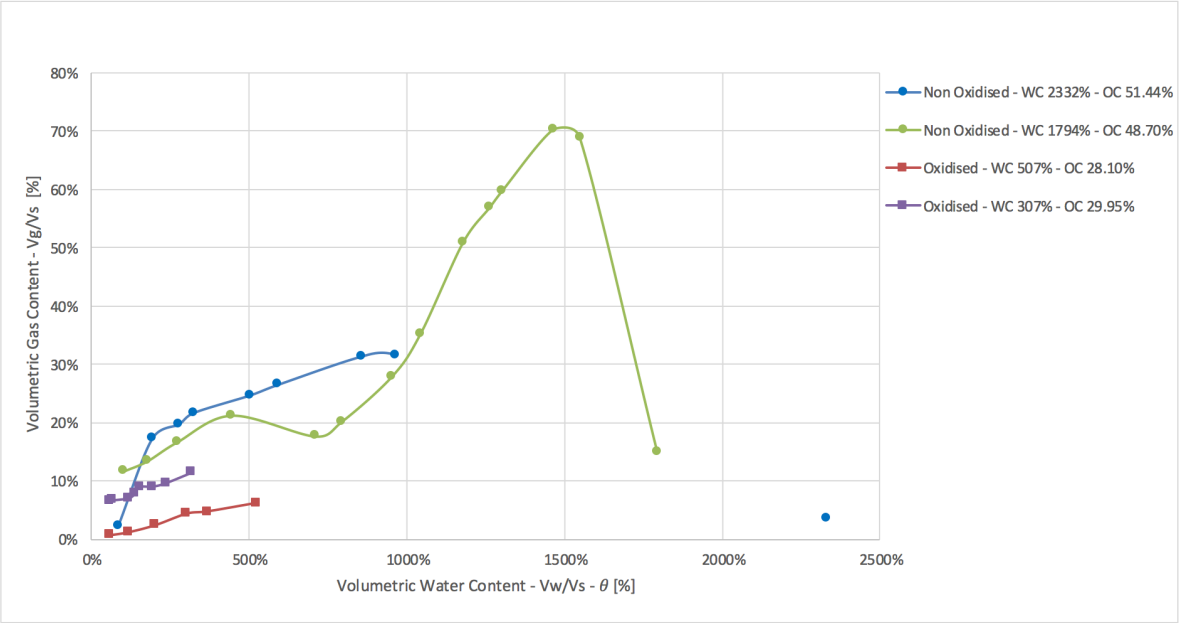

Figure 5.11: Volumetric gas content over the volumetric water content for all Hyprop tests

Figure 5.12 displays the volumetric gas content over tension measurements. Notable are the low suction values at which gas bubbles were being developed for the non-oxidised & partially air dried campaign. Peak gas volume was around 10 hPa. Similar behaviour is expected for the non-oxidised & undried campaign but has not been documented due to lack of CT-scans during this period. Also, the initial volumetric gas content of 4% could not be plotted in this graph because of negative initial tensions even when the correction methods were applied.

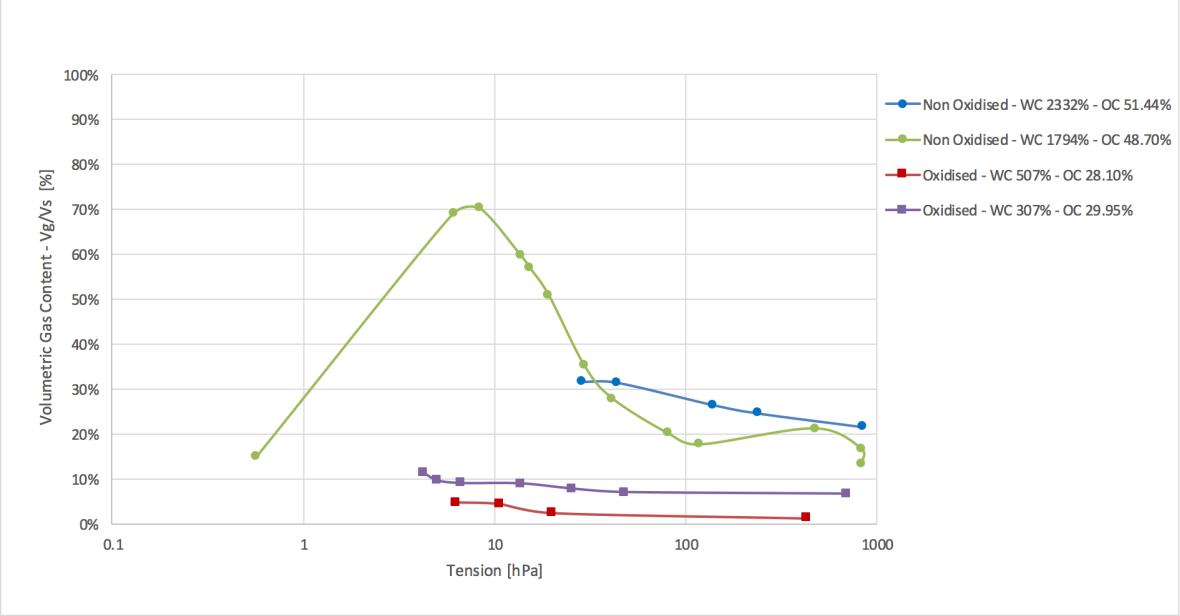

Figure 5.12: Volumetric gas content over the volumetric water content for all Hyprop tests.

Figure 5.13 illustrates the void ratio plotted over the tension measurements. The dataset is limited due to the amount of CT-scans made during the test. The volumetric soil water retention curves are expected to be almost identical to the void ratio versus tension graphs due to the linear relationship of the soil shrinkage curve seen previously in Figure 5.10. The same points were plotted in Figure 5.14 to verify this. The two graphs clearly show that they are virtually identical, only varying for the non-oxidised tests. The slight deviation is caused by the increase of gas volume in the early stages of the experiments. Inversely, the oxidised samples do not vary due to lack of gas accumulation during its desiccation process.

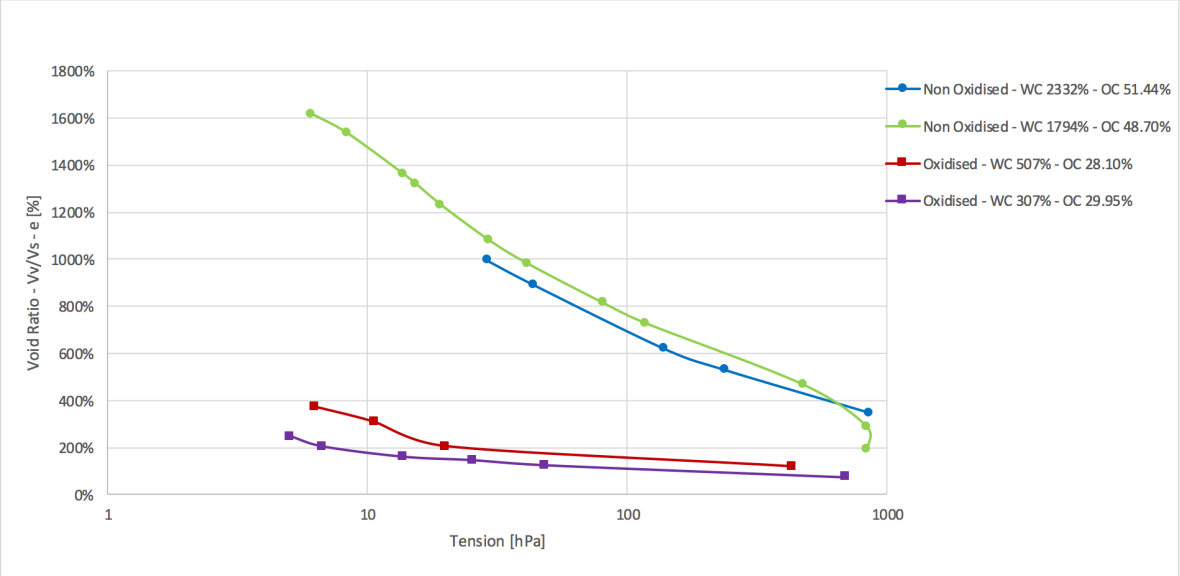

Figure 5.13: Void ratio vs tension for all Hyprop tests

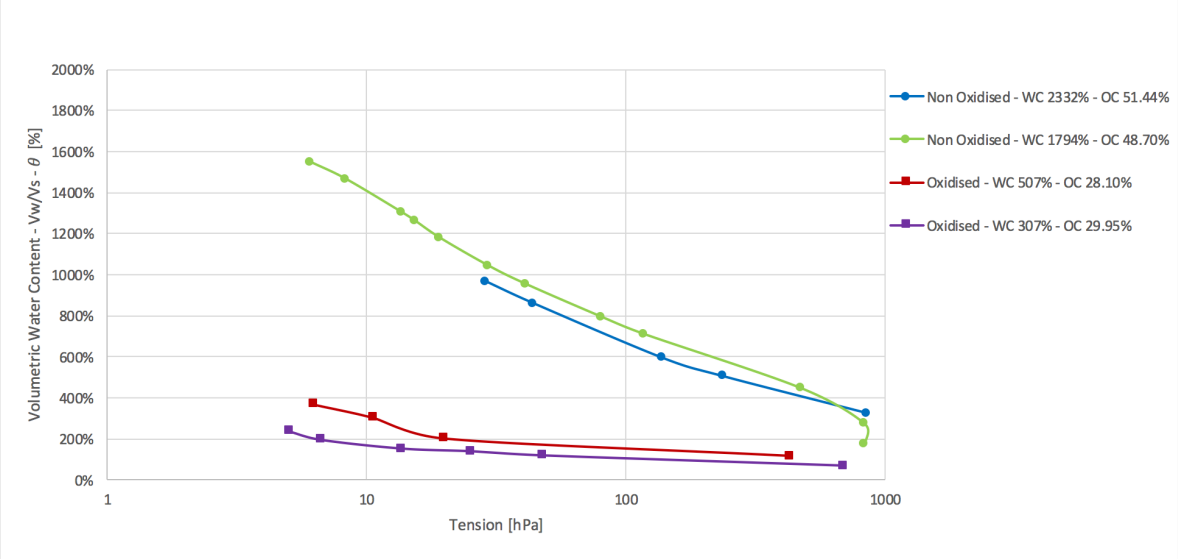

Figure 5.14: Volumetric soil water retention curves for all Hyprop tests - data points on CT-scans

6

DISCUSSION

6.1. INTRODUCTION

The previous chapters described the methodology, data processing and the results of the experiments carried out. This chapter shall discuss and evaluate these chapters individually. The highly shrinkable organic dredged sediment combined with the procedure of the Hyprop tests, CT-scans, organic oxidation and data processing are relatively new to the Geo-Engineering field of study. Thus, a critical evaluation is needed of the aforementioned points and the results it produced.

6.2. DISCUSSION OF METHODOLOGY

The testing methods shall be discussed in this section, which will include the complications encountered during testing and advantages and objections of using such methods.

6.2.1. HYPROP

The Hyprop is a simple device to continuously measure mass and suction values of the soil during desiccation. However, soils are generally assumed to be rigid during loss of water on drying and as such the Hyprop was mainly designed for such soils. Highly shrinkable soils that we are dealing with in this thesis was the first issue encountered when applied to Hyprop. Previous research done by Tollenaar [35] has shown punching of the top tensiometers when dealing with such shrinkable soils. To avoid this issue, the original sampling ring was extended from a height of 5 cm to 12 cm. This increased the distance of the tensiometers to the surface of the soil column considerably, which must be taken account for when processing the results.

Other technical issues encountered with the Hyprop are related to the macro CT-scanner. To avoid scanning disturbance in the CT-scanner metal components were removed from the Hyprop. The majority of these components were removed, such as the fastening clips and the metal sampling ring. These were replaced with plastic and PVC counterparts. However, metal components inside the Hyprop's main body were not removed. In hindsight, an additional few components could have been removed from inside the main body such as screws. However, units such as the temperature and tension sensors can not be removed from the main body. Therefore, artefacts produced from these metal components were removed manually during data processing. Manual removal of artefacts is very time consuming and is subject to error if not done accurately. This directly affects the accuracy of the soil volume measurements.

The final technical issue with using the Hyprop for highly shrinkable soil is the deformation of the tensiometers as the soil dries. Figure 6.1 illustrates this for the non-oxidised & partially air dried Hyprop campaign. Shrinkage of the dredged sediment causes the tensiometers to experience lateral stress from the soil. The lateral stress on the fixed tensiometers causes the shafts to behave as a cantilever as it displaces. The extent of this effect is greater for the top tensiometer due to its length, which subsequently causes the base of the top tensiometer to bend towards the center of the soil column. Such bends in the shaft can negatively influence the performance of the tensiometer with consecutive use.

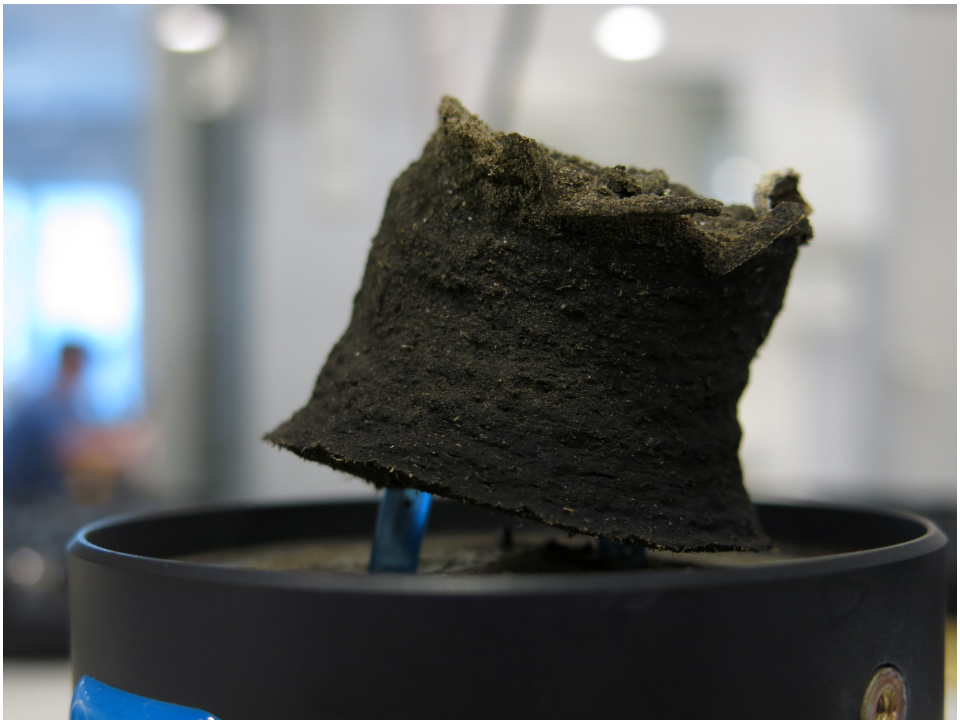

Figure 6.1: Bend of the top tensiometer due to the shrinking soil - Non-oxidised & partially air dried Hyprop campaign

6.2.2. HYPROP ASSEMBLY

Assembly of the Hyprop was executed in two ways depending on the consistency of the dredged sediment. The two assembly methods utilised were: (1) fasten the sampling ring to the main body with the tensiometers attached and pour the liquid formed dredged sediment into the sampling ring or (2) place the sampling ring on a flat tile, fill the ring with a partially air dried viscous sediment, flip the main body with the tensiometers attached and insert into the sampling ring filled with soil, then flip the assembled unit back up right, slowly slide off the flat tile and finally fasten the assembled units. Irregular tension measurements occurred only for the second assembly method. The first assembly method showed no irregular measurements, because pouring of the liquid slurry does not disturb the tensiometers. However, the second method was rather intrusive for the initial tension measurements. Firstly, penetrating the viscous material with the tensiometers caused an initial pressure buildup for one campaign. Where ordinarily an auger is used to drill a hole in the soil for the tensiometers to be placed in. But, the use of an auger was not possible for this viscous soil as the auger works poorly in these conditions and the drilled hole would collapse back immediately. Secondly, the removal of the flat tile caused a vacuum effect which resulted in irregular initial tension to be measured. Rapid removal by pulling enhances this effect. Thus, slowly sliding the tile off was adopted in subsequent tests. The vacuum effect was still visible, but to a lower extent.

Irregular assembly measurements are only noticeable for the first few days of testing, but are still evident when plotting soil water retention curves such as in Figure 5.4 from the previous chapter. Such irregular behaviour is naturally unwanted as it does not accurately describe the soil's hydraulic behaviour in its initial phase. Additionally, the correction methods applied in this thesis, which corrects for negative initial tension, enhances the offset of the irregular assembly values as well.

Testing has shown that the initial vacuum caused by tile removal causes greater disturbance in the measurements than initial pressure buildup due to soil penetration. Proposed method to solve this issue is to use a fabric mesh to cover the soil with a perforated tile. The perforated tile would prevent tension to form when removing the soil and the fabric mesh prevents the loss of soil through the perforated tile. However, the fabric mesh must allow air to pass through. The traditional method combines the fabric mesh with a perforated cap. But, pulling off the perforated cap also causes tension to form. Thus, a flat perforated tile would be a more suitable option.

6.2.3. MACRO CT-SCANNER

Employing a medical CT-scanner on soil bodies has numerous advantages for this type of research. The ability to 3D reconstruct the soil body without the boundary restraints of the Hyprop allows for geometrical changes to be observed and the nondestructive method of measuring the soil and pore volume are the main advantages of utilizing the CT-scanner. However, a number of aspects must be considered when making use of a medical CT-scanner. A few aspects one must consider when utilizing computed tomography are the size, shape and material of the object to be scanned, the allowable budget for the research, artefacts that could influence the images, resolution of the images, etc.

Size of the object to be scanned and the amount of scans to be made are interrelated with the cost when considering the budget for the research. As the size of the object determines the scanning time, where one second of scanning amounts to approximately €20 in expenses. Consequently, one CT-scan of the Hyprop with its modified sampling ring cost approximately €80. The shape and density of the object directly affects the quality of the CT-scans. Medical CT-scanners are optimal for cylindrical shapes, such as a person. For a cylindrical object, x-rays passing through the middle portion experience equal amount of hardening regardless of the x-ray's origin of projection. Whereas, a rectangular object will experience additional hardening because they are passing through more material depending on the x-ray's origin of projection.

Additionally, the density of the object must be within the range that can be handled by the computer. Metal objects for instance leads to severe streaking artefacts because its density is beyond the computer's normal measuring range. Although the majority of the metal components were removed from the Hyprop, the artefacts caused by the remaining metal components were removed manually. Removal of metal artefacts with Avizo's image segmentation function is a time consuming process, but can greatly influence the results if not taken into consideration. In the case that the artefacts are not removed, these streaks will then be misinterpreted as gas within the soil. This would lead to gas volume overestimation of nearly a factor two in a few Hyprop cases for the given dredged sediment and laboratory conditions. An alternative option to reduce metallic interference is to increase kilovoltage, which may help penetrate the metal objects.

Other density related concerns are the sampling ring. Clearly discerning the dredged sediment from the sampling ring with the Volume Edit module was difficult at times. Utilizing a sampling ring with a contrasting density the dredged sediment would provide a clear distinction of the soil and ring. Metal sampling rings would once again have to be avoided. This is only a minute detail, but would make post processing slightly more manageable.

Voxel resolution and voxel size is another contributing factor to CT image quality. The CT-scanner has a minimum voxel size of 0.33 mm. For the tests the voxel size was fixed at 0.4x0.4x0.6 mm with a voxel resolution of 512x512x512 in a local 3D (XYZ) coordinate system. The voxel size determines the smallest visible particle at 0.4 mm. Thus, individual particles smaller than 0.4 mm will not be visible in these images. To acquire higher image resolution, one would have to make use of micro CT-scanners. The micro CT-scanner from the TU Delft has a maximum voxel size of 0.5 - 1 micron. However, the disadvantage of these machines are the long scanning periods (in the order of a few hours) and the limited area that can be scanned at once.

6.2.4. OXIDATION PROCEDURE

The oxidation procedure was performed according to the British Standard. However, the prescribed pretreatment for organic matter can only be considered a guideline due to the lack of specific instructions. The main shortcoming of the British Standard is the lack of correlation of the organic content with the suggested amount of initial soil to be treated and the prescribed amount of hydrogen peroxide to be used. Furthermore, the standard does not state the concentration of the hydrogen peroxide and the size of the filter paper. Regarding chemical removal of organic matter, there is no general consensus on the correct oxidation method and chemical to be used. Thus, the standard was treated as a rough guide. The principle of the oxidation procedure was applied, but the exact amount of hydrogen peroxide and initial soil to be treated was determined based on other literature.

Two calculation methods were considered when determining the amount of hydrogen peroxide needed for 100 gr of wet soil. The first method uses Schumacher's conversion factor. The total amount of organic matter in the soil is divided by the conversion factor to estimate the amount of carbon. The second method is the

Rock-Eval method, which was previously carried out by another TU Delft researcher on the same dredged sediment. The Rock-Eval method involves measuring the amount of hydrocarbons and carbon dioxide released when the organic content is pyrolyzed in the absence of oxygen. When comparing both methods, the calculated amount of carbon was similar magnitude. The lower boundary value of Schumacher was slightly more conservative, thus it was decided to use Schumacher's calculation to increase the likelihood of achievable oxidation. See Appendix A for calculation details.

Hydrogen peroxide was used for this study as it is the most most widely used chemical reagent for organic matter destruction. However, the issue with hydrogen peroxide is the unknown negative effects the reagent has on the mineral fraction of the soil and its incomplete removal of organic matter. Thus, research is currently being carried out on alternative reagents in an attempt to improve these deficiencies. Sodium hypochlorite (NaOCl) and disodium peroxodisulfate ($Na_2S_2O_8$) have emerged recently with the greatest potential to replace hydrogen peroxide. Depending on the soil's mineral composition, these reactants are possibly more effective in organic carbon removal and could be considered for further research.

The observed removal of organic matter was checked with the loss on ignition (LoI). LoI tests were carried out according to the RAW standard, where the soil is heated for 4 hours at 500 °C after having dried the soil at 105 °C. Organic matter combusts, and subsequently the organic matter can be calculated as the difference between the initial and final sample weights. The main concern with this method is the destruction of mineral matter present in the soil, leading to an overestimation of organic matter content. The amount of mineral matter lost in this manner, if at all, is not known and must be taken into consideration for the organic content values presented in this thesis.

Concerning the filtration process, suggested is to wash the oxidised material with the on site water instead of demineralised water. When studying gas bubble formation in dredged sediment, the use of demineralised water could have a negative effect on this process.

The final point of note is the use of sodium hydroxide (NaOH) to neutralise the soil's pH. Sodium hydroxide is more commonly used for industrial cleaning, but not so much for civil engineering practices. Sodium hydroxide is a highly reactive solution and most likely also alters the soil's properties. Ongoing research involves applying sodium hydroxide for soil stabilisation. Researchers Olaniyan et al [36] has found an increase in the soil's compressive strength when applying sodium hydroxide as an stabilisation additive. Contrarily, Nyamangara [37] has observed a decrease in structural stability and hydraulic conductivity with increasing hydroxide solutions. Apparent is that sodium hydroxide does have some type of effect on structural and hydraulic properties. The exact nature of this effect is not clear, but it is clear that sodium hydroxide will influence the soil's behaviour, and thus the results presented in this thesis. An additional control test could be carried out to observe the effects of sodium hydroxide on the soil sample.

6.3. DISCUSSION OF DATA PROCESSING

Data processing topics that will be discussed are the thresholding accuracy and the negative initial pore water tension observed during testing.

6.3.1. THRESHOLDING ACCURACY

The greyscale images produced by computed tomography can be represented by a histogram, where voxel frequency distribution is plotted over the voxel intensity. A threshold value can be chosen to separate the various phases in the soil. Air is the easiest to discern from these images and are characterised as black voxels. However, water and solids are not discernable from each other and at present there is no effective algorithm that could segment out the solid and liquid fractions. The lower and upper threshold values were determined visually with Avizo. The accuracy of the calculated volume is heavily influenced by the threshold criteria. The precision of the solid and liquid fraction can be confirmed by the weight measurements registered from the Hyprop, assuming the weight of the gas/air to be naught.

Weight measurements can be converted to a combined soil and water volume with the help of the water density and the specific gravity, where the specific gravity was determined previously by Zain [28]. An Avizo volume error was derived by calculating the difference between the weight converted volume and the Avizo calculated volume divided by the weight converted volume. Avizo volume errors ranged from 1 to 20 %. Accuracy appears to decrease as the desiccation process proceeds, with the largest volume errors observed in the final stages of the test. Threshold values were moderately adjusted when it became apparent that the previous values did not represent the non-void voxels accurately. This was caused by the increasing bulk density as the soil dries out. However, attempting to lower the Avizo error by drastically adjusting the threshold values does not properly describe the soil and liquid fraction within Avizo. These errors are attributed to the voxel size of the images. Voxel size of the images are 400x400x600 μm. As the soil shrinks, the size of the voxels becomes more significant to the analysis module of Avizo. Smaller voxels will reduce the error and inversely larger voxels will increase the error as the soil shrinks.

Concerning the gas/air phase, the lower threshold value is equal to the left boundary of the histogram, namely a voxel intensity of -1024 HU (Hounsfield Units). The upper threshold value is then equal to the lower threshold value of the solid and liquid fraction. Thus, the assigned threshold values of the liquid and solid fraction directly influences air/gas phase fraction. If the computed soil and liquid fraction is accurate, then one can assume that the computed gas volume would be accurate as well. However, the accuracy of the computed gas volume is difficult to verify, as there are no reference measurements, as is the case for the solid and liquid fraction. A method of confirming the gas measurements are by means of sensitivity analysis. Where the upper threshold value is varied until the variance of the gas volume measurements are deemed acceptable. The aforementioned sensitivity analysis would be very time consuming with the basic Avizo software package, especially when a considerate amount of CT-scans were made. Suggested, is to export the data to Matlab for data analysis. Alternatively, open source software such as ImageJ in Java would be more suited for such data analysis.

The remaining un-thresholded area represents the Hyprop testing device and its various components. This area was not needed for the analysis. Figure 6.2 illustrates the three thresholded states.

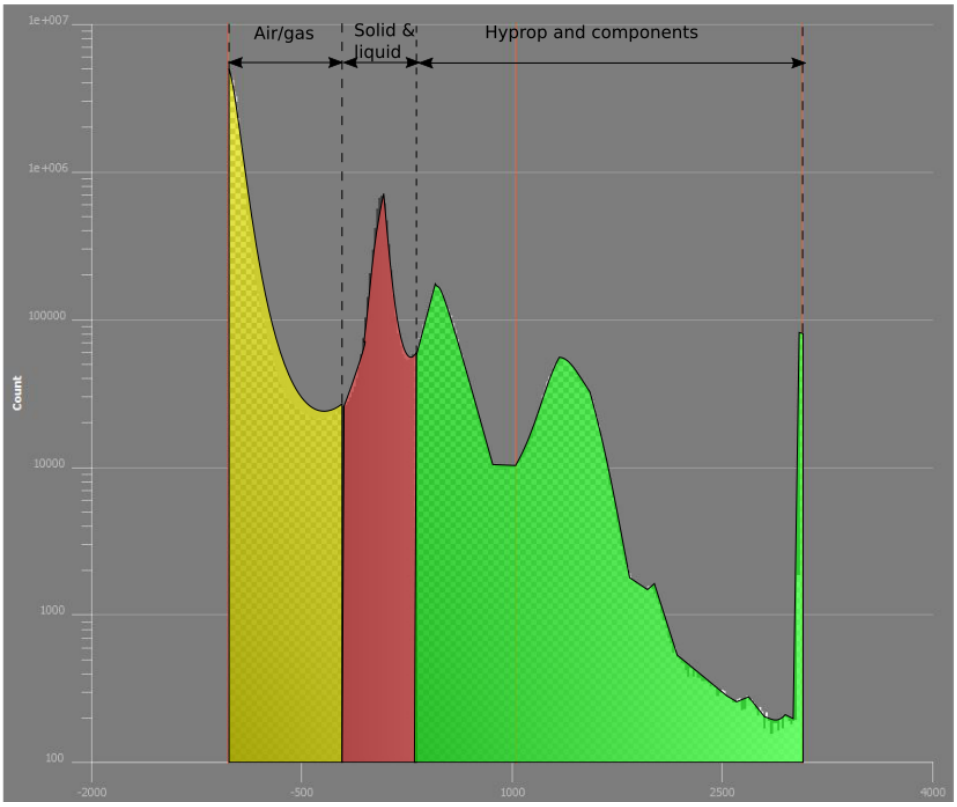

Figure 6.2: Threshold segmentation - From left to right: air/gas fraction, solid & liquid fraction and the Hyprop and its components

6.3.2. NEGATIVE INITIAL PORE-WATER TENSION

Negative initial pore water tension becomes an issue when processing the results in various diagrams. Commonly, tension measurements are plotted on a logarithmic scale, such as in a soil water retention curve. Thus, it becomes impossible to depict these negative measurements on a log scale graph. To correct these measurements, two correction methods were applied, namely: “liftup” of the measurements based on the initial slurry column height and by correlating the loss of slurry column height to positive tension.

Correcting based on the initial slurry column height was most accurate when the dredged sediment behaved fluidlike. In this state, the initial tension coincides with the hydrostatic pressure of the slurry column, with the exception of irregular measurements due to assembly. This was the case for the non-oxidised campaigns, where the negative initial tension more or less corresponded with their respective slurry column height. However, for the drier oxidised campaigns, column slurry height deviated substantially from the negative initial tension. Table 6.1 illustrates the variance between the oxidised and non-oxidised campaigns. Ignoring the irregular measurements due to assembly, the significant discrepancy between the column height and initial tension of the oxidised campaigns can be explained by the soil having a limited amount of water retaining capacity in its initial state. Thus, the “liftup” corrections for these campaigns essentially over calibrates the measurements.

The second correction method assumes only vertical shrinkage throughout the entire drying process and correlates the amount of vertical shrinkage to positive tension. The correction method aims to improve the accuracy of tension measurements in the early stages of the test where indeed only vertical shrinkage takes place. In the later stages this correction becomes invalid as lateral and vertical shrinkage from becomes evident. Nevertheless, for consistency the correction was applied for the entire lifetime of the various Hyprop experiments. The applied correction ranges from 6- 10 hPa, thus barely influencing the measurements in its final stage.

Collectively, both correction methods utilised, overly compensates for negative tension but overall does give a more accurate representation of tension development in the soil. Suggested, is to calibrate the Hyprop unit prior to starting the campaign, thus after the complete assembly of the Hyprop. Generally, the Hyprop unit is calibrated after degassing the water and prior to installation of the tensiometers. By calibrating after complete assembly, this should set the zero point in its initial state and remove any initial negative tension. However, this will not correct for subsequent negative tension buildup as the soil equalizes.

Hyprop Campaign	**Column Height [cm]**	**Measured Initial Tension Bottom [hPa]**	**Measured Initial Tension Top [hPa]**
Non-oxidised & undried	10.17	-11.39	-13.47
Non-oxidised & air dried	10.21	-9.64	33.43*
Oxidised & undried	9.85	-36.8*	-0.7
Oxidised & air dried	9.86	-5.6	-0.1

Table 6.1: Initial column height with corresponding uncorrected initial tensions for the Hyprop campaigns
* = Irregular measured values due to assembly

6.4. DISCUSSION OF RESULTS

The final results acquired from the experiments and subsequent data processing produced 3D reconstructed images of the drying process of the soil and a series of graphs that describes the shrinkage characteristics, gas formation and the water retention characteristics. Recent studies related to computed tomography, pore size distribution and biogenic gas bubble development in peat consists of either core samples taken from the field, gas traps for gas collection and/or pressure plate method to obtain hydraulic properties ([13], [14], [16], [17], [25], [26],[27], etc). The combination of computed tomography and the extended evaporation method used in this research has not been seen before in previous studies, apart from TU Delft colleagues, whose work is still in preparation. Benefits of this research combination are continuous suction measurements, the quick procedure of making CT-scans and a complete 3D profile of the soil can be reconstructed as it dries. Whereas, other researchers used μCT-scanners and/or pressure plates for their studies [25], [26], [27].

The soil was reconstructed successfully, removing any unwanted objects such as the Hyprop and its components. The majority of the artefacts present were also removed and a distinction was made between entrapped gas bubbles and air/gas open to the atmosphere. However, the main mechanism for gas formation and the type of gas entrapped can not be derived from these experiments. Research have shown that the main components of gas produced by peatlands are carbon dioxide (CO_2) and methane (CH_4). CO_2 is released under aerobic conditions due to oxidation of organic matter, and CH_4 is released due to diffusion, plant transport and as exsolution of dissolved bubbles in the pore water under waterlogged anaerobic conditions. CO_2 release under these test conditions is possible, as the sample is placed under aerobic conditions during drying. Release of CH_4 via plant transport can be ruled out due to the absence of living plants. Diffusion through pore water is possible and gas bubble accumulation is evident, with sudden release to the atmosphere when cracking at the surface occurs. Thus, according to literature, the apparent gas bubble formation in the dredged sediment can most likely be attributed to the exsolution of dissolved gas in the pore water, oxidation of organic matter or a combination of the two mechanisms. Ultimately, the CT images does clearly confirm the accumulation of gas bubbles, gradual movement of the bubbles, the growth of larger bubbles and sudden release of the gas (ebullition) to the atmosphere in a few cases.

The shrinkage characteristic was obtained by combining the gas volume measurements from the CT-scans and the soil mass measurements registered by the Hyprop. Results from the shrinkage characteristic curve were satisfactory as it clearly depicts the soil's shrinkage behaviour in their respective states. However, one must consider that the tensiometers and the boundary effects of the sampling ring affects shrinkage behaviour of the soil. Shrinkage is influenced once the soil releases from the sampling ring. The soil also released from the bottom of the Hyprop device by being supported by the tensiometers. Additionally, for future research, the shrinkage range should be extended by allowing the desiccation process to continue until zero volume change is recorded. The shrinkage characteristic measured solely proportional shrinkage during the Hyprop's period of testing. By extending the drying period, air entry and the zero shrinkage stage can then be observed as well.

Graphs that describe the gas bubble development within the dredged sediment are dependent on the CT-scans made during the Hyprop campaigns. Graphs representing the gas development are described by the volumetric gas content over the volumetric water content or the tension. Volumetric water contents were obtained by converting the mass based measurements with the water density and specific gravity. Where ρ_w = 1 g/ml, $G_{s;non-ox}$ = 1.8 - 1.82 and $G_{s;ox}$ = 1.86 - 2.03. The range of the specific gravity implies that the converted volumetric water content could vary somewhat. In this thesis, the lower bound values were used. Furthermore, for every scan point measurements for the void ratio and volumetric gas content were acquired. Thus, the amount of scans will directly influences the continuity of these diagrams. In hindsight, it became apparent that the early stages of the drying process is critical, the period where the majority of gas bubbles were formed. Due to lack of CT-scans during this period for the non-oxidised & undried campaign, 15 days between the first and second scan, peak gas volumes were not measured. A significant gap is visible in the graphs because of this. In subsequent Hyprop tests, more frequent scans were made in the early stages of drying, namely within 2 to 5 days from each other. As a result the continuity of the graphs improved for the remaining Hyprop campaigns. Arguably the period between the first and second scan from the non-oxidised & partially air dried campaign could have been reduced even further, as there still appears to be a slight gap in the gas bubble development. Scan frequency for the oxidised campaigns is deemed sufficient, as there appears to be no gas bubble formation and only a steady decrease in gas volume.

The water retention characteristics were constructed exclusively from the Hyprop data. These results were also satisfactory as a clear and continuous graph was constructed with minimal irregular values. Irregular values were only visible for the oxidised campaigns in their initial stage of the test, due to the intrusive assembly procedure.

7

CONCLUSIONS & RECOMMENDATIONS

7.1. INTRODUCTION

The final conclusions of the thesis shall be given in this chapter and will consist of the conclusions of the results, the practical and scientific relevance of the research and final recommendations for further research.

7.2. RESULT CONCLUSIONS

The main conclusion about the effect of organic matter on the water retention behaviour can be derived from the water retention characteristics. Varying the organic content by means of chemical oxidation greatly reduces the volumetric water content at a given suction level. Supported by the reduction in liquid limit with decreasing organic content, which corresponds to literature such as Hobbs 1986 [10]. The effect of organic matter on the shrinkage characteristics is not significant for the range of water contents relevant during the desiccation process observed in the field. During the desiccation process, normal shrinkage is observed at near saturated conditions, where the loss of water volume is equal to the loss of bulk soil volume. The gas fraction is negligible over the full range of shrinkage for the desiccation period tested. The gas fraction is relative small when compared to the water and solid fraction of dredged sediment. Thus, gas buildup barely influences the degree of saturation. However, these results are obtained in a climate controlled environment and will most likely differ under field conditions.

Varying the initial water content changes the onset of the water retention characterstics. Its shape is barely influenced by the lowered initial water content, where the sample with the lowered water content wants to follow the path of its undried counterpart. The initial water content only influences the onset of the shrinkage characteristic, normal shrinkage commenced afterwards.

The observed results indicate that the effect of organic matter stimulates gas formation. Immediate gas accumulation was witnessed for the non-oxidised campaigns until peak gas volume was reached. Peak gas volume was realised at low tension values of around 10 hPa. Removal of organic matter by chemical oxidation dismisses the possibility of gas accumulation. Visual observation of the 3D reconstructed CT images indicated gradual movement of the gas bubbles within the dredged sediment. Aggregation of bubbles were clearly visible as the sediment dried, resulting in larger gas bubbles. Once the peak gas volume was achieved, gradual decrease of total gas volume was observed within a confined area of soil. In the early stages of drying, no connection of the gas bubbles to the open atmosphere was visible. This leads one to believe that the gradual decrease in gas volume was caused due to diffusion through the pore water. In the end phase of a few campaigns, ebullition events occurred, where gas was abruptly released to the atmosphere due to cracks.

The observed gas bubbles partly consists of air entrapped during the assembly procedure and by an unknown gas as drying of the soil takes place. Researchers such as Tokida, Strack, Kellner and Kettridge propose that methane is dissolved in the pore water under anaerobic conditions. Gas accumulation is then suggested to have been caused by exsolution of the dissolved methane in the pore water, where variation of the gas volume is described by Henry's law and the ideal gas law. Considering that the Hyprop tests were carried out under aerobic conditions, the gas accumulated could also partly be carbon dioxide caused by oxidation of organic

matter. However, from the experiments performed it is simply not possible to verify the gas entrapped in the sediment. Further research would be needed to confirm the gas composition.

7.3. THESIS VALUE

From a practical standpoint the results from the research has led to a greater understanding of the shrinkage and water retention behaviour of the dredged sediments in Wormer & Jisperveld, an area that generates large amounts of dredged sediments due to unstable conditions. Mobile flow of these sediments throughout the entire area causes significant hindrance for the environment and surrounding community. Thus, creative reapplication of dredged sediments are currently being developed and tested to solve the issue. One of the main methods being utilised is storage of excess dredged sediment in depots to compensate for subsidence and to improve soil fertility by dewatering/ripening. Shrinkage and water retention characteristics are of value for improved soil ripening models of the depots. Although, one must consider the difference between laboratory and field environment. Weather, scaling and boundary effects must be taken into consideration as it will directly influence shrinkage and water retention behaviour. Field data and weather prediction models can be correlated with laboratory results for a more accurate interpretation of dredged sediment behaviour during ripening. Such knowledge is of value to predict the optimal period of land reclamation to further proceed with agricultural use of the land. From the observed measurements of the core samples, ripening of dredged sediment seems to have a positive effect on the soil. Organic content increased and immense amount of plant growth was noticeable. Soil strength and stability is expected to increase as a result.

From a scientific standpoint the shrinkage characteristics contradicts claims from authors such as van den Akker [3] and Schothorst [4], where stated that the majority of subsidence is attributed to oxidation of organic matter. The soil's composition makes it impossible to assign the majority of the subsidence due to oxidation. If 5-10% of the soil's total volume consists of organic matter, with an original peat layer of 5m, then only 0.5m of surface subsidence can directly be attributed oxidation of organic matter. A more likely explanation is that oxidation of organic matter indirectly causes surface subsidence due to loss of soil structure. Supported by laboratory results where there was a substantial loss of water retention when organic matter was removed.

The use of computed tomography in combination with the extended evaporation method can be considered a novel approach as it has not been seen before in previous literature. The value of the combined techniques are continuous suction measurements of the soil while being able to generate a complete 3D profile at various stages of the desiccation process. CT images visually confirms the common belief under researchers such as (Tokida [13], Strack [14], Waddington [17], [25]) that there is gas bubble development, gradual movement, aggregation, growth and eventual ebullition of gas.

7.4. RECOMMENDATIONS

This section shall discuss the recommendations for further research. The section shall be divided once again in the recommendations for the methods, data processing and the results.

7.4.1. RECOMMENDATIONS FOR METHODS

Consistency Limits

Plastic limit was not determined for the oxidised samples due to insufficient oxidised dredged material. Liquid limit was determined for the oxidised sample, however only a single point measurement was acquired. The pH of the oxidised material from Zain was not neutralised with sodium hydroxide, therefore Zain's liquid and plastic limit values will differ. Suggested is to repeat the consistency limits for the oxidised material. When repeating the oxidation procedure, keep in mind the low yield of oxidised material.

Hyprop Testing Conditions

Testing conditions varied slightly for the oxidised Hyprop campaigns due to time constraints. For the oxidised campaigns, it was decided to use an air pump to accelerate the desiccation process. Ideally, the same testing conditions should be applied for all experiments to enable better comparison of results.

Chemical Reagents

Hydrogen peroxide is a very invasive chemical and does not completely remove the organic matter. Alternative reagents, such as NaOCl and $Na_2S_2O_8$, could be experimented with to improve efficiency of organic

matter removal and to reduce possible effects of hydrogen peroxide on minerals. Conservative amounts of hydrogen peroxide was used to ensure optimum removal of organic matter. Determining the optimal amount of chemicals could also be studied further.

Contrasting Sampling Ring Density
With the CT images, it was challenging at times to discern the sampling ring from the soil within Avizo. The sampling ring was constructed from a light-weight PVC. A simple solution would be to replace the light PVC ring with a denser substance, which will allow for a clear distinction between the light-weight soil and dense boundary.

Gas Verification
Verifying the entrapped gas observed in the dredged sediment is not possible with the applied testing methods. Gas traps could be used to collect the gas and can be analysed by gas chromatograph. Bioreactor can also be used to study the chemical processes within the dredged sediment.

7.4.2. RECOMMENDATIONS FOR DATA PROCESSING

Thresholding
Thresholding accuracy is an area that can vastly be improved upon in the scientific community. In this study, and also in other research, the solid and liquid fractions of the histograms were not separated as there is at present no effective algorithm that could do so. If one is able to develop an accurate algorithm to separate the solid and liquid fraction from each other, this would prove valuable as an alternative soil characterisation method.

Recommended for further research is a sensitivity analysis of the acquired soil fraction volumes. A preliminary analysis was carried out for the solid and liquid fractions by comparing the computed volume with the mass based measurements of the Hyprop. No such reference values are available for the gas fraction, thus a more in depth sensitivity analysis is needed for this phase.

7.4.3. RECOMMENDATIONS FOR RESULTS

CT-Scan Frequency
The first five days were crucial for gas bubble development for the non-oxidised campaigns. However,this period was not captured for the non-oxidised & undried campaign. After peak gas volumes were reached, the entrapped gas volume slowly decreased in time. Proposed are more frequent CT-scans, especially in the first week of testing.

Extend Desiccation Period
Desiccation period carried out for the thesis was solely based on the measuring range of the Hyprop. The experiment was stopped once air entry of the tensiometers occurred. This point is characterised by the sudden collapse of tension values to 0 kPa. The resulting measuring range for the shrinkage characteristic was up to a volumetric water content of approximately 60%. In this range only normal shrinkage was observed. Extending the desiccation period despite failure of tensiometers will expand the shrinkage characteristic, giving more insight to shrinkage behaviour in drier conditions. Particularly, air entry points and shrinkage limits are of great interest. Naturally, the Hyprop must be left running to register evaporation and continued CT-scans must be made for additional data points.

Dewpoint Tests
Additional suction measurements can be made with dew point tests if one opts to extend the desiccation period. Dew point devices has a measuring range of -0.1 to -300 MPa. Although, one has to consider the relevant measuring range applicable for (Dutch) field conditions.

Rewetting and Drying Cycles
Studying multiple cycles of rewetting and drying behaviour is an aspect not studied in this thesis. This is an important matter, as it more accurately simulates field conditions. Additionally, for future research seasonal effects can also be considered, taking into account for dry summers and wet winters.

BIBLIOGRAPHY

[1] G. Ven, *Leefbaar laagland: geschiedenis van de waterbeheersing en landaanwinning in Nederland* (2003).

[2] J. M. Ewing and M. J. Vepraskas, *Estimating primary and secondary subsidence in an organic soil 15, 20, and 30 years after drainage,* Wetlands **26**, 119 (2006).

[3] J. van den Akker and P. Kuikman, *Emission of CO2 from agricultural peat soils in the Netherlands and ways to limit this emission.* Statewide Agricultural Land Use Baseline **1**, 8 (2008), arXiv:arXiv:1011.1669v3 .

[4] C. Schothorst, *Subsidence of low moor peat soils in the western netherlands,* **17** (1977).

[5] L. Pons and Zonneveld.I.S., *Soil Ripening and Soil Classification,* **15** (1965).

[6] Tauw, *The Sediment Storer,* (2015).

[7] Hoogheemraadschap Hollands Noorderkwartier, *Syntheserapport uitgevoerde studies naar de grote plassen van het Wormer- en Jisperwater*, Tech. Rep. (2013).

[8] Hoogheemraadschap Hollands Noorderkwartier, *Advies ontmanteling depot K*, Tech. Rep. (2013).

[9] P. M. Hayward and R. S. Clymo, *Profiles of Water Content and Pore Size in Sphagnum and Peat, and their Relation to Peat Bog Ecology,* Proceedings of the Royal Society B: Biological Sciences **215**, 299 (1982).

[10] N. B. Hobbs, *Mire morphology and the properties and behaviour of some British and foreign peats,* Quarterly Journal of Engineering Geology and Hydrogeology **19**, 7 (1986).

[11] E. Gorham, *Some chemical aspects of wetland ecology,* (1967).

[12] T. D. Sharkey, E. a. Holland, and H. a. Mooney, *Trace Gas Emissions by Plants* (1991).

[13] T. Tokida, T. Miyazaki, M. Mizoguchi, O. Nagata, F. Takakai, A. Kagemoto, and R. Hatano, *Falling atmospheric pressure as a trigger for methane ebullition from peatland,* Global Biogeochemical Cycles **21**, 1 (2007).

[14] M. Strack and E. Kellner, *Dynamics of biogenic gas bubbles in peat and their effects on peatland biogeochemistry,* Global Biogeochemical (2005).

[15] J. Couwenberg, *Methane emissions from peat soils,* Wetlands International , 16 (2009).

[16] E. Kellner and J. Waddington, *Dynamics of biogenic gas bubbles in peat: Potential effects on water storage and peat deformation,* Water Resources Research (2005).

[17] J. M. Waddington, K. Harrison, E. Kellner, and A. J. Baird, *Effect of atmospheric pressure and temperature on entrapped gas content in peat,* **2980**, 2970 (2009).

[18] A. Verruijt and S. V. Baars, *Soil mechanics* (VSSD, 2007) pp. 28–32.

[19] K. R. Everett, *Chapter 1,* in *Pedogenesis and Soil Taxonomy. II. The Soil Orders*, edited by W. L.P., N. Smeck, and G. Hall (Elsevier Science Publishers B.V., Amsterdam, 1983) Chap. 1, pp. 1–53.

[20] E. P. Querner, P. C. Jansen, J. J. H. van den Akker, and C. Kwakernaak, *Analysing water level strategies to reduce soil subsidence in Dutch peat meadows,* Journal of Hydrology **446-447**, 59 (2012).

[21] U. Schindler, J. Doerner, and L. Mueller, *Simplified method for quantifying the hydraulic properties of shrinking soils,* Journal of Plant Nutrition and Soil Science **178**, 136 (2015).

[22] S. Kazemian, B. B. K. Huat, a. Prasad, and M. Barghchi, *A state of art review of peat: Geotechnical engineering perspective,* International Journal of Physical Sciences **6**, 1974 (2011).

[23] K. &. Mikutta, R., Kleber, M., Kaiser and R. Jahn, *Review : Organic Matter Removal from Soils using Hydrogen Peroxide ,,* Soil Science Society of America **69**, 120 (2005).

[24] K. Soga and J. Mitchell, *Fundamentals of soil Behavior,* John Wiley& Sons, Hoboken, New Jersey, USA (2005).

[25] N. Kettridge and A. Binley, *Characterization of peat structure using X-ray computed tomography and its control on the ebullition of biogenic gas bubbles,* Journal of Geophysical Research: Biogeosciences **116**, 1 (2011).

[26] F. Rezanezhad, W. L. Quinton, J. S. Price, D. Elrick, T. R. Elliot, and R. J. Heck, *Examining the effect of pore size distribution and shape on flow through unsaturated peat using 3-D computed tomography,* Hydrology and Earth System Sciences Discussions **6**, 3835 (2009).

[27] F. Rezanezhad, W. L. Quinton, J. S. Price, T. R. Elliot, D. Elrick, and K. R. Shook, *Influence of pore size and geometry on peat unsaturated hydraulic conductivity computed from 3D computed tomography image analysis,* Hydrological Processes **24**, 2983 (2010).

[28] N. Zain, L. van Paassen, and C. Jommi, *Effects of in-situ oxidation on the compression behaviour of organic soils: Part I Compressibility (in preparation),* (2016).

[29] British Standard, *Methods of test for soils for civil engineering purposes (1377),* British Standard Institution (1990).

[30] B. Schumacher, *Methods for the Determination of Total Organic Carbon (TOC) in Soils and Sediments*, Tech. Rep. April (Ecological Risk Assessment Support Center, U.S. Environmental Protection Agency, Las Vegas, 2002).

[31] W. McLean, *the Nature of Soil Organic Matter As Shown By the Attack of Hydrogen Peroxide,* Journal of Agricultural Science **21**, 595 (1931).

[32] U. Schindler, *Ein Schnellverfahren zur Messung der Wasserleitfahigkeit im teilgesattigten Boden and Stechzylinderproben,* Archiv fur Acker-und Pflanzenbau und Bodenkunde (1980).

[33] U. Schindler and L. Müller, *Simplifying the evaporation method for quantifying soil hydraulic properties,* Journal of Plant Nutrition and Soil Science **169**, 623 (2006).

[34] F. E. Boas and D. Fleischmann, *CT artifacts: causes and reduction techniques,* Imaging in Medicine **4**, 229 (2012).

[35] R. Tollenaar, L. Van Paassen, and C. Jommi, *Assessing the water retention characteristics of shrinking soils with high initial water content using the HYPROP device (in preparation),* (2016).

[36] O. Olaniyan, R. Olaoye, O. Okeyinka, and D. Olaniyan, *Soil stabilization techniques using sodium hydroxide additives,* International Journal of Civil **11**, 9 (2011).

[37] J. Nyamangara, S. Munotengwa, P. Nyamugafata, and G. Nyamadzawo, *The effect of hydroxide solutions on the structural stability and saturated hydraulic conductivity of four tropical soils,* South African Journal of Plant and Soil **24**, 1 (2007).

A

Oxidation Sheet

The calculations for the required amount of hydrogen peroxide (H_2O_2) to ensure maximum removal of organic matter is illustrated in this appendix. Two calculation methods were considered, namely the Rock Eval method and the Schumacher conversion method. Both calculation methods are displayed in the Table A.1.

The first section of the table illustrates general information and assumptions required for the calculations. Assumed was a partially air dried sediment of 500% water content. Dry solid was calculated to be 16.67% at the assumed water content, along with a 50% organic content estimate. All calculations were carried out for a starting weight of 100g of sediment. The dry solid and water mass were calculated based on the corresponding ratio values. The total organic carbon (TOC) (from total dry soil) of 23.85% was derived from the Rock Eval experiment which was previously carried out by another researcher. Schumacher's lower bound conversion factor of 1.724 is listed as well.

The amount of carbon was calculated by multiplying the Rock Eval's TOC ratio value by the dry soil mass. The mass of carbon was then converted to molecular units. Equation 3.2 displays the amount of oxygen (O_2) needed to react with 1 mol of carbon (C), namely a 1:1 ratio. The amount of hydrogen peroxide (H_2O_2) per mol oxygen is a 2:1 ratio based off Equation 3.1. Once the molecular weight of hydrogen peroxide was calculated, it was then converted back to regular mass units and subsequently to volumetric units. The final amount needed according to the Rock Eval method was 225ml.

The same process was essentially applied with Schumacher's method, except the total organic carbon was calculated by dividing the organic matter by the conversion factor. The calculated amount of hydrogen peroxide with Schumacher's method was 275ml. The more conservative Schumacher's method was used for the experiments.

General Information & Assumptions

	Unit	Amount	Comments
Initial moisture content partially dried	[%]	500%	[Mw/Md]
Dry solid content	[%]	16.67%	[Md/Mt]
Organic Content	[%]	50%	[Morg/Md]
Total (wet) soil	[g]	100	Mw - Starting weight
Total (dry) soil	[g]	16.67	Md
Mass water	[g]	83.33	Ms
Total organic carbon (from total dry soil)	[%]	23.85%	TOC
Molecular Weight Carbon	[g/mol]	12.0107	Mcarbon
Molecular Weight Oxygen gas	[g/mol]	31.9988	Moxygen
Molecular Weight Hydrogen	[g/mol]	1.00794	Mhydrogen
Molecular Weight Hydrogen peroxide	[g/mol]	34.01468	M_H2O2
H2O2 wt. content in stock	[g/mol]	10.00%	
Density H2O2 stock solution	[g/ml]	1.11	
Conversion factor Schumacher		1.724	

Rock Eval Method

	Unit	Amount	Comments
Total organic carbon content_ Rock Eval method	[g/100 g wet soil]	3.98	TOC * Md
Total organic carbon content_ Rock Eval method	[mol/100 g wet soil]	0.33	Divide by Mcarbon
Total O2 as electron acceptor	[mol/100 g wet soil]	0.33	1 O2 per C
Total H2O2 needed to supply the electron acceptor	[mol/100 g wet soil]	0.66	2 H2O2 needed
Total H2O2 needed to supply the electron acceptor	[g/100 g wet soil]	22.52	Multiply by M_H2O2
Total H2O2 stock solution needed for electron acceptor	[ml/ 100 g wet soil]	225.19	10% wt H2O2

Schumacher Conversion Method

	Unit	Amount	Comments
Total organics	[g/100 g wet soil]	8.34	Md * organic content
TOC based on conversion factor	[g/100 g wet soil]	4.83	Divide by conversion factor
Total organic carbon content	[mol/100 g wet soil]	0.40	Divide by Mcarbon
Total O2 as electron acceptor	[mol/100 g wet soil]	0.40	1 O2 per C
Total H2O2 needed to supply the electron acceptor	[mol/100 g wet soil]	0.81	2 H2O2 needed
Total H2O2 needed to supply the electron acceptor	[gr/100 g wet soil]	27.38	Multiply by M_H2O2
Total H2O2 stock solution needed for electron acceptor	[ml/ 100 g wet soil]	273.84	10% wt H2O2

Table A.1: Chemical oxidation H_2O_2 calculation sheet

B

Titration Curves

After chemical oxidatoin, the acidic oxidised slurry was neutralised with sodium hydroxide (NaOH). The titration process was documented for the initial batches, because it was not known how the oxidised material would react to NaOH. The pH was checked with the Consort pH meter. The titration curves illustrated in Figure B.1 and B.2 consisted of 100g batches of oxidised material. The first batch was carried out with a 0.1M NaOH concentration. The second and third batch was performed with 2M NaOH concentration. All subsequent titration batches were then performed with 2M concentration and were not registered, as it was too time consuming. The titration curves were used to obtain a rough estimate of the necessary amount of NaOH to neutralise to safe levels of pH 5.5 - 7.

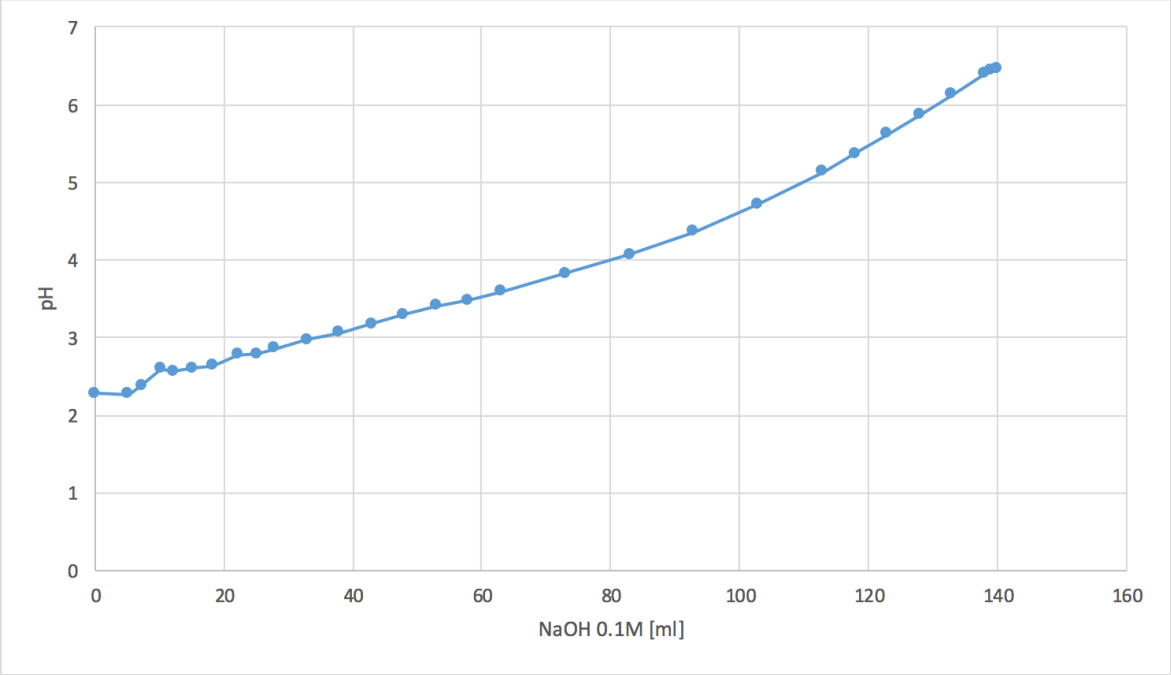

Figure B.1: Titration curve for a 0.1M (molar) concentration of sodium hydroxide (NaOH)

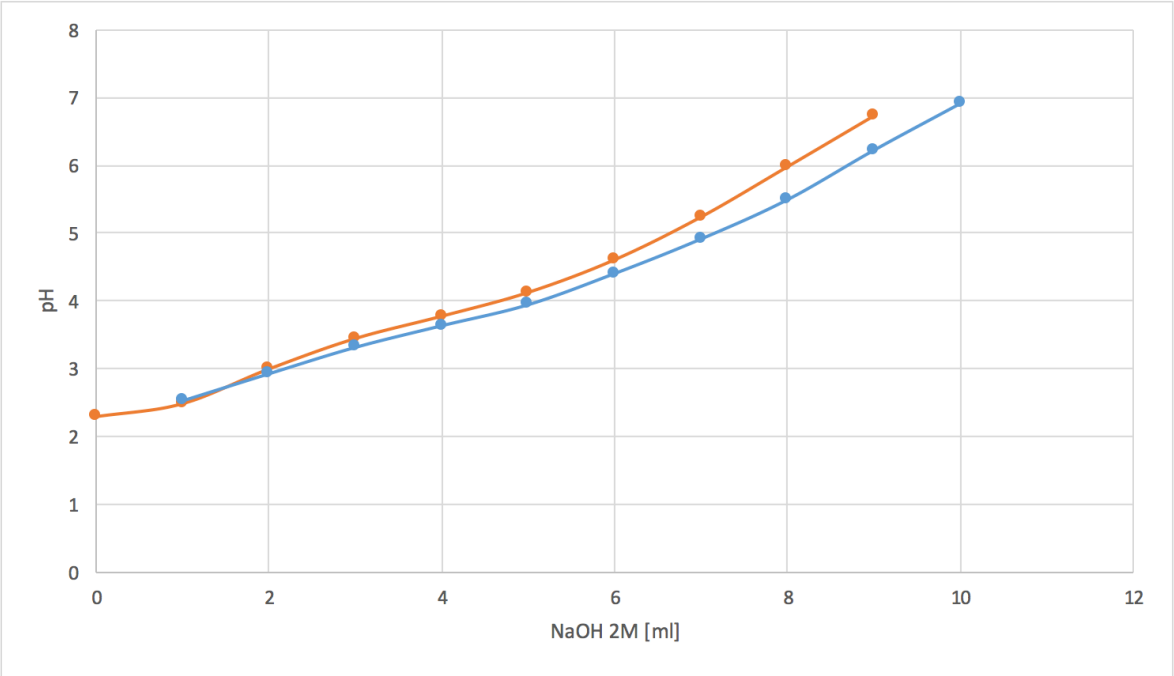

Figure B.2: Titration curves for 2M (molar) concentration of sodium hydroxide (NaOH)

C

HYPROP TEST LOG

Non-Oxidised & Undried

Date	Time	Activity	Comments
25-04-16	13:00	CT-scan	Due to software issues no evaporation rates were measured. Tension and weight measurements made at different time intervals for entire test
28-04-16	15:08	Start of test	Start of test - 3 days of unregistered evaporation
02-05-16	9:18	Start of air pump	Air pump used for 2 days
04-05-16	15:38	End of air pump	
10-05-16	9:47	CT-scan	
12-05-16	13:10	CT-scan	
17-05-16	13:20	CT-scan	
19-05-16	10:02	CT-scan	
23-05-16	10:15	CT-scan	
24-05-16	11:56	CT-scan	
26-05-16	13:56	CT-scan	
30-05-16	13:38	CT-scan	End of test + CT-scan

Non-Oxidised & Partially Air Dried

Date	Time	Activity	Comments
12-05-16	15:38	CT-scan + Start test	
17-05-16	13:23	CT-scan	
19-05-16	10:03	CT-scan	
23-05-16	10:16	CT-scan	
24-05-16	11:57	CT-scan	
26-05-16	13:57	CT-scan	
26-05-16	16:00		Power outtage for 1 hour
30-05-16	13:39	CT-scan	
02-06-16	14:35	CT-scan	
07-06-16	08:28	CT-scan	
09-06-16	14:13	CT-scan	
17-06-16	10:15	CT-scan	
23-06-16	15:39	CT-scan	
27-06-16	9:26	CT-scan	
30-06-16	15:30	End of test + CT-scan	

Oxidised & Undried

Date	Time	Activity	Comments
03-08-16	9:32	CT-scan + Start test	Use of air pump entire test
08-08-16	9:37	CT-scan	
11-08-16	15:04	CT-scan	
15-08-16	9:18	CT-scan	
18-08-16	12:46	CT-scan	
22-08-16	14:46	End of test + CT-scan	

Oxidised & Partially Air Dried

Date	Time	Activity	Comments
18-08-16	13:22	CT-scan + Start test	Falling cone prior to test - penetration 21mm
18-08-16	13:22		Use of air pump entire test
22-08-16	14:49	CT-scan	
25-08-16	16:07	CT-scan	
29-08-16	8:37	CT-scan	
30-08-16	14:36	CT-scan	
01-09-16	8:45	CT-scan	
05-09-16	8:31	CT-scan	
06-09-16	12:42	End of test + CT-scan	

D

CT MEASUREMENTS

Listed in this chapter are the calculated volume measurements derived from the CT-data. Volume measurements calculated were the volume of water and solids (Vw + Vs), gas volume (Vgas) and the volume of scatter and beam hardening effects (Vscat). A distinction is made between the volume of entrapped gas (Vgas) and gas volume that was entrapped and also open to the atmosphere (Vgas/air). The non-oxidised & partially air dried test was the only occasion where cracks did not develop, thus the entrapped gas was not exposed to the atmosphere. For the void space, Vgas/air is considered, because the phenomenon of air entry of the soil is studied in shrinkage characteristic curves. The volume of solids and water were corrected by the addition of the artefact volumes.

Bulk density was calculated by the net weight of the soil registered by the Hyprop divided by the total volume of the soil (Vt). Where the total volume is defined as $Vt = Vs + Vw + Vscat + Vgas$. Void space that is open to the atmosphere is not included in this definition of total soil volume. As time passed, the bulk density increased due to evaporation of the water which leads to the removal of buoyant forces.

Furthermore, a comparison was made between the mass based volumes acquired from the Hyprop, with the volume measurements from the CT-data. This was done to examine the accuracy of the CT measurements, assuming the mass based measurements were dependable. The “CT Volume Error” column was calculated by the volume differential of the mass based volumes and the CT volumes, and then divided by the mass based volume at that their respective time. Volume errors increased in time due to the increasing influence of the voxel size as the soil shrinks, which results in an underestimation of the volume measurements. Maximum error calculated was a 20% deviation from the mass based values.

Ratio values used for the final analyse of the results, such as the shrinkage characteristic curve and the soil water retention curve were derived from the volume measurements in this appendix. Ratio values derived were: void ratio ($e = \frac{V_v}{V_s}$), volumetric gas content ($V_g = \frac{V_g}{V_s}$), degree of saturation ($S = \frac{V_w}{V_v}$) and volumetric water content ($\theta = \frac{V_w}{V_s}$).

Table D.1: CT volume and Hyprop mass based measurements and calculations- Non Oxidised & Undried

Non-Oxidised & Undried

Date	Volume Solids + Water Vs+Vw [cm^3]	Volume Gas Vgas [cm^3]	Volume Gas+Air Vgas/air [cm^3]	Volume Scatter Vscat [cm^3]	Corrected Volume Solids+Water Vs+Vw+Vscat [cm^3]
25-04-16	444.89	0.69	0.69	4.38	449.27
10-05-16	196.18	6.03	6.14	1.82	198.00
12-05-16	176.79	5.99	5.99	1.76	178.54
17-05-16	119.11	5.06	5.06	0.77	119.88
19-05-16	101.97	4.71	4.98	0.43	102.40
23-05-16	71.28	4.14	4.14	0.13	71.40
24-05-16	58.81	3.76	3.89	0.13	58.93
26-05-16	45.84	3.29	3.32	0.03	45.87
30-05-16	28.21	0.42	3.34	0.00	28.21

	Volume Water Mass Based Vw [cm^3]	Volume Voids Vv Vgas/air+Vw [cm^3]	Total Volume Vt Vs+Vw+Vscat+Vgas [cm^3]	Net Weight Mt [g]	Bulk Density Mt/Vt [g/cm^3]
25-04-16	445.33	446.023442	449.97	479.70	1.07
10-05-16	184.14	190.281394	204.03	218.51	1.07
12-05-16	164.03	170.017304	184.53	198.40	1.08
17-05-16	113.18	118.241614	124.94	147.55	1.18
19-05-16	96.12	101.101394	107.11	130.49	1.22
23-05-16	62.04	66.1786641	75.54	96.41	1.28
24-05-16	53.19	57.0843941	62.70	87.56	1.40
26-05-16	36.95	40.2713941	49.17	71.32	1.45
30-05-16	16.26	19.5983121	28.63	50.63	1.77

	Volume Solids+Water Mass Based Vs+Vw [cm^3]	Δ Volume Solids+Water Mass - CT [g]	CT Volume Error
25-04-16	464.43	15.15	3%
10-05-16	203.24	5.24	3%
12-05-16	183.13	4.58	3%
17-05-16	132.28	12.39	9%
19-05-16	115.22	12.82	11%
23-05-16	81.14	9.73	12%
24-05-16	72.29	13.35	18%
26-05-16	56.05	10.17	18%
30-05-16	35.36	7.15	20%

Table D.2: CT volume and Hyprop mass based measurements and calculations - Non Oxidised & Partially Air Dried

Non-Oxidised & Partially Air Dried

Date	Volume Solids + Water Vs+Vw [cm^3]	Volume Gas Vgas [cm^3]	Volume Scatter Vscat [cm^3]	Corrected Volume Solids+Water Vs+Vw+Vscat [cm^3]
12-05-16	449.27	3.66	5.69	454.96
17-05-16	377.09	16.81	6.47	383.56
19-05-16	362.50	17.09	3.88	366.38
23-05-16	323.45	14.53	3.91	327.36
24-05-16	313.84	13.83	4.04	317.88
26-05-16	295.43	12.39	3.12	298.55
30-05-16	267.50	8.58	0.84	268.33
02-06-16	245.28	6.79	0.70	245.98
07-06-16	203.76	4.91	0.72	204.48
09-06-16	183.80	4.30	0.62	184.42
17-06-16	117.30	5.17	0.80	118.11
23-06-16	75.51	4.06	0.04	75.55
27-06-16	55.32	3.26	0.02	55.34
30-06-16	41.00	2.85	0.42	41.42

	Volume Water Mass Based Vw [cm^3]	Volume Voids Vv Vgas+Vw [cm^3]	Total Volume Vt Vs+Vw+Vscat+Vgas [cm^3]	Net Weight Mt [g]	Bulk Density Mt/Vt [g/cm^3]
12-05-16	436.48	440.14	458.62	480.27	1.05
17-05-16	376.29	393.10	400.36	420.08	1.05
19-05-16	356.26	373.35	383.47	400.05	1.04
23-05-16	316.88	331.41	341.89	360.67	1.05
24-05-16	307.14	320.97	331.71	350.93	1.06
26-05-16	286.74	299.13	310.93	330.53	1.06
30-05-16	253.87	262.45	276.91	297.66	1.07
02-06-16	231.77	238.56	252.77	275.56	1.09
07-06-16	193.07	197.98	209.39	236.86	1.13
09-06-16	172.77	177.07	188.72	216.56	1.15
17-06-16	108.35	113.52	123.28	152.14	1.23
23-06-16	66.09	70.15	79.61	109.88	1.38
27-06-16	42.89	46.15	58.60	86.68	1.48
30-06-16	25.19	28.04	44.27	68.98	1.56

Table D.3: CT volume and Hyprop mass based measurements and calculations - Non Oxidised & Partially Air Dried continued

	Volume Solids+Water Mass Based Vs+Vw [cm^3]	**ΔVolume Solids+Water Mass - CT [g]**	**CT Volume Error [%]**
12-05-16	460.81	5.85	1%
17-05-16	400.62	17.06	4%
19-05-16	380.59	14.21	4%
23-05-16	341.21	13.85	4%
24-05-16	331.47	13.59	4%
26-05-16	311.07	12.52	4%
30-05-16	278.20	9.87	4%
02-06-16	256.10	10.12	4%
07-06-16	217.40	12.92	6%
09-06-16	197.10	12.68	6%
17-06-16	132.68	14.57	11%
23-06-16	90.42	14.87	16%
27-06-16	67.22	11.88	18%
30-06-16	49.52	8.10	16%

Table D.4: CT volume and Hyprop mass based measurements and calculations - Oxidised & Undried

Oxidised & Undried

Date	Volume Solids + Water Vs+Vw [cm^3]	Volume Gas Vgas [cm^3]	Volume Gas+Air Vgas/air [cm^3]	Volume Scatter Vscat [cm^3]	Corrected Volume Solids+Water Vs+Vw+Vscat [cm^3]
03-08-16	435.03	4.42	4.42	6.27	441.31
08-08-16	323.01	3.41	3.41	4.69	327.71
11-08-16	271.18	3.14	3.14	5.08	276.26
15-08-16	197.55	1.75	1.75	2.70	200.25
18-08-16	140.30	0.91	16.75	0.00	140.30
22-08-16	98.62	0.55	17.75	0.00	98.62

	Volume Water Mass Based Vw [cm^3]	Volume Voids Vv Vgas/air+Vw [cm^3]	Total Volume Vt Vs+Vw+Vscat+Vgas [cm^3]	Net Weight Mt [g]	Bulk Density Mt/Vt [g/cm^3]
03-08-16	375.78	380.20	445.73	509.19	1.14
08-08-16	264.06	267.46	331.11	397.47	1.20
11-08-16	217.12	220.26	279.41	350.53	1.25
15-08-16	144.94	146.69	202.00	278.35	1.38
18-08-16	83.89	100.64	141.21	217.3	1.54
22-08-16	41.43	59.18	99.17	174.84	1.76

	Volume Solids+Water Mass Based Vs+Vw [cm^3]	ΔVolume Solids+Water Mass - CT [g]	CT Volume Error [%]
03-08-16	447.50	6.198	1%
08-08-16	335.78	8.079	2%
11-08-16	288.84	12.582	4%
15-08-16	216.66	16.416	8%
18-08-16	155.61	15.315	10%
22-08-16	113.15	14.530	13%

Table D.5: CT volume and Hyprop mass based measurements and calculations - Oxidised & Partially Air Dried

Oxidised & Partially Air Dried

Date	Volume Solids + Water Vs+Vw [cm^3]	Volume Gas Vgas [cm^3]	Volume Gas+Air Vgas/air [cm^3]	Volume Scatter Vscat [cm^3]	Corrected Volume Solids+Water Vs+Vw+Vscat [cm^3]
18-08-16	420.85	12.10	12.10	4.12	424.97
22-08-16	344.25	10.22	10.22	2.98	347.24
25-08-16	296.33	9.58	10.75	3.05	299.38
29-08-16	253.24	9.51	11.99	1.94	255.18
30-08-16	236.91	8.30	11.97	1.52	238.43
01-09-16	219.72	7.47	17.29	0.88	220.60
05-09-16	165.81	7.09	23.67	0.00	165.81
06-09-16	156.31	6.91	19.68	0.00	156.31

	Volume Water Mass Based Vw [cm^3]	Volume Voids Vv Vgas/air+Vw [cm^3]	Total Volume Vt Vs+Vw+Vscat+Vgas [cm^3]	Net Weight Mt [g]	Bulk Density Mt/Vt [g/cm^3]
18-08-16	335.83	347.93	437.07	532.60	1.22
22-08-16	250.19	260.41	357.46	446.96	1.25
25-08-16	205.97	216.72	308.96	402.74	1.30
29-08-16	160.82	172.81	264.69	357.59	1.35
30-08-16	146.70	158.68	246.73	343.47	1.39
01-09-16	125.21	142.50	228.07	321.98	1.41
05-09-16	71.83	95.50	172.91	268.60	1.55
06-09-16	61.49	81.18	163.22	258.26	1.58

	Volume Solids+Water Mass Based Vs+Vw [cm^3]	ΔVolume Solids+Water Mass - CT [g]	CT Volume Error [%]
18-08-16	441.62	16.65	4%
22-08-16	355.98	8.74	2%
25-08-16	311.76	12.38	4%
29-08-16	266.61	11.43	4%
30-08-16	252.49	14.06	6%
01-09-16	231.00	10.40	5%
05-09-16	177.62	11.81	7%
06-09-16	167.28	10.97	7%

E

Core Sample Testing

Presented are the gravimetric water and organic contents averaged over the depth. Core samples had a depth of 1.5 - 2m. Core samples originated from from Depot X. No measurements were avalaible for the years 2013 and 2015.

Date	Average Gravimetric Water Content [%]	Average Organic Content [%]
04-03-14	1730	53.46
08-04-14	830	50.59
08-04-14	977	50.44
08-04-14	743	47.93
03-06-14	791	50.47
24-07-14	839	53.57
24-07-14	849	-
24-09-14	902	53.56
09-10-14	990	52.18
13-11-14	868	52.97
12-12-14	895	-
04-03-14	622	53.79
25-08-16	550	57.16

Table E.1: Gravimetric water and organic contents averaged over the depth of the soil column.

F

Post Hyprop Images

F.1. Non-Oxidised & Undried

F.1a illustrates cracking of the surface. F.1b indicates clear elevation of the soil, supported by the two tensiometers. A slight bend is visible for the tensiometer on the left, which is the top tensiometer. Figure F.1c shows the bend of the tensiometer more clearly. Additionally, the organic fibers can be viewed here as well. Dredged sediment was very hard at this stage.

(a)

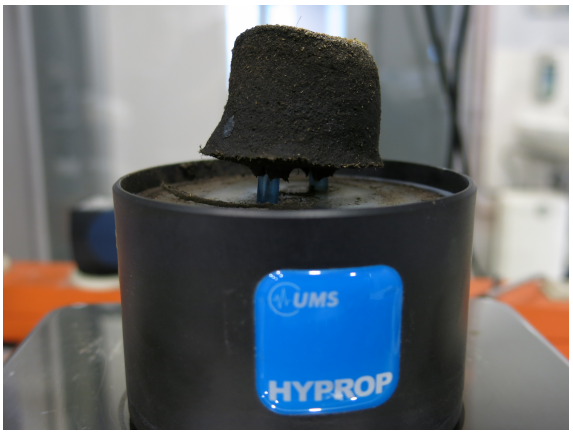

(b)

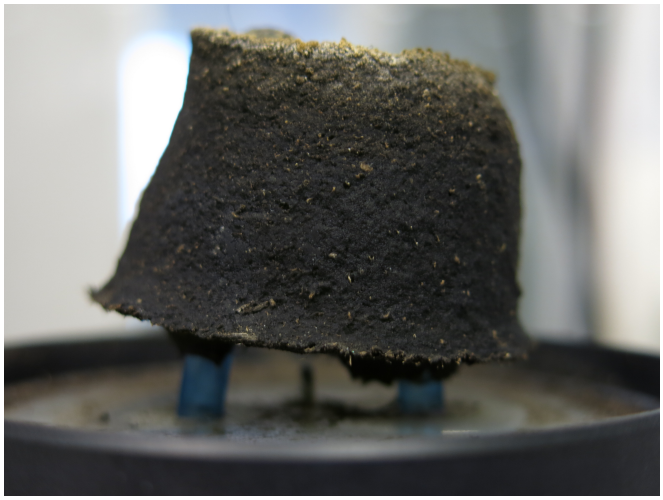

(c)

Figure F.1: Images post Hyprop experiment for the non-oxidised & undried campaign.

F.2. NON-OXIDISED & PARTIALLY AIR DRIED

F.2a displays the top view of the dredged sediment. Unlike previous campaign, no cracks are visible on the surface. F.2b shows once again the soil hanging on the tensiometers. Greater bend than the non-oxidised & undried campaign is visible in F.2c. Very hard texture is once again present, with organic fibres visible. F.2d displays the bend of the top tensiometer more clearly when detached from the Hyprop.

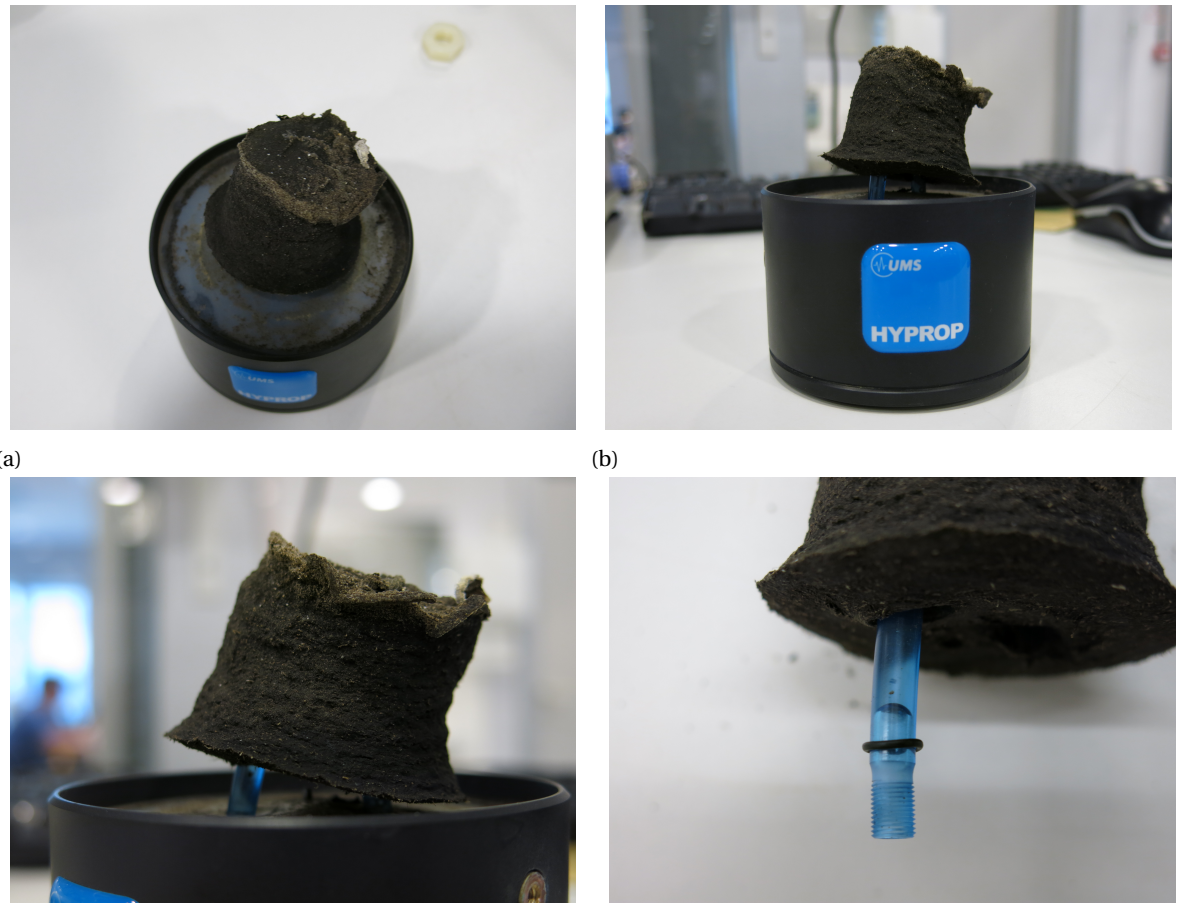

(a) (b)

(c) (d)

Figure F.2: Images post Hyprop experiment for the non-oxidised & partially air dried campaign.

F.3. OXIDISED & UNDRIED

Top view is given in F.3a, where no surface cracks are visible. However, some form of fungi is visible. This could possibly indicate oxidation of dredged sediment as fungus is known to cause decomposition of organic matter. Side view in F.3b displays plenty more fungi. Additionally, a larger soil body remains after the experiment as there were more solids present. Slight elevation of the soil is also visible. CT-scans showed cracks and thus air penetration in the bottom of the sample. Texture of the soil is more visible in F.3c, where the sediment was glossy and sticky with no fibers visible. F.3d illustrates the tensiometers after removal of the sediment. Slight bend is visible for the top tensiometer and air entry of this tensiometer is clearly visible.

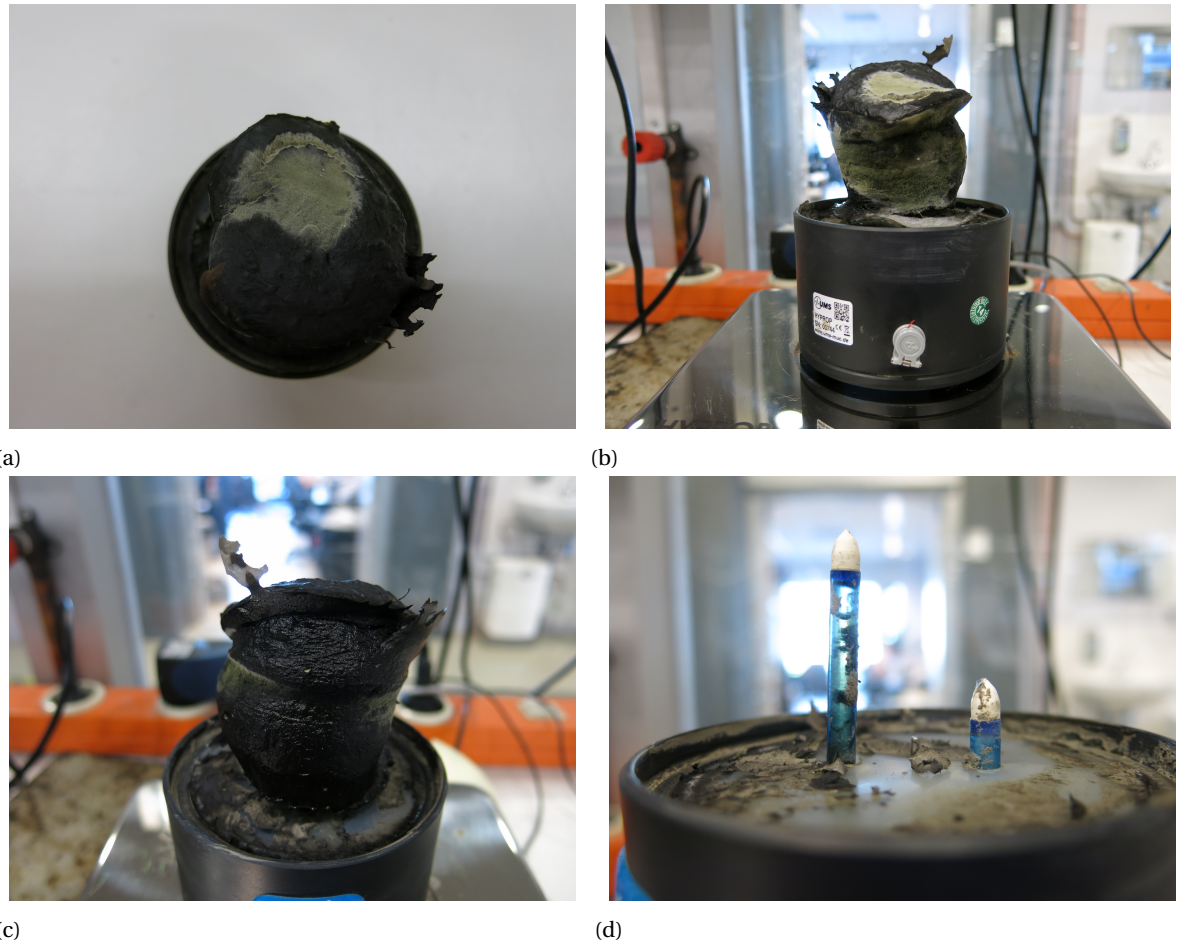

(a) (b)

(c) (d)

Figure F.3: Images post Hyprop experiment for oxidised & undried campaign.

F.4. OXIDISED & PARTIALLY AIR DRIED

Top view in F.4a exhibits a large crack on the surface with no fungus visible. Side view in F.4b does show fungi. Texture was very hard, glossy and sticky. A large soil body remains after the evaporation test due to the large amount of solids that were present. In F.4c cracks on the side of the body is visible. When the soil along the surface crack was removed, large amounts of fungi was visible as well. Other areas within the soil body, F.4e, that was not subject to the open atmosphere displayed no fungi. This indicates that sediment must be subjected to the open atmosphere to enable fungus growth. No fibers were visible in this sample. Cracks formed on the bottom of the soil as well, which caused large voids to form, visible in F.4f when the soil body was dissected once more. Around the air voids fungi is noticeable again.

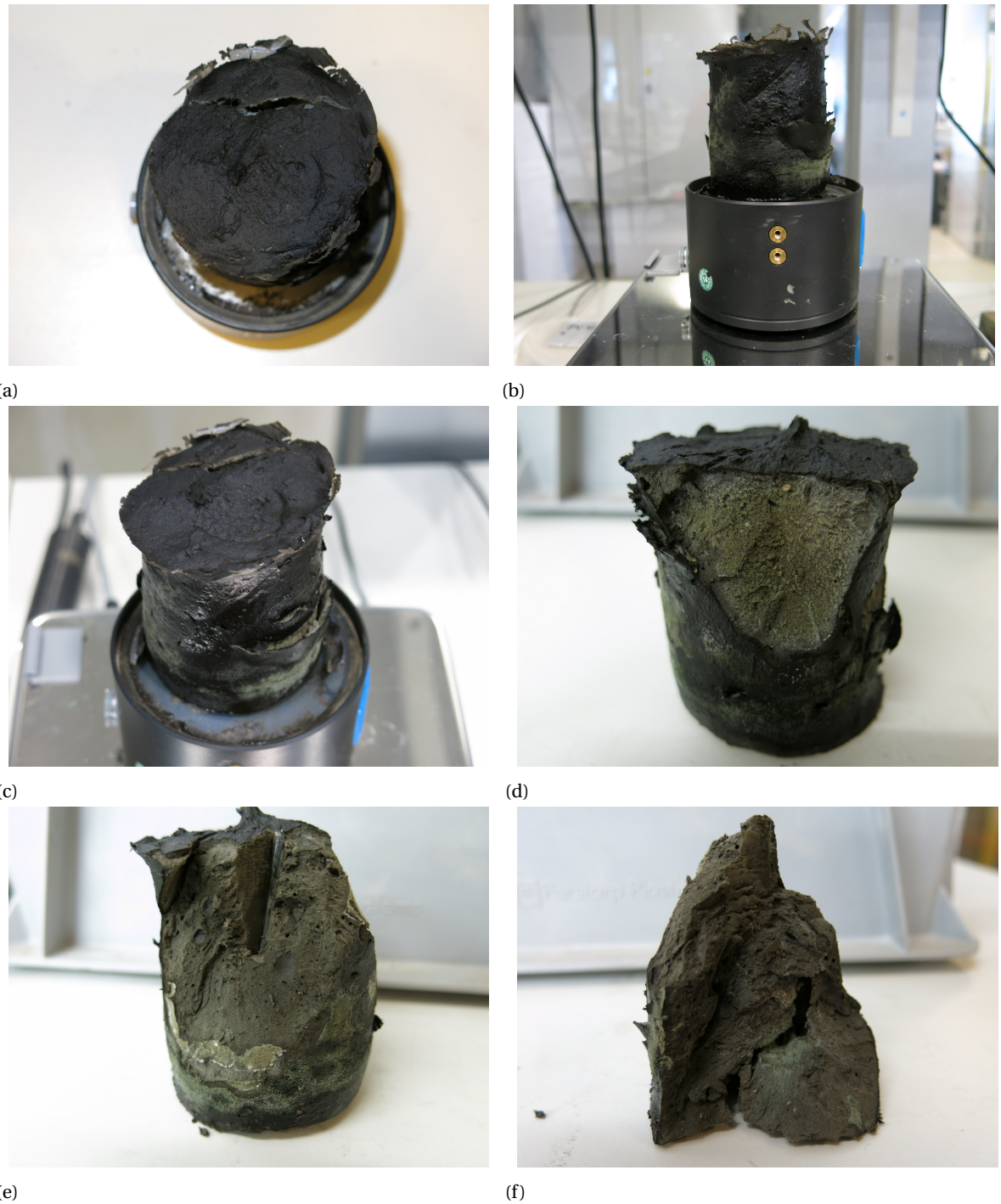

(a) (b) (c) (d) (e) (f)

Figure F.4: Images post Hyprop experiment for the oxidised & partially air dried campaign.